A morphological study of the parasitic barnacle, *Anelasma squalicola* (Lovén, 1844)

Helge Olsen Theil Bergum

Thesis submitted in partial fulfillment of the Master's degree in Marine Biology: Marine Biodiversity

Institute of Biology
University of Bergen, Norway

June 2016

Acknowledgements

I would first like to thank my supervisor, Professor Henrik Glenner of the Marine Biodiversity group at the University of Bergen. He always had a spare moment when I got stuck, and helped out greatly with his knowledge of *Anelasma* and Cirripedia in general. I would also like to thank my co-supervisor professor Frank Nilsen for helping me with my work in histology, and assisting me in interpreting the findings.

A special thank goes to the Zoological Institute of Rostock and Professor Stefan Richter and all of his colleagues for welcoming me into their group and letting me use their equipment. Their knowledge of µCT-scanning and 3D-reconstruction were a great help to me in my work on remodeling *Anelasma*.

I would also like to thank Professor Andreas Hejnol and everyone in his group for letting me use their equipment and including me in their group, making my modeling work much more enjoyable.

I would also like to thank Teresa Cieplinska at the Institute for Biology for helping me with histology and sectioning, and Professor Emeritus Harald Kryvi for sharing his knowledge of histology and providing me with invaluable help in interpreting my sections.

Lastly I would like to thank Brith Bergum and Richard Davies for proofreading, and everyone in the Marine Biodiversity group for helping me with equipment, answering all my questions and providing a nice working environment.

Objectives and Summary

The pedunculate barnacle, *Anelasma squalicola,* is found parasitizing various squaloid sharks of the family Etmopteridae. Its peduncle has been modified to bury in the flesh of its host, and has replaced its cirri as a feeding device. It is however still in possession of its cirri, albeit reduced, and digestive tract, both believed to be of a vestigial nature. Due to the curious appearance of *Anelasma* it has been of great interest to scientists since its first description in the 18th century. Despite this it has rarely been studied, due to a low frequency and a seemingly patch distribution, and many details of its morphology and adaptations to a parasitic mode of life remains unclear. By employing new methodologies including SEM, histology, micro-CT scanning 3D-reconstruction, this study aims to investigate and clarify *Anelasmas* morphology and adaptations to a parasitic way of life.

Through micro-CT scanning and 3D-reconstruction the intricacy of the root system of *Anelasma* has been revealed, showing an extensively branching system, penetrating deep into the tissue of its host. Histology reveals that the cuticle of the peduncle and the roots is thinning with distance from the mantle, and in the roots the exocuticle has been entirely reduced. It can be seen covering the tips of the roots to the very end. Its reproductive system is very well developed and takes up most of the space in the peduncle and thorax. The cement glands are numerous, and can be seen throughout the lower part of the mantle and in the waist, they have been seen emptying into the lacunae and I hypothesize that their function in *Anelasma* is to aid in the digestion of or nutrient uptake from its host. The lacunar system has also been seen in great detail, originating from the great central lacunae running axially through the peduncle and branching out to envelop the ovarian tubes and out into the tips of the roots. It is likely that the function of the lacunae is to transport absorbed nutrients throughout the body of *Anelasma.* All in all, *Anelasma* seems beautifully adapted to a life as a parasite.

Contents

Introduction

Historical summery

The stalked barnacle *Anelasma squalicola (Lovén 1844)* is found partially embedded in the flesh of various deep-sea squaloid sharks of the familiy Etmopteridae. It is mainly found parasitizing *Etmopterus Spinax (Linnaeus 1758,* Fig. 1) but it has also been reported to parasitize *Centroscyllium fabricii* and *Etmopterus princeps, unicolor (Yano and Musick 2000, Rees et al. 2014). Anelasma* was first described in 1763 by Norwegian naturalist J. E. Gunnerus while researching *E. spinax*. On some of the individuals he found the barnacles attached to the sharks at the base of the dorsal fins. This is the most common site of attachment, but they have also been found behind the eyes, behind the gills and at the base of the anal fins in *E. spinax* (Johnstone J, Frost WE, 1927, pers. com. Glenner, H.). Gunnerus made a cursory description and drawings, recognizing the crustacean nature of the parasite, but no name was given to the parasite, and his paper was later forgotten (Broch H., 1919). *Anelasma* was later described by Lovén in 1845, and placed among the cirripedes, as Alepas squalicola. In 1851 Charles Darwin included it in "A Monograph on the Sub-class Cirripedia", where it was given its current name, *Anelasma squalicola,* due to the largely modified peduncle and rudimentary cirri (Fig. 2). The peduncle and its rootlets were merely considered as a means of adhesion by Darwin (Fig. 3), attaching the cirripede to the shark. Kossmann (1874) considered the filaments of the peduncle as feeding organs that provided the organism with most of its food, comparing it to those of rhizocephala. The stomach contents as well as the trophic level, based on stable isotopes of *Anelasma,* has also been investigated. All specimens investigated were completely devoid of food in their intestines and the isotopes indicate that *Anelasma* inhabits a similar trophic level as *E. spinax* (Ommundsen A., 2014). These findings are further supported by the large amount of ovaries and testes in *Anelasma* in comparison to the filter feeding cirripede, *Scapellum strømii,* (Broch H., 1919) who found upwards to 2000 eggs in *Anelasma* compared to only 60 in *S. strømii*. This seems to far exceed the nutrient uptake it would obtain from filter feeding alone, and indicates further that it would require another means of nutrient uptake, i.e. through parasitizing its host (Broch H., 1919).

Within Cirripedia there are many species that have adapted to a parasitic lifestyle, but only a few by means of roots. Among them Rhizocephala with around 250 species, all parasitizing crustaceans, and 2 species of Rhizolepas, parasitizing polychaetes. Both Rhizocephala and

Rhizolepas are highly reduced, showing little resemblance to crustaceans as both both cirri and the mantle are largely reduced or absent (Rees et al. 2014). Barnacles in the superfamily Coronuloidea also use a similar mode of attachment to that of *Anelasma*, attaching to the host surface, or embedded in the skin as in Xenobalanus (Hayashi et al., 2013). The whale barnacles are, however, still in possession of fully functional cirri and obtain their nourishment through filter feeding and are therefore considered epibiotic. The assumption that *Anelasma* was related to the acorn barnacles was considered by Darwin, but due to *Anelasma* possessing features not seen in the acorn barnacles, he placed it in its own genus. It has later been shown that *Anelasma* is most closely related to pedunculated filter feeding barnacles in the Indo-pacific *Capitulum mitella* (Rees et al. 2014*)*. *Anelasma* is the only cirripede known to parasitize a vertebrate. Due to the distance to and the dissimilarity between the habitat of its closest relative, it is believed to be the only extant member of a larger clade of filter feeding cirripedes that only recently evolved parasitic traits (Rees et al. 2014).

Anatomical description of *Anelasma*

Anelasma is generally divided into two parts for morphological studies. The “capitular region” and the “penduncular region” (Johnstone J, Frost WE, 1927). When dissected out the size of *Anelasma* ranges from 0.4-3 cm and individuals less than 1 cm in total length have generally been found to be immature. The mantle generally makes up for a little more than half of the parasites total length. The “capitular region” consists of the part that is visible while attached to the host, the part of the body with the biramous appendages, the probosciform mouth, the penis, in some cases up to 3, (Ommundsen A., 2014), two egg sacks and the mantle (Fig. 3.). The mantle is soft with a dark purple-brown color, both on the inside and outside. It is completely devoid of calcareous shell plates and contain a large portion of the cement glands (Fig 4.), believed to produce vitelline for the eggs (Johnstone J, Frost WE, 1927). The remainder of the structures inside the mantle have the same coloration apart from the two white egg sacks, this is believed to be due to the relative openness of the mantle (Darwin, 1851). The mantle is characterized by Darwin as unusually flexible for a cirripede, owing to its thin outer membrane, while the inner membrane is relatively thick for a cirripede. The mantle is thickest towards the waist (Fig. 3.), and tapers towards the edges of the mantle. The mantle contains large muscle bundles believed to be adductor muscles, a system of lacunar spaces, cementary glands and connective tissues and diffuse muscle bundles (Johnstone J, Frost WE, 1927). In living specimen the mantle has been seen to completely

enclose the exposed “capitular region”. The parasite is embedded in the tissue of the host with the “peduncular region” towards the anterior, while the “capitular region” is towards the posterior in relation to the host.

The peduncle is bulbous and cause a swelling that can be seen in the dermis of the host. The diameter of the peduncle is larger than the diameter of the waist of the parasite and the constriction of the surrounding host tissue alone is enough to keep the parasite in place. To remove the peduncle from the host it is necessary to cut through the hosts’ skin and underling tissue. The peduncle can then be separated from the surrounding tissue, this however breaks off the root filaments penetrating the surrounding tissue (Johnstone J, Frost WE, 1927). In mature specimen the peduncle mainly contains ovarian follicles and ovarian ducts while most of the space in the thorax is taken up by the testis (Fig. 4). The ovaries are connected to the rootlets by the large lacunar vessel running axially through the peduncle and branching into smaller vessels running into the roots.

The roots cover the peduncle uniformly, growing out from the integument of the peduncle and penetrating the tissue of the host. Each root normally branches into several offshoots and can be up to 1 cm long. The diameter of the roots is about 0.1 mm and terminate in a rounded and sometimes enlarged tip (Darwin, 1851). Looking at lengthwise section of the rootlets it can be seen that the layering of the rootlets is the same as in the peduncle itself. The function of the roots is likely the acquisition of from the host. The mechanism for how the nutrients are absorbed and transported into the main body of *Anelasma* is unknown, but it has been proposed that the lacunar vessels combined with peristalsis may serve this purpose (Johnstone J, Frost WE, 1927).

The cephalothorax and abdomen are found between the mantle lobes. On the anterior end the probosciform mouth is found followed by six pairs of biramous appendages, and on the posterior end one can find the anus and the probosciform penis. *Anelasma* mouth parts are rather small, and reduced when compared to other cirripedes (Ommundsen A., 2014). The thoracic appendages are similarly reduced, no longer possessing setae which would normally be used in filter feeding. They show abnormal shapes compared to the biramous cirri of other filter feeding cirripedes, with shorter unsegmented cirri, some of which are uniramous, triramous and tetraramous. This indicates that the feeding apparatus in *Anelasma* is no longer under a positive selection pressure due to it no longer being used for feeding (Ommundsen A., 2014).

Aim of the study

The main goal of this master's thesis was to study the functional morphology of *Anelasma squalicola*, building on the work of Johnstone and Frost, using modern methodologies. Methods including micro-CT scanning, 3d-reconstruction, SEM and histology.

Figure 1. Two of the *E. spinax* caught in Sognefjorden that were parasitized by *Anelasma*. The red circle marks the site of infection.

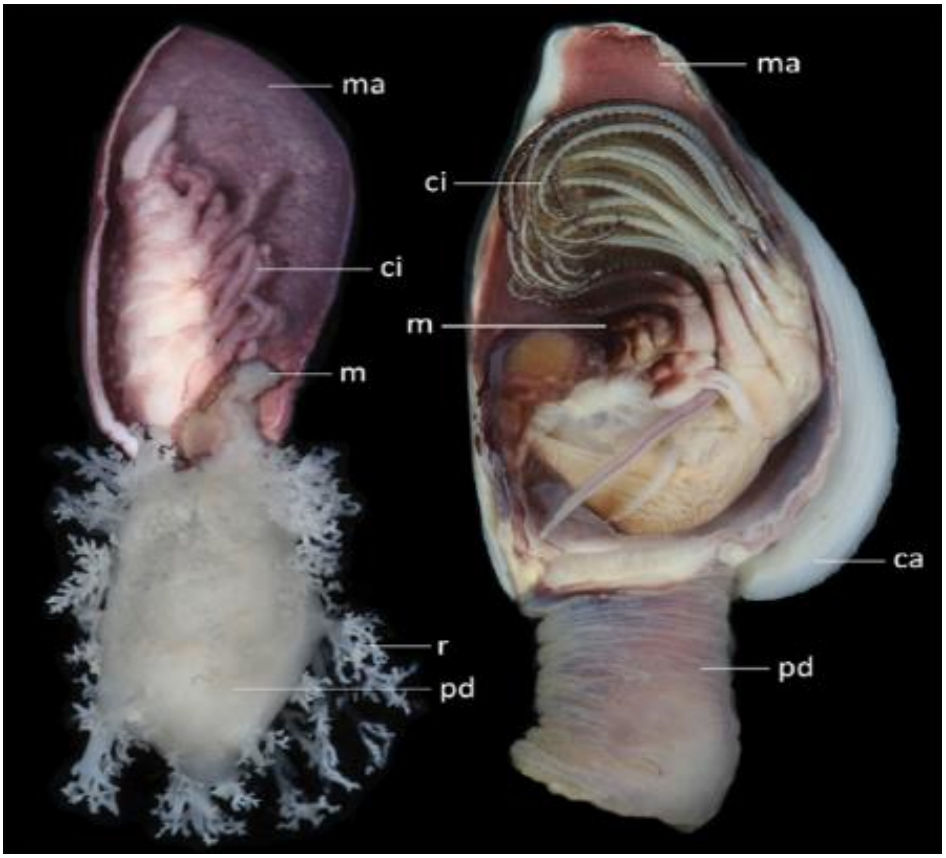

Figure 2: Anatomical comparison of *Anelasma* (left) and *Lepas sp.*, (right). Both with the mantle, and the shell plate in *Lepas sp.*, removed on the side facing the viewer. Ma = mantle, ci = cirri, m = mouth, ca = carina, pd = peduncle, r = rootlets. Picture taken from Rees et al, 2014. Current Biology.

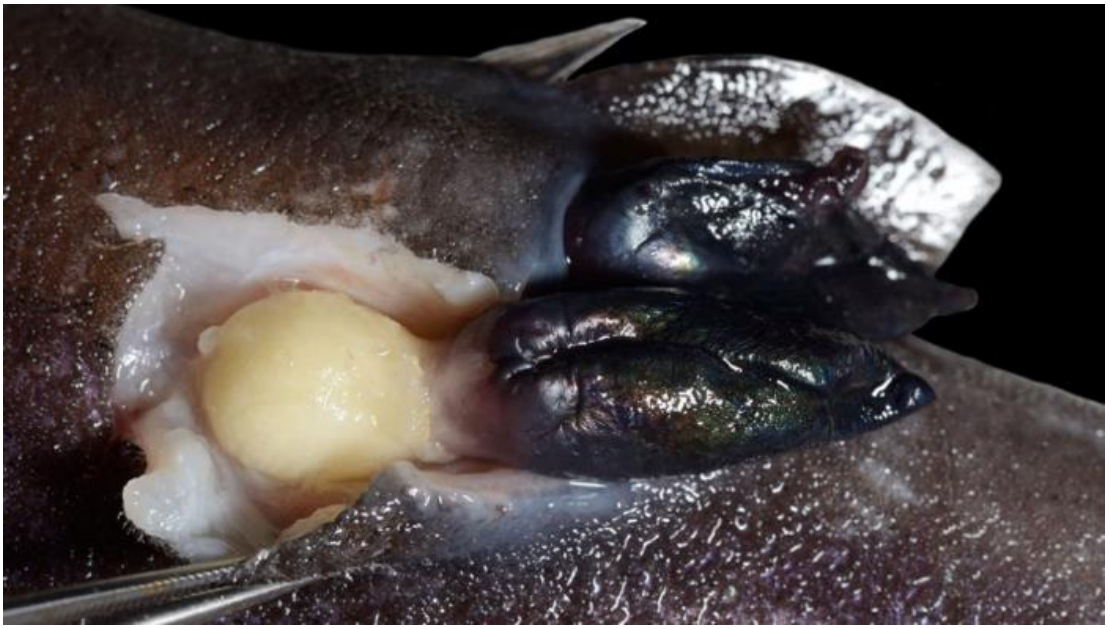

Figure 3: A partially exposed *Anelasma* on the back of an *E. spinax*, revealing its peduncle. Around the waist the skin of the host is visibly paler then the skin away from the parasite.

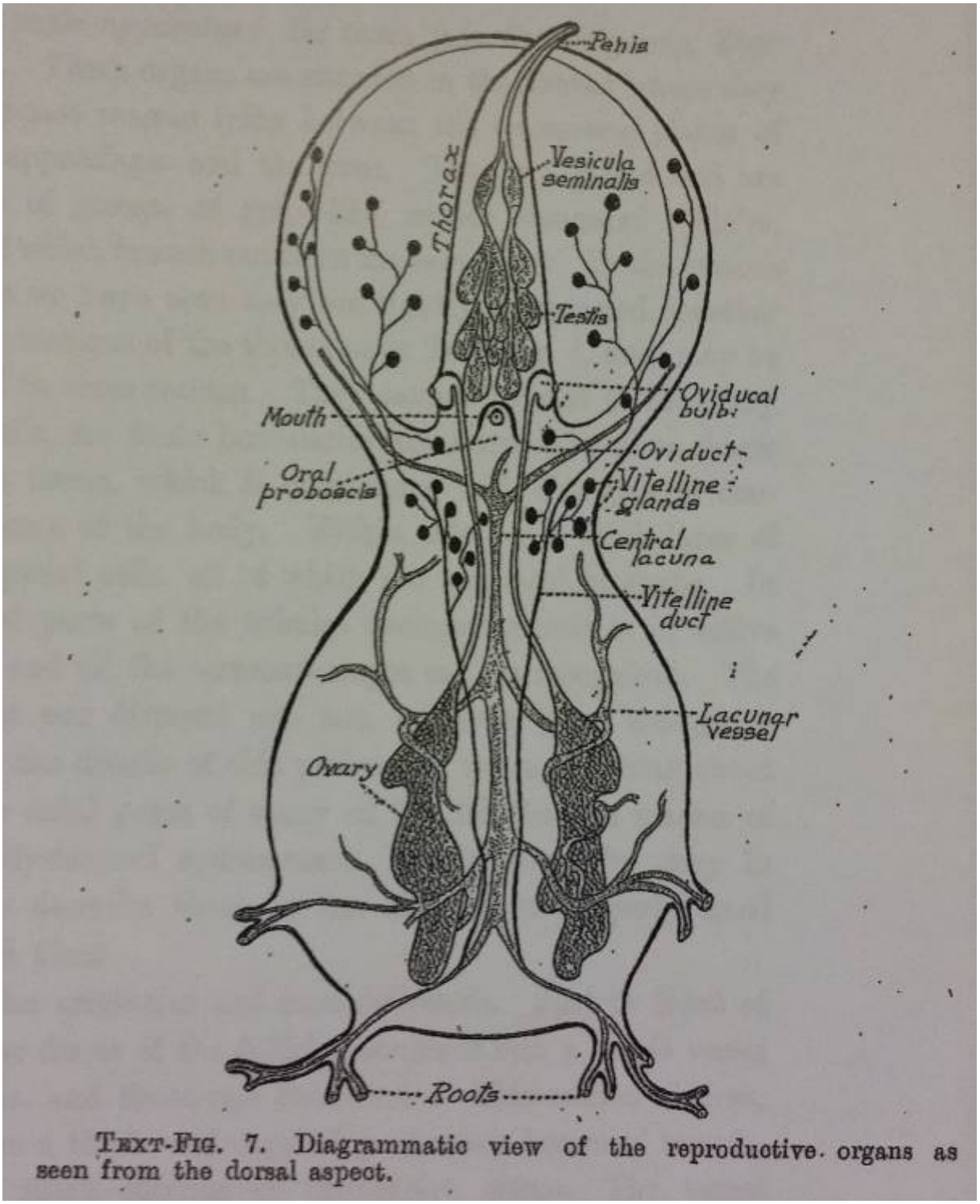

TEXT-FIG. 7. Diagrammatic view of the reproductive organs as seen from the dorsal aspect.

Figure 4: Drawing of the reproductive system, cement glands (vitelline glands) and their ducts and the "lacunar vessels" of *Anelasma*. Picture taken from Johnstone and Frost, 1927.

Materials and methods

Sampling and sampling site

Sampling of *E. spinax* and *Anelasma* was carried out in Lustrafjorden, a small tributary to Sognefjorden, north of Bergen, Norway. Sampling took place on board RV Hans Brattstrøm between the 18th and 22nd of May, 2015, using a winged shrimp-trawl, produced for UIB by Nett & Tau Bergen AS. Two trawls were completed (See table 2 for coordinates). Of the 256 *E. spinax* caught 7 were found to be parasitized by 1-3 individuals of *Anelasma.* All specimen of *E. spinax* were measured, weighed, sexed, checked for parasites and photographed (Canon EOS w/ MP-E 65mm lens) prior to freezing. For the individuals of *E. spinax* parasitized by *Anelasma* extra pictures were taken, and the site of attachment was recorded. They were later dissected out together with a large piece of host tissue and placed in specific fixatives, depending on what use they were intended for. Individuals that were to be used for morphological studies were fixed in Bouin's fluid (Sigma Life Science) to preserve gross morphological features. Four specimen from this trip were used, along with two specimen caught on earlier trips, the exact date and location for when and where these were caught was not logged (Table 1.). The specimen have been designated as P1, P7, P8 and P9 following our sampling protocol, while the remaining two have been designated as "Adult" and "Juvenile" and will be referred to as such in the text for clarification when writing about specific specimen.

Table 1. Detailed list of individual specimens used, catch location, date, size, fixative and use. All specimen measurements are given as distance from the site of implementation to the furthest point of the mantle.

Barnacle ID	Location	Date	Size (mm)	Fixative	Use
P1	Lustrafjorden	18.-22. May 2015	7	Bouin's fluid	µCT, 3D-reconstruction, SEM
P7	Lustrafjorden	″	4	″	″
P8	Lustrafjorden	″	6	″	Histology
P9	Lustrafjorden	″	6	″	″
Adult	NA	NA	8	Alcohol	SEM
Juvenile	NA	NA	5	Glutaraldehyde	µCT, 3D-reconstruction,

Table 2. List of trawl stations, coordinates are given as degrees, minutes and seconds.

Station	Start coordinates	End coordinates
HB2015-05-1A	61°26'03.8"N 7°28'26.1"E	61°24'24.1"N 7°27'21.1"E
HB2015-05-1B	61°26'03.8"N 7°28'26.1"E	61°24'01.7"N 7°26'24.4"E

µCT and 3D-reconstruction

Specimens

For 3D-reconstruction 3 individuals of *Anelasma* were investigated (P1, P7 and juvenile). The smallest individual was a recently settled juvenile protruding 5 mm from the shark's skin, caught on a previous cruise and stored in glutaraldehyde, while the two others were sub-adults protruding 4 and 7 mm from the site of attachment, caught in Lustrafjorden in May, 2015.

Specimen preparation

All specimen were washed in distilled water for at least 12 hours after storage in 25% glutaraldehyde (Sigma-Aldrich) and bouins fluid, with water being changed at regular intervals. After rinsing out excess glutaraldehyde/bouins, the specimens were stained for 26-30 hours using Lugol's Solution. After staining all specimens were treated twice with 10% DMSO in distilled water for twenty minutes, then freeze-dried for a minimum of 12 hours using a UniCryo MC2L (UniEquip, Munich, Germany).

Specimen preparation and scanning

Wet specimens were placed in a piece of a plastic straw or a pipette and fixed using damp cotton to avoid movement during the scan, the container was then sealed using plastelina to keep the specimen from drying out during the scanning period. Dried specimens were mounted on glass rods using a hot glue gun with a small plastic spacer between the specimen and the glass rod. The spacer was used to avoid excess refraction of the laser, from passing through the glass rod, and addition of noise to the scans.

All scans were performed using a nanotom (Phoenix|x-ray; GE Measurement & Control, Wunstorf, Germany) high resolution µCT in high resoultion mode and a molybdenum target. The data was recorded using datos|x acquisition. Several shorter scans were performed between each step after washing in purified water to pinpoint the optimal settings for

achieving a good contrast between the tissue of the *Anelasma* and the surrounding *E. spinax* tissue This was done due to a lack in knowledge of how to best treat *Anelasma* to obtain high contrast scans. All final scans were done after washing, staining with Lugol's solution and freeze drying, using a molybdenum target, voxelsize: ca. 3-6 µm, voltage: 25-30W, current: 420-450mA, mode: 0, detector timing: 1000ms, number of projections: 1440 and a rotation of 360 degrees. A volume file was generate using datos|x reconstruction and an 8-bit image stack was created using VGStudio Max (Volume Graphics, Heidelberg, Germany).

3D-Reconsruction and imaging

The data exported from VGStudio was loaded with the imaging software Imaris 7.6.5 (Bitplane, Zuric, Switzerland). A scene was created in the "Surpass mode" and surfaces were created manually using the "Surface" tool. The contours of each organ was outlined using vertices on every 1-5 virtual sections depending on the size and intricacy of the organ. An automatic surface was then created over the vertices. The channel containing the entire dataset was duplicated and the volume outside the surface was masked to get a channel containing only the structure of interest. After isolating each structure, the "surface" tool was used again to make an automatic surface rendering. Images of the structures were taken using the "snapshot" mode in Imaris. Pictures of the dried specimens were taken using a lupe (Leica MZ16 A, Leica Microsystems AG, Wetzlar, Germany) connected to a camera (Nikon Digital Sight DS-SM, Nikon Corporation, Tokyo, Japan) and the the software ACT-2U, version 1.31.76.212 (Nikon Corporation, Tokyo, Japan). Upon completion the 3D-models were exported from Imaris and implemented into PDF files for easy access (see appendix for detailed steps.)

Scanning electron microscopy

For SEM 3 individuals were used. (P1, P7 and adult) The mantles were dissected away to reveal the main body and cirri. The mantle in P1 & P7 were not kept due to the samples being previously dried, and the mantle crumbling during dissection. For adult the mantle was dissected into two pieces, to study the internal and external surfaces of the mantle. All samples were then critical point dried before they were then mounted on a small pedestal using carbon tape and placed in a sputter coater (Polaron SC502 Sputter Coater, Quorum Technologies, East Sussex, England). After the chamber was evacuated and filled with argon,

the samples were coated using gold/palladium for 45 seconds. After coating the samples were moved to a scanning electron microscope (ZEISS Supra 55VP scanning electron microscope, Carl Zeiss AG, Oberkochen, Germany) for imaging.

Histology

For histology 2 specimens (P8/9) fixed in Bouin's fluid were used to investigate the internal and external morphology of the parasite and the effect of the surrounding tissue of *E. spinax*. Both specimens were measured to 6 mm from the site of attachment to the furthest part of the mantle. The samples were decalcified using buffered formic acid for approximately 12 hours to dissolve the cartilage and placoid scales in the shark tissue. They were then stored in 70% ethanol prior to dehydration and fixation. To dehydrate the samples, they were placed in 96% ethanol for at least 2x 15 minutes depending on size. After dehydrated they were placed in a 1:1 solution of 96% ethanol and basic Technovit for approximately 2 hours, then Technovit over night while under light stirring. The samples were placed in a casting tray and covered with a 1:15 mix of infiltration solution and hardener, then left to dry for 2 days.

After the blocks had hardened, 2 µm thick sections were made using a microtome (Leica RM2165). The sections were placed three and three on frosted microscope slides and dried before staining with 1% toluidine blue (Philpott, 1966). Excess staining was rinsed out using running water. After the staining had dried, cover slips were mounted on top of the sections, using DPX (Merck KGaA, Darmstadt, Germany).

The slides where then examined using a microscope (Leica DM 2000 LED) with four lenses (5x, 10x, 40x and a 100x immersion lens) and an attached camera (Leica DFC 450). The areas of interest were captured in the imaging software (Leica Application Suite, V. 4.5.0 [build :418]).

Results

General body form

Looking at specimens of *Anelasma,* ranging from recently settled to mature individuals, clear differences can be seen in the implementation and the morphology of the peduncle. In the largest individual (Fig. 5, 3D-model of P1) it closely resembles what has been described previously (Johnstone and Frost, 1927). Here the parasite is clearly divided into the peduncular and capitular region, separated by the waist. The peduncle has obtained a bulbous form, and there is a uniform cover of roots penetrating into the host tissue. For an in depth explanation of how to access and get the most out of the 3D-models see the appendix under "Directions for viewing 3D-models "

In the recently settled individual (Fig. 6, 3D-model of Small) the parasite only has a few rather large roots penetrating into the tissue of the host and a long stalk raising the mantle from the site of attachment and there are no clear signs of a peduncle forming.

In the second smallest *Anelasma* (Fig. 7, 3D-model of P7) the peduncle has developed and there is a narrowing at the waist, but the mantle is still slightly raised above the site of attachment. The roots are also more developed and make finer branches then in the recently settled individual, but only appear in patches on the peduncle.

Across the different stages the capitular region appears to resemble each other closely, despite it being raised and slightly elongated in the younger individuals.

External characteristics

The mantle

The outside of the mantle lacks any sort of calcareous plates, spines or granules. It appears completely smooth (Adult, Fig. 8). The inside of the mantle of Adult is covered by indents made by the ovigerous lamella (Adult, Fig. 9). At higher magnification retinacula (Mean=12.6 µm) can be seen forming a dense cover of the inside of the mantle (Fig. 10). The cuticle covering the mantle is thicker on the outside of the mantle than in the mantle cavity (Fig. 11).

The cirri

The cirri of *Anelasma* appear to be contorted and malformed compared to what one would expect to see in a filter feeding cirripede (Fig. 2). In the individuals studied they appear to be either biramous or uniramous (Fig .12 & 13). Histological sections of the cirri show clear muscle bundles (Fig. 14), and in live specimen both the cirri and thorax have been seen moving actively (H. Glenner 2016, pers. Comm.). SEM images of the cirri show an even cover of fan shaped setules (Fig. 15, P1). They appear in groups of approx. 12 individual setae with a mean length of 2.95 µm. There is also a very limited number of spines on the cirri (Fig. 16, P1). The remainder of the thorax appear to have no spines or seta at all. When stained with toluene blue the endo- and exo-cuticle of the cirri can be seen as two distinct layers, the exocuticle staining in a much deeper blue then the endocuticle (Fig. 18).

The peduncle

In the largest individual the peduncle is approximately the same length as the visible parts of the parasite, excluding the roots. The roots penetrate quite a bit deeper into the tissue of the host (Fig. 5, 3D-model of P1). The musculature of the peduncle forms three distinct layers, one inner layer running from the top to the bottom, and 2 layers running obliquely (left-right, and right-left) on the outside (Fig. 18 & 19) All the musculature appears to be restricted to the outer layer of the peduncle and no musculature can be seen crossing through the central part of the peduncle in either the micro-CT scans or the histological sections.

The cuticle of the peduncle starts out quite thick near the waist and tapers off with distance away from the capitular region, the division of endo- and exo-cuticle is not clear in the peduncle (Fig. 20). In histological sections of the peduncle the columnar cells supporting the cuticle can be seen clearly, forming a dense layer in direct contact to the cuticle (Fig. 21 & 22, top down and side view respectively). This arrangement seems to hold true for most parts of the parasite.

Cuticle of the roots

The cuticle of the roots is in direct continuation of the cuticle of the peduncle but tapers off even further towards the tips of the roots (Fig. 23), as in the peduncle it is not possible to distinguish between endo- and exo-cuticle in the roots, and it seems as if the exocuticle has been reduced entirely. The cuticle can be traced all the way to the tip of the roots (Fig. 24 & 25), forming a continuous sheath covering the roots. Towards the tips of the roots striped

muscle bundles can be seen crossing the roots from side to side anchoring into the cuticle (Fig. 26).

In some of the roots there are still two separate layers of cuticle (Fig. 27), but there is no difference in the color of these layers, it appears as if the roots are molting. Using an oil immersion lens a dark blue layer covering the inside of the outer layer can be seen (Fig. 28), this appears to be the ecdysial membrane that is left over on the inside of the molted endocuticle.

The reproductive organs

Anelasma is a hermaphrodite and has well developed male and female reproductive organs. The male reproductive system consists of the testis, seminal vesicle, vas deferens and the probosciform penis. The female reproductive system consists of the large ovaries, the oviducts and the oviducal bulbs opening up in the mantle cavity at the base of the first pair of cirri.

The male reproductive system

The testis takes up a large portion of the thorax (Fig. 5, 3D-model of P1). The 3D reconstruction only shows the general location and not the distinct morphological features of the testis due to low contrast between each follicle. The overall shape of the testis appears more like clusters of grapes (Fig. 4), and a cross section of one individual vesicle can be seen in figure 29. The vesicles connect into two separate ducts running towards the penis and merging to form the vas deferens. The probosciform penis is primarily located on the posterior segment of the body. The cuticle of the penis appears highly folded and the musculature in the penis seems to be mostly longitudinal but any details are hard to make out due to the poor fixation of the tissue (Fig. 30).

In the individual used for remodeling the reproductive system a second vas deferens can be seen running into a secondary penis attached to the body segment carrying the 5th pair of cirri (Fig 5. & 12). The secondary penis also appears to be somewhat functional, but it is not as highly folded as the primary penis (Fig. 12), but the meatus can still be seen (Fig. 31).

The female reproductive system

The ovaries take up most of the space of the peduncle, extending to just below the waist (Fig. 5, 3D-model of P1). The ovarian follicles merge into two large ovarian tubes leading up to the ovarian bulbs situated at the base of the first pair of cirri (Fig. 32). The opening of the ovarian bulbs points down towards the bottom of the mantle cavity and is clearly visible in cross sections of the 3d model (Fig. 33). The ovarian follicles branch out from the central ovarian tube and end in bulbs that contain the oogonia and ova, in P8 they appear to be mostly immature, and no large ova can be seen (Fig. 34). In the sections from P9 the different developmental stages of the oocytes are all visible in the peduncle at the same time (Fig. 35). ranging from small oocytes consisting of the cytoplasmic blastoderm and the yolk-appendage (Fig. 36), larger oocytes with a more granular deeper staining yolk appendage (Fig. 37) and large oocytes under the process of atresia (Fig. 38). In histological sections the lipids in the yolk appendage are washed out due to the treatment of the samples, and appear as white circular spots.

The lacunar system

The great central lacunae can be seen originating in the waist and running downwards through the central part of the peduncle (Fig. 5, 3D-model P1). Looking at cross sections of the micro-CT data the great central lacunae is already clearly visible in the juvenile specimen (Fig. 42). In the mature individual smaller lacunae run out from the great central lacunae to the peripheral parts of the peduncle and out into the roots, the walls of the lacunae are made up by a dense layer of connective tissue (Fig. 39). The lacunae appear to be present in all the roots, and can be seen branching when the roots themselves branch out (Fig. 40). In lengthwise sections of the roots the lacunae appear to be continuous, stopping just before the tip of the roots (Fig. 41).

The cement glands

The cement glands extend from the top third of the peduncle and up into the dorsal side of the mantle. Towards the opening and distal parts of the mantle there are no cement glands (Fig. 5, 3D model P1). The largest number of cement glands can be found in the waist, just below the mantle cavity (Fig. 43). The lower extent of the cement glands seems to be limited by the ovarian follicles. Several ducts can be traced form the interior of each cement gland and out

into the surrounding tissue, here they join together with the ducts from other cement glands (Fig. 44). Due incomplete serial sections it was not possible to trace the ducts to the end.

The digestive system

The esophagus runs slightly downwards towards the waist before it opens up into the stomach, the stomach arches backwards and runs dorsally until it terminates at the base of the penis (Fig. 5, 3D model P1). The stomach is highly folded and in most parts it consists of a layer of high columnar cells with large nuclei. The supporting cells below this layer appear to continuous with the remaining tissue of the thorax (Fig. 45).

In parts of the stomach the columnar cells are replaced by smaller cells with a much darker staining surface (Fig. 46). The cells continue into the connective tissue surrounding the intestines and their apparent function is unknown. Peduncular to the stomach the digestive glands can be seen (Fig. 47). Their extent and whether or not they open up into the stomach could not be accounted for due to poor fixation of the tissue in the area and difficulties obtaining serial sections.

Occurrence of *Anelasma* on the host

The *Anelasma* studied were located by the first dorsal and by the pectoral fins. Host 213 had one pair of *Anelasma* by its right pectoral fin (P8 & P9), and one on the left side of the front dorsal fin (P7), while host 37 only had one *Anelasma* by the front dorsal fin (P1, Fig. 1). The two remaining parasites (Juvenile and Adult) had been removed from the host without noting site of attachment.

Host reaction to the parasite

Looking at the site of attachment there is a clear whitening of the host tissue surrounding the waist of the parasite (Fig. 3). There is also a noticeable difference between histological sections of the host epithelium surrounding the peduncle and sections taken farther away. In the tissue directly in contact with the peduncle there is a visible thickening of the epithelium and a reduction of Melanophores (Fig. 48). A rather large blood vessel can also be seen at the ridge surrounding the waist of the parasite. Away from the site if infection the thickness of the

epithelium is more even, and the melanophores are evenly spread and of rather uniform size (Fig. 49).

The changes in the host tissue appear to be very localized around the peduncle and roots. The surrounding myotomes appear healthy given that they are not penetrated by the roots of *Anelasma*. Figure 50. shows three intact myotomes, each separated by a layer of connective tissue, and above these there is a layer affected by the presence of the roots of *Anelasma*.

Close to the peduncle the host tissue is completely riddled by roots (Fig. 51) and there is no apparent structure left in the tissue. The muscle fibers that appear in dense layers away from the parasite only appear in small bundles and appear to mostly be replaced by connective tissue. A high degree of cellular infiltration and granulocytes can also be seen (Fig. 52). Surrounding the roots there is a layer of fibroblast cells, making a barrier between the host and the parasite (Fig. 53).

Looking at musculature away from the peduncle one can clearly see the striation of the musculature. The muscles are organized into large bands of uniform appearance, separated by connective tissue (Fig. 54a). The musculature in proximity of the roots appears necrotic and has a less ordered appearance. The striation of the musculature is fading and there is a high degree of cellular infiltration into the bundles of muscle fibers (Fig. 54b).

In the tissue affected by *Anelasma* there is also a large increase in the number of blood vessels (Fig. 55). For the most part the erythrocytes appear to be healthy and approximately 18 μm across, there are, however, some smaller erythrocytes that appear to be paler in color (Fig. 56) as well as some that appear to be crenated (Fig. 57).

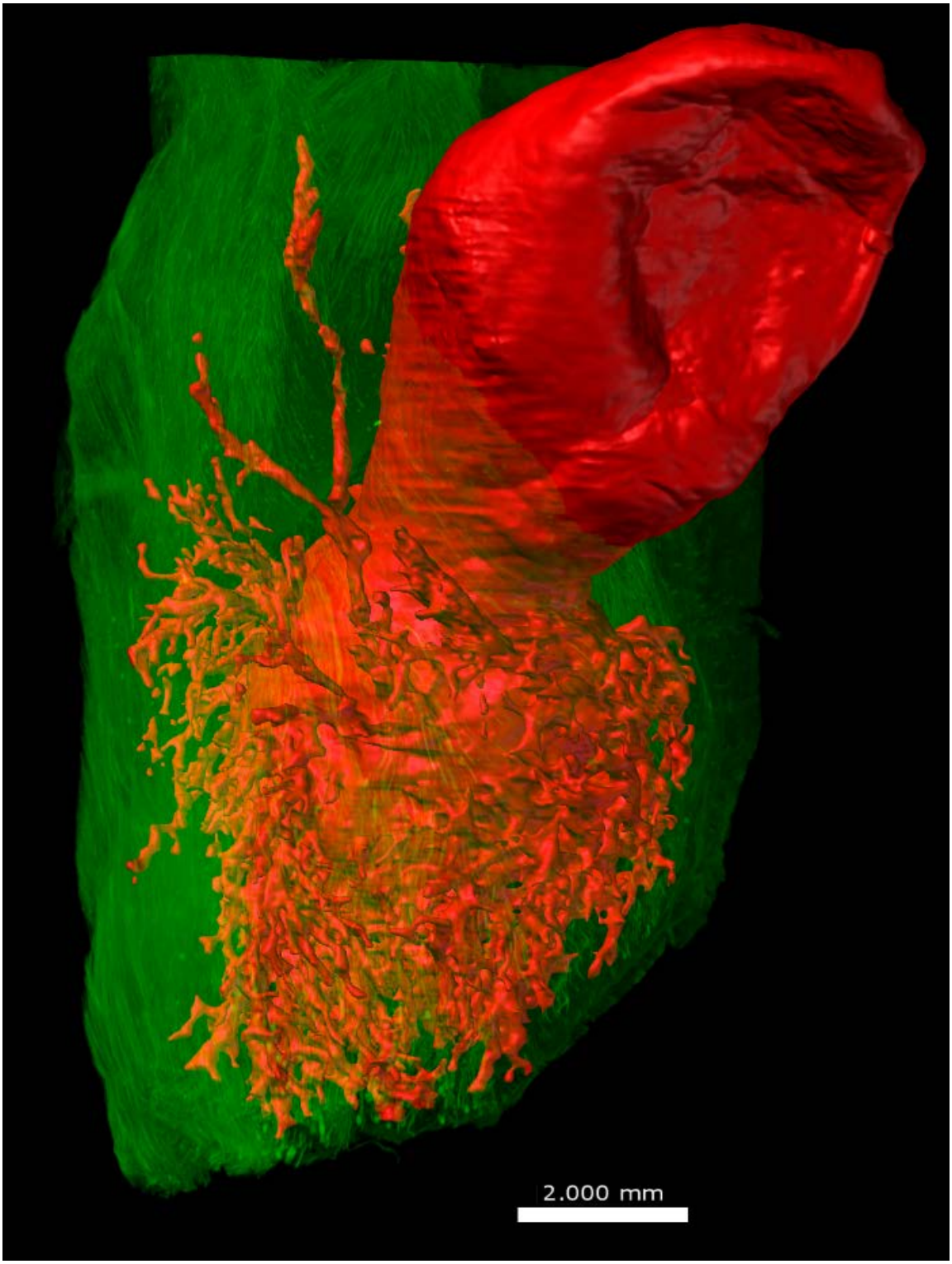

Figure 5: 3D-reconstruction of P1. Parasite (red) embedded in the host tissue (green) is shown. Scale bar: 2 mm.

This figure, as well as Fig. 6 & 7, contain interactive 3D-models. For an in depth explanation of how to access and get the most out of the models see the appendix under “Directions for viewing 3D-models “.

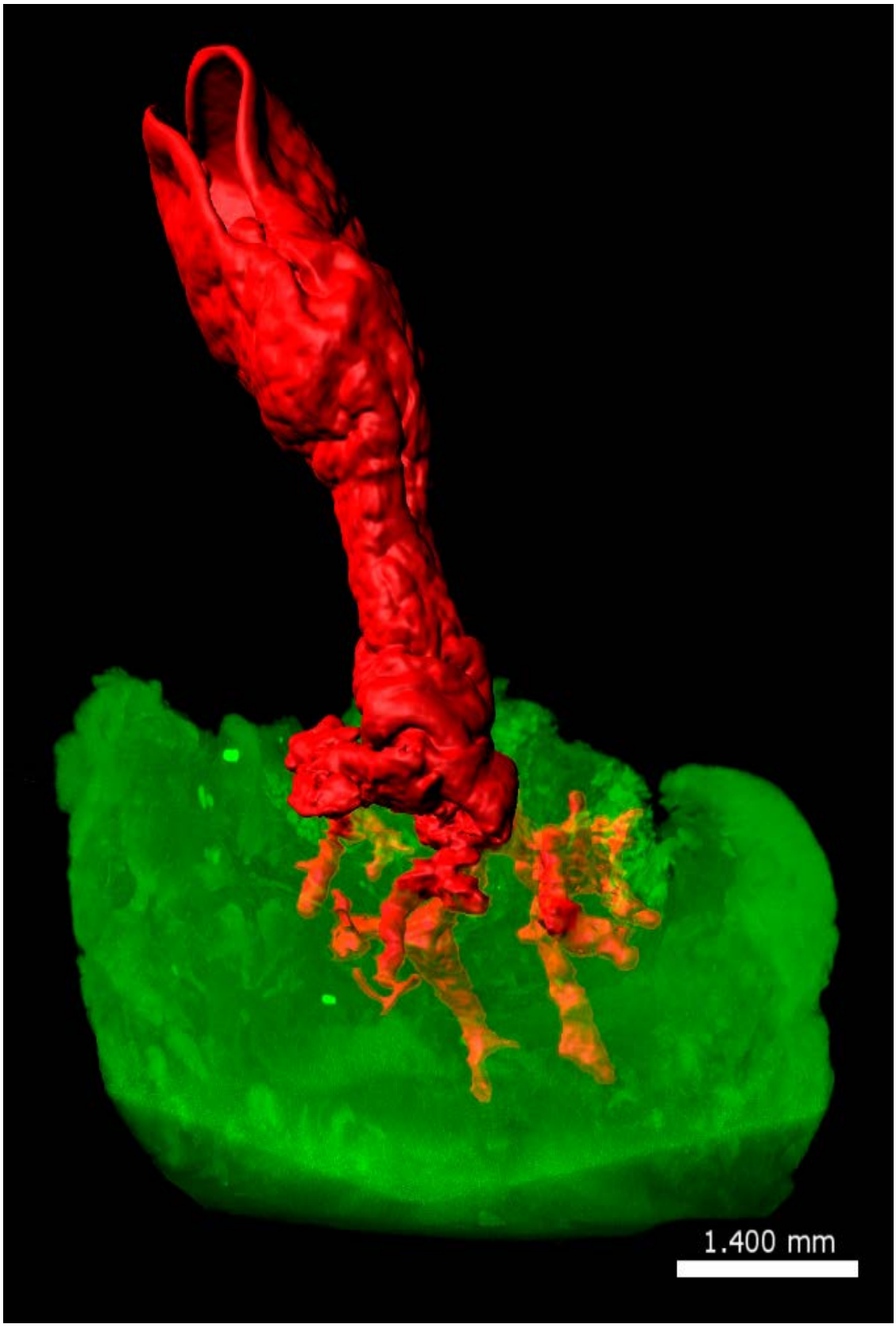

Figure 6: 3D-reconstruction of Juvenile. Parasite (red) embedded in the host tissue (green) is shown. Scale bar: 1.4 mm.

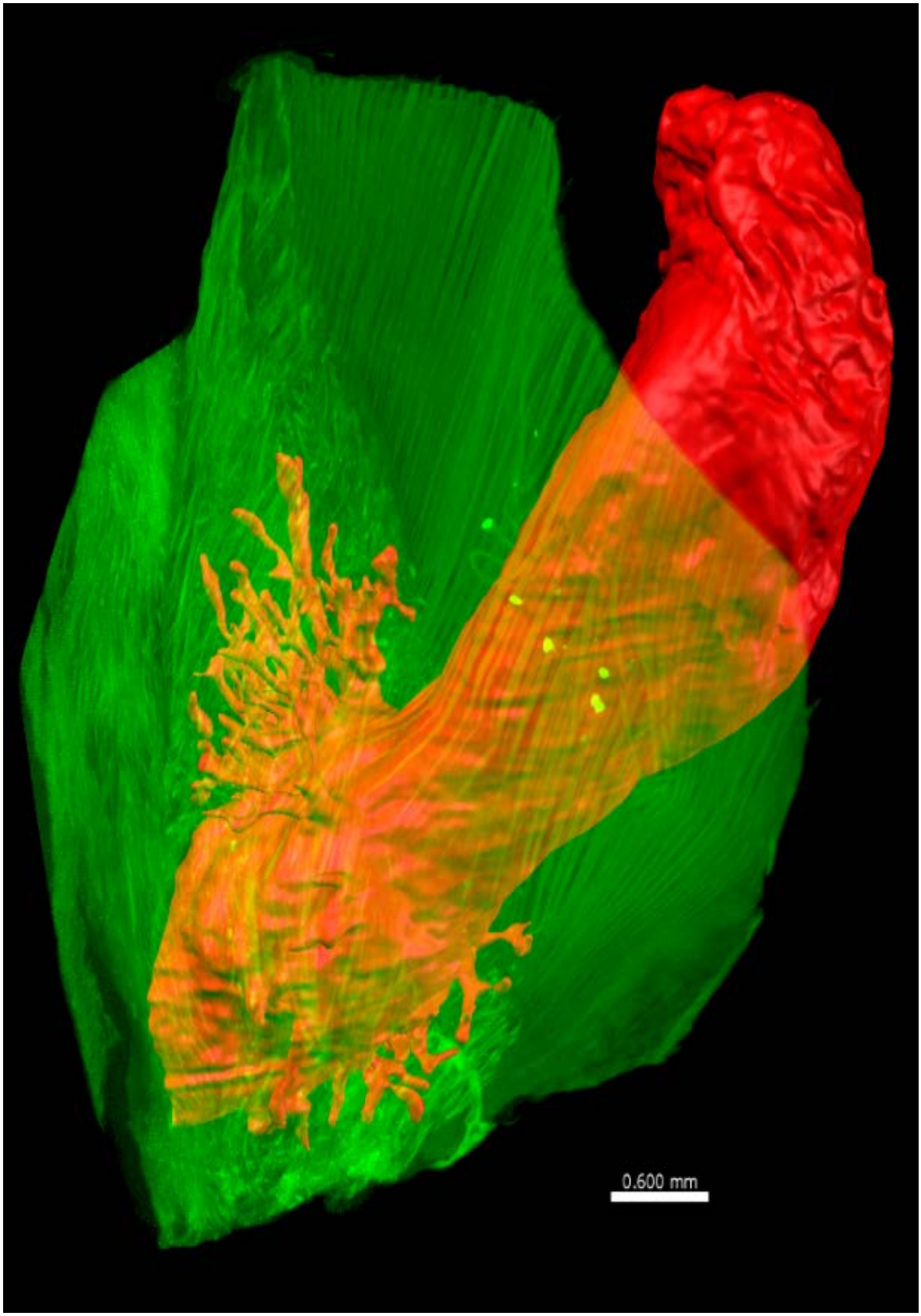

Figure 7: 3D-reconstruction of P7. Parasite (red) embedded in the host tissue (green) is shown. Scale bar 0.6 mm.

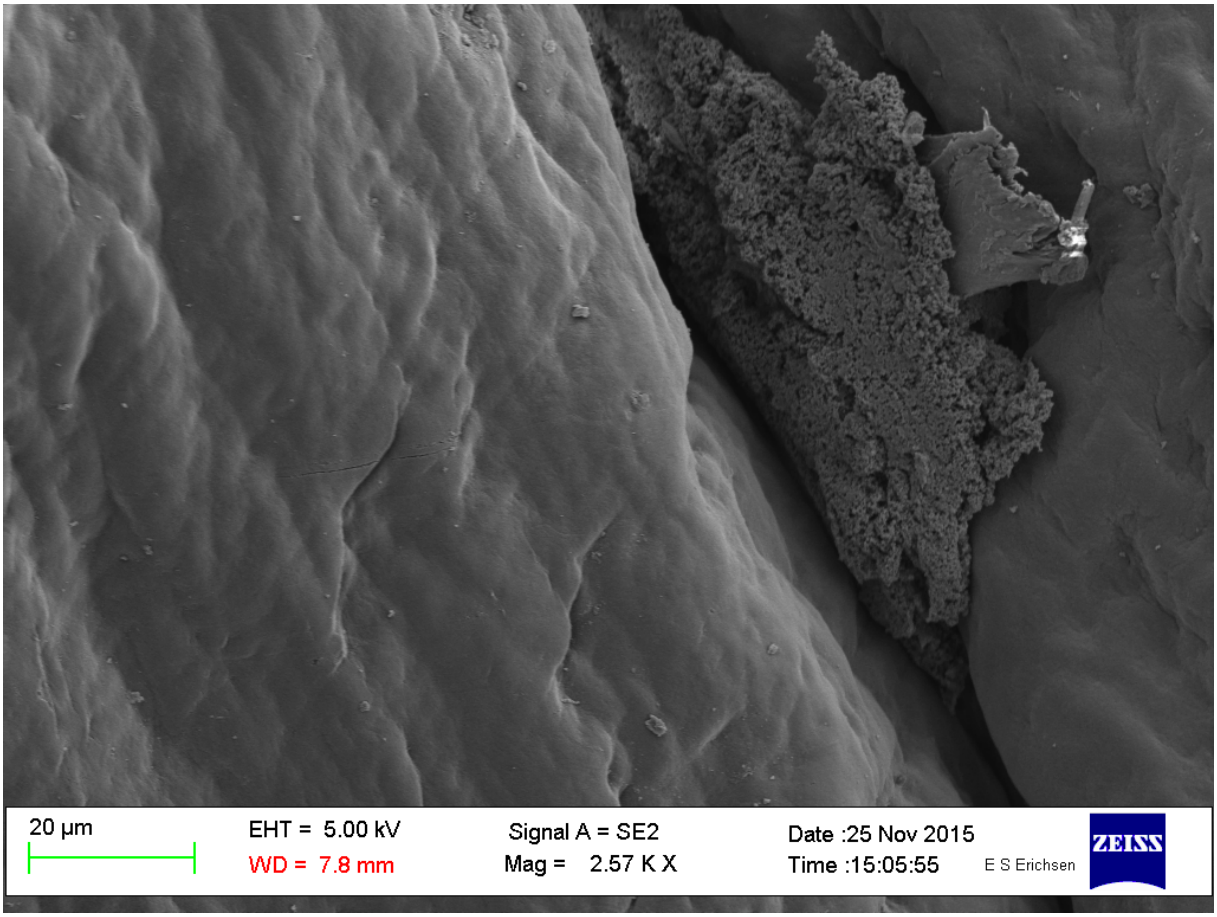

Figure 8: SEM of the outside of the mantle (Adult). The outside of the mantle is shown to be devoid of spines or seta. Scale bar: 20 µm.

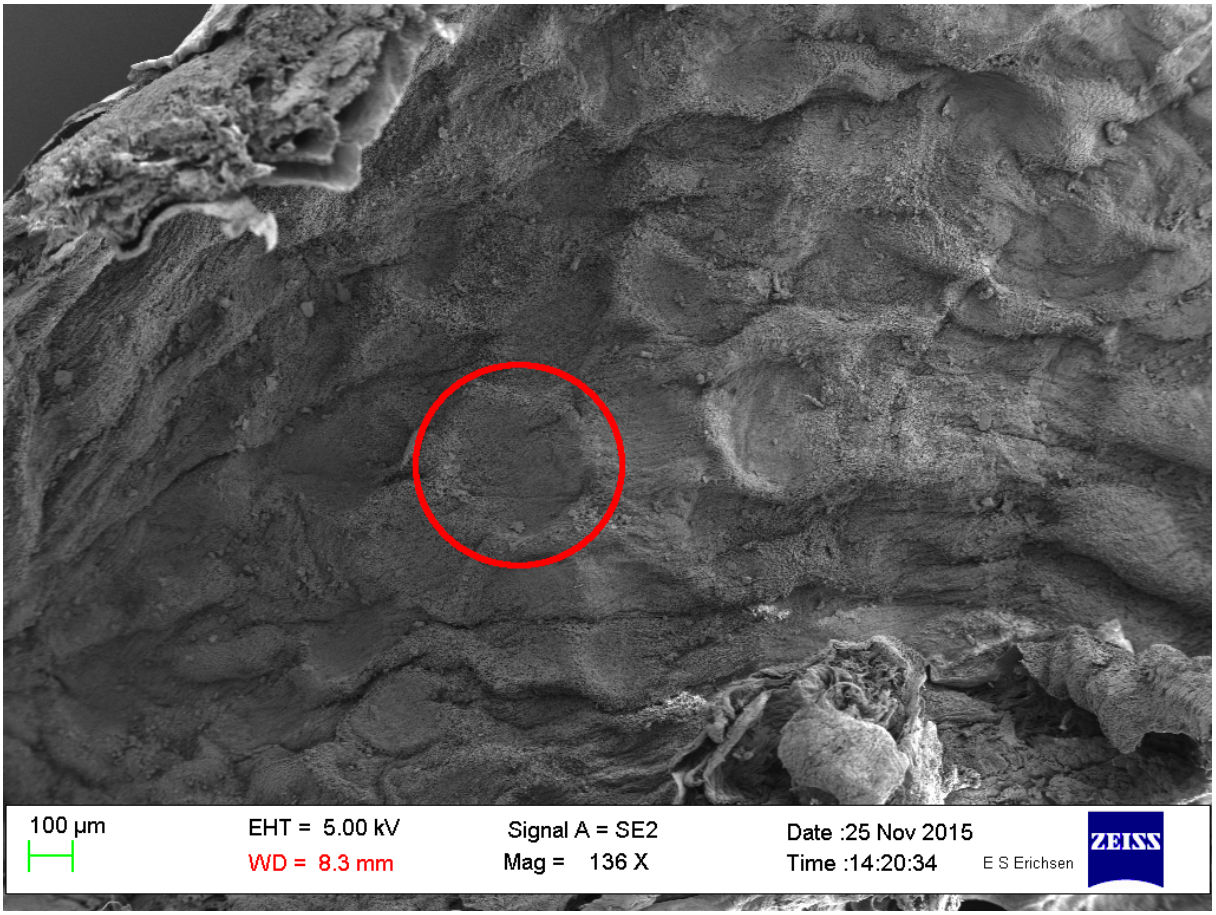

Figure 9: SEM of the inside of the mantle (Adult). Image shows the circular indents made by the ovigerous lamellae. Red circle highlights one individual indent. Scale bar: 100 µm.

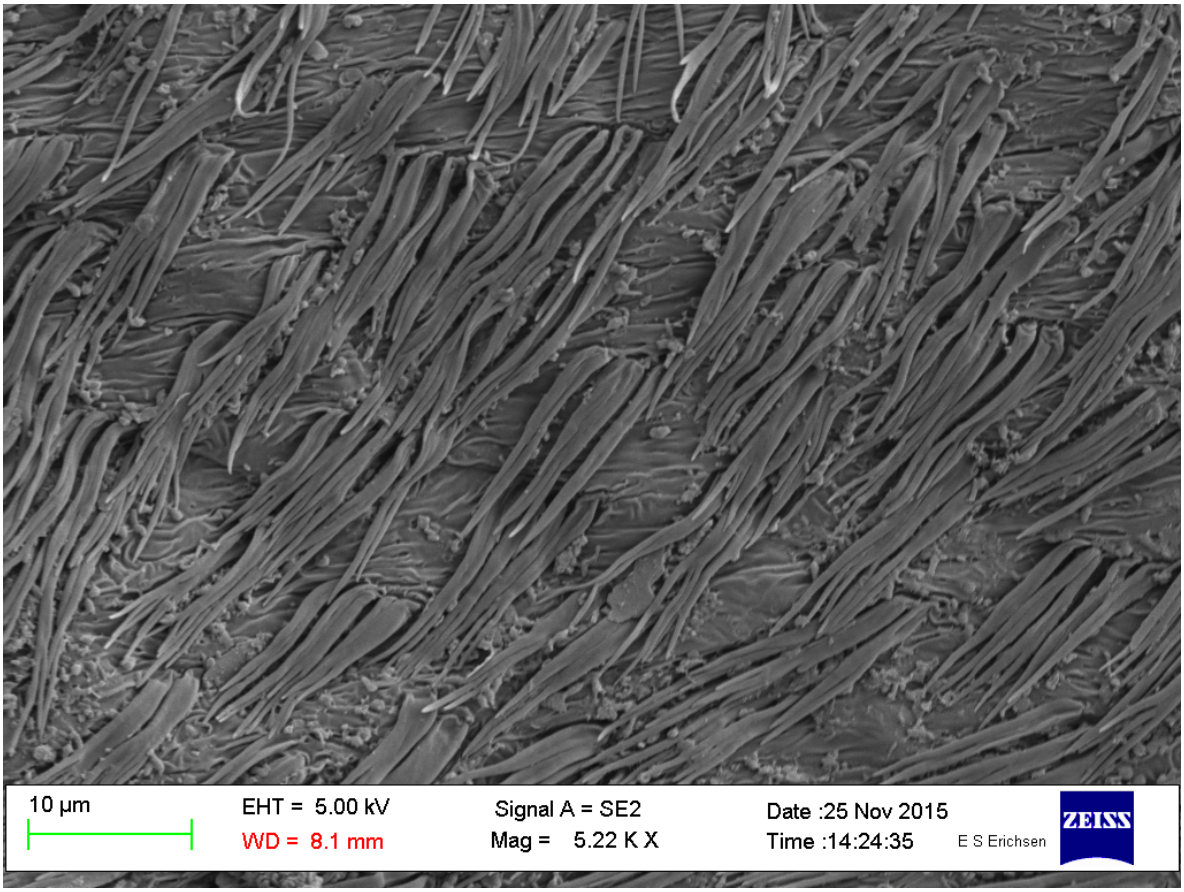

Figure 10: SEM of the ultrastructure on the inside of the mantle. A dense cover of retinacula covers most of the inside. Scale bar: 10 µm.

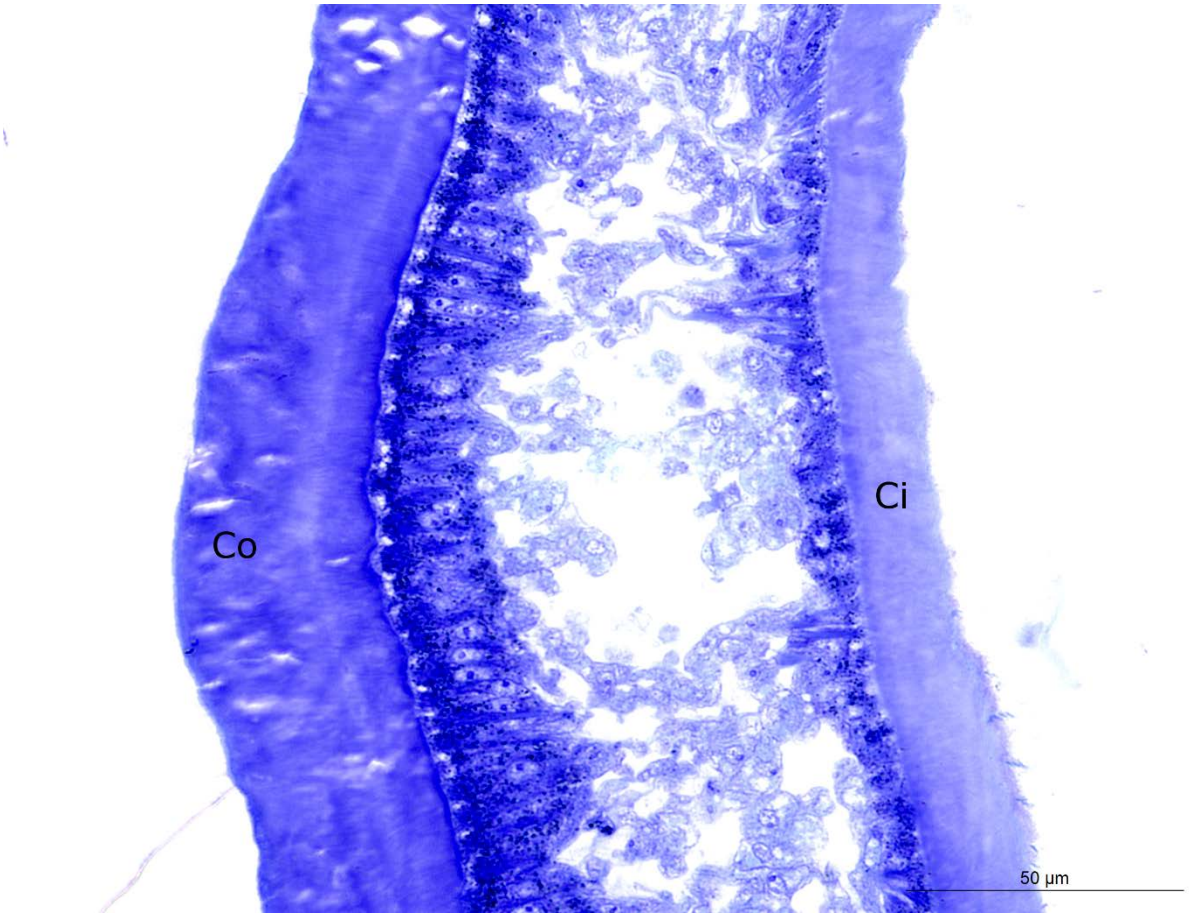

Figure 11: Cross section of the mantle is shown. The difference in thickness between the inside and outside cuticle can be seen with the outside cuticle being notably thicker. Co, cuticle outside; Ci, cuticle inside. Scale bar: 50 µm.

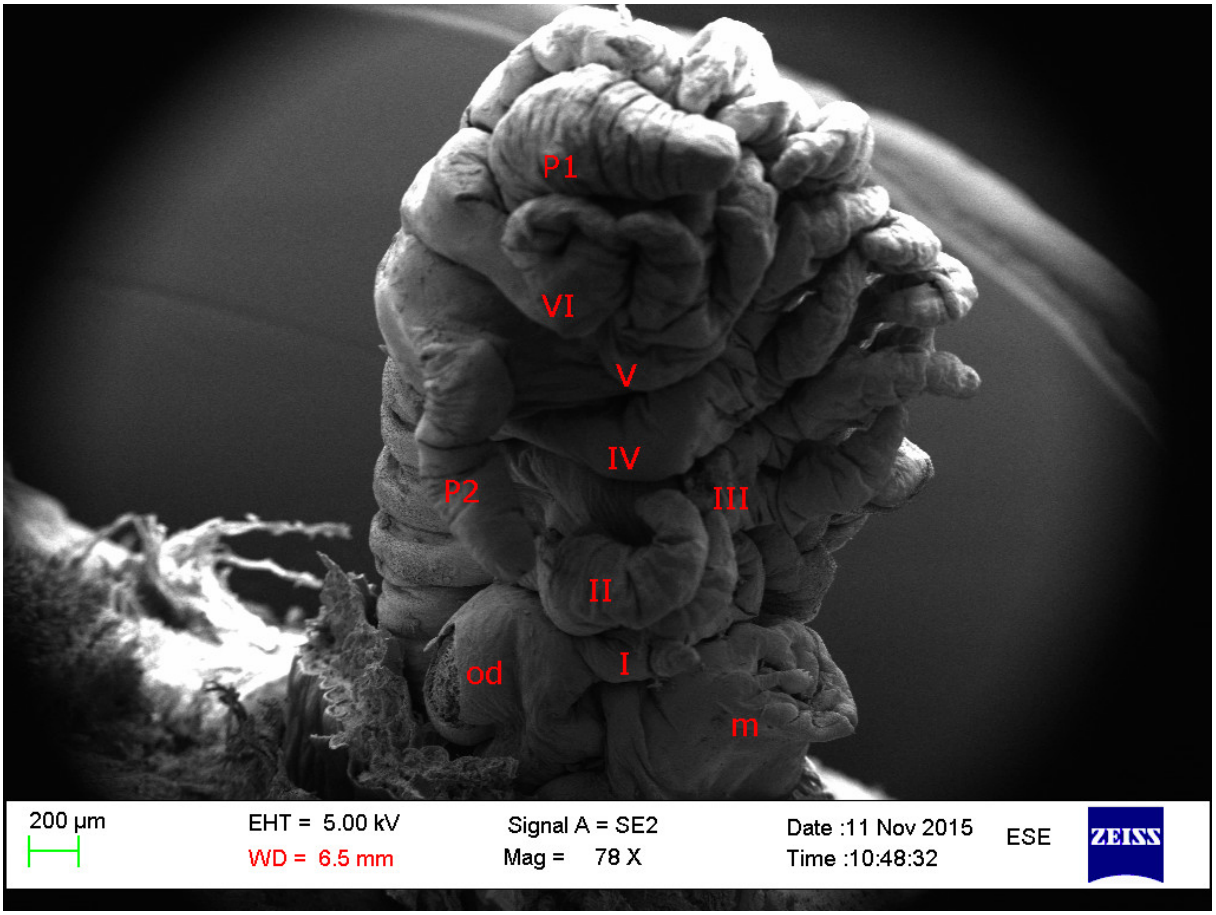

Figure 12: SEM of P1 with the mantle removed, exposing the thorax. The cirri, penis, oviducal bulb and the probosciform mouth can be seen. Cirri are numbered from I-VI; od, oviducal bulb; m, mouth; P1, primary penis; P2, secondary penis. Scale bar: 200 µm.

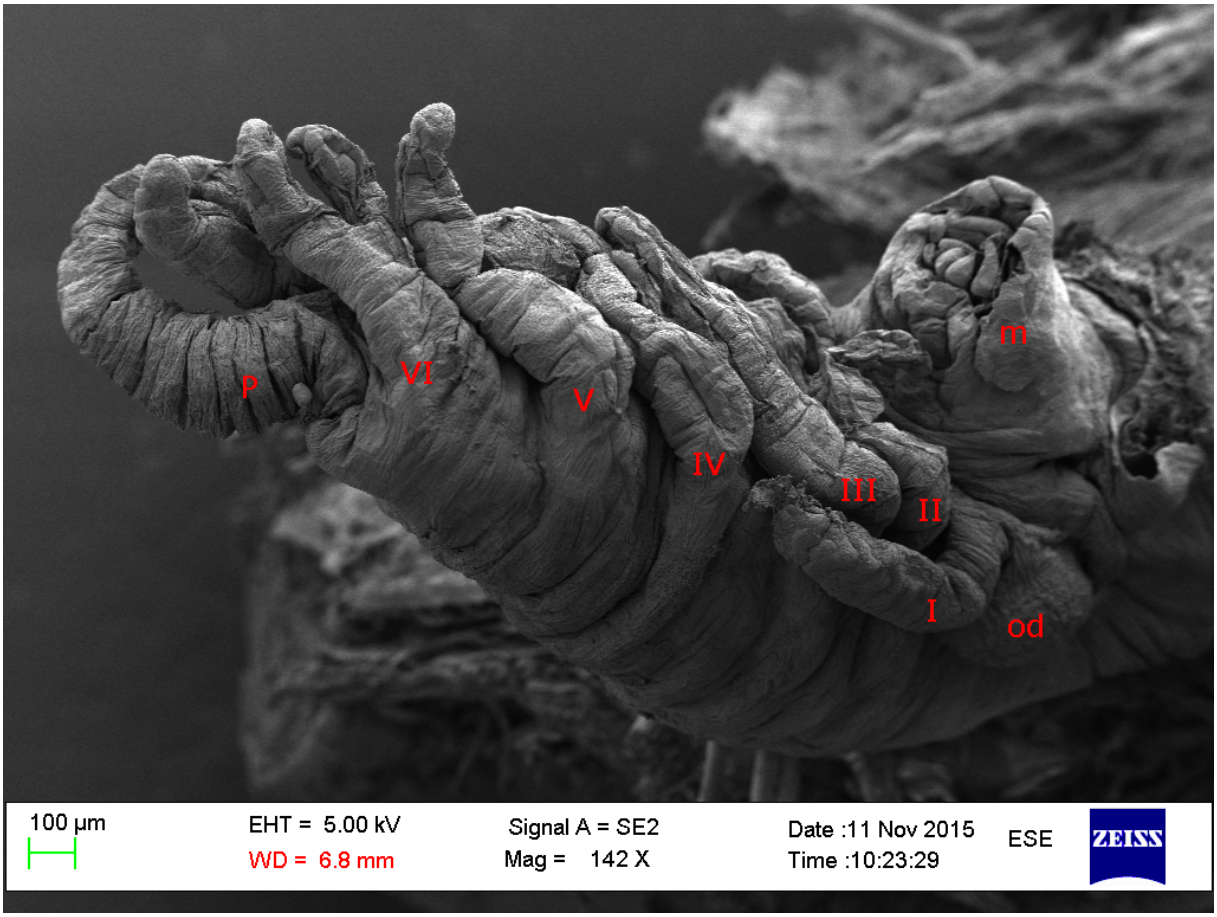

Figure 13: SEM of P7 with the mantle removed, exposing the thorax. The cirri, penis, oviducal bulb and prosbosciform mouth can be seen. Cirri are numbered from I-VI; od, oviducal bulb; m, mouth; P, penis. Scale bar: 100 µm.

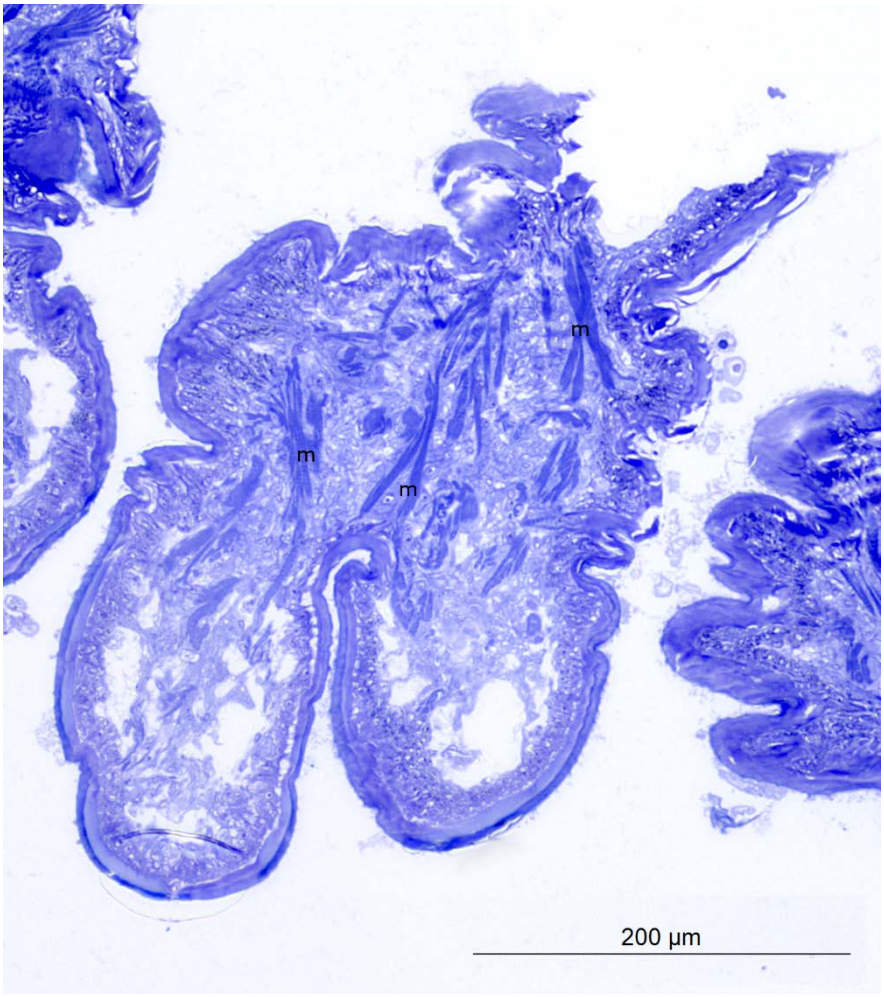

Figure 14: Histological section of cirri showing longitudinal muscle fibers. M, muscle fibers. Scale bar: 200 µm.

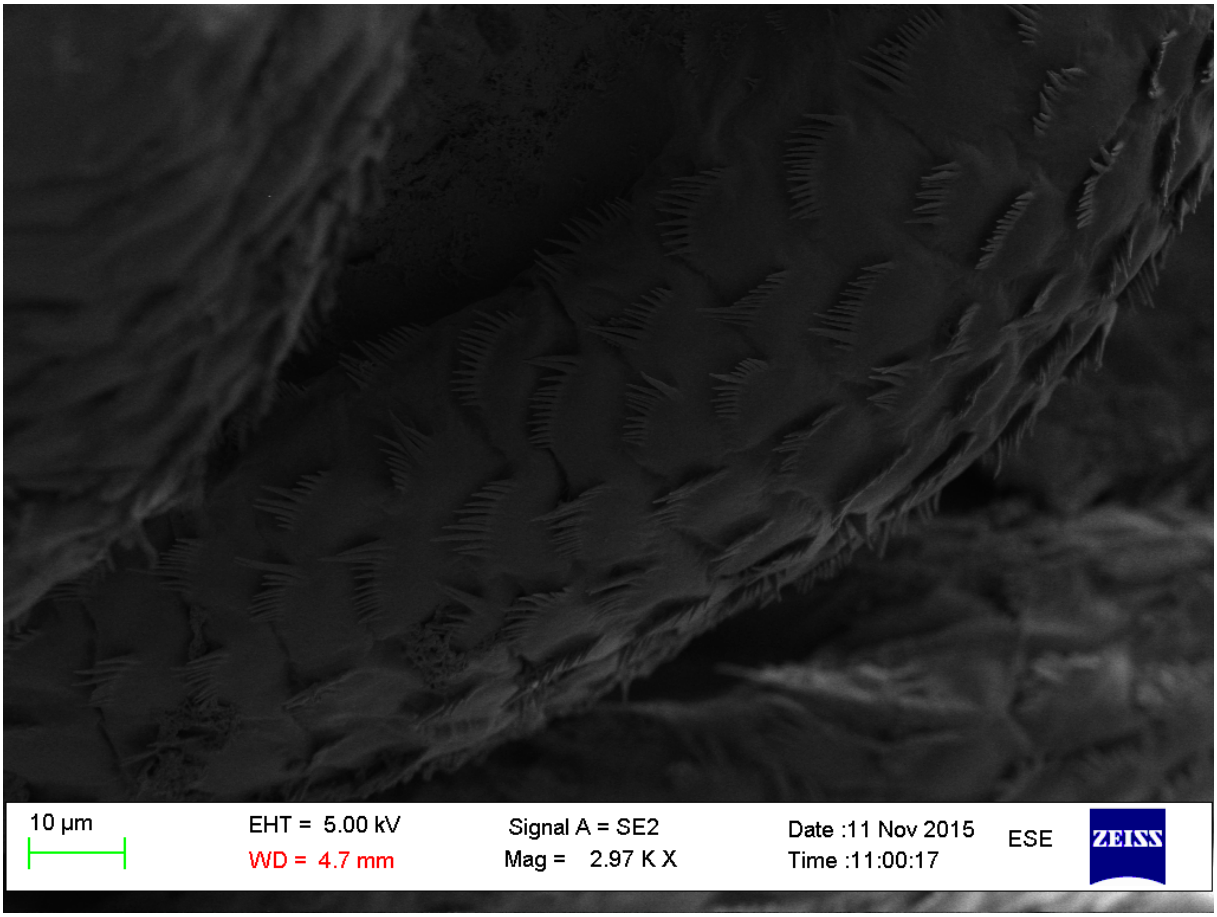

Figure 15: High magnification SEM of cirri (P1) showing an even cover of fan shaped setules. Scale bar: 10 µm.

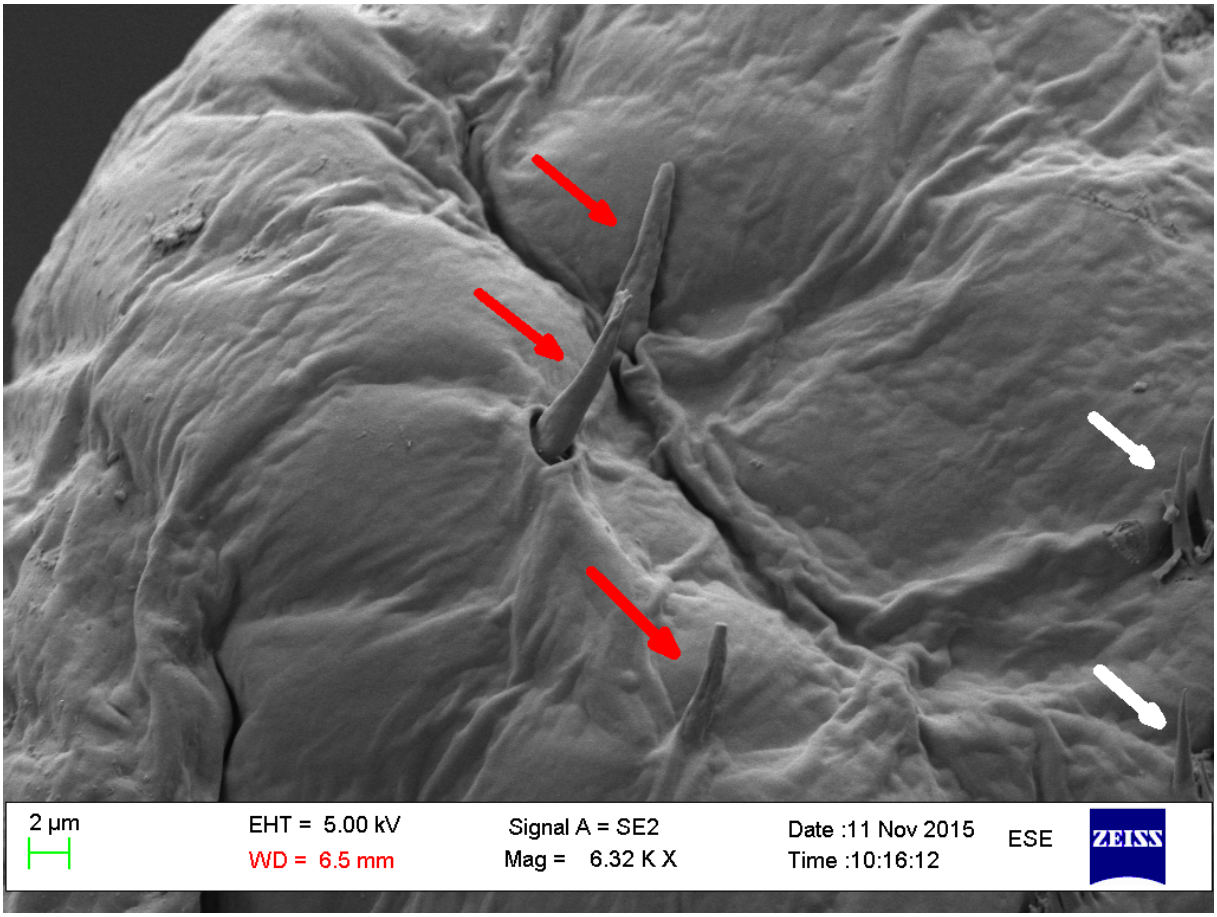

Figure 16: High magnification SEM of cirri (P1). Three single spines are highlighted by red arrows and the edge of two fan shaped setules are highlighted by white arrows. Scale bar: 2 µm.

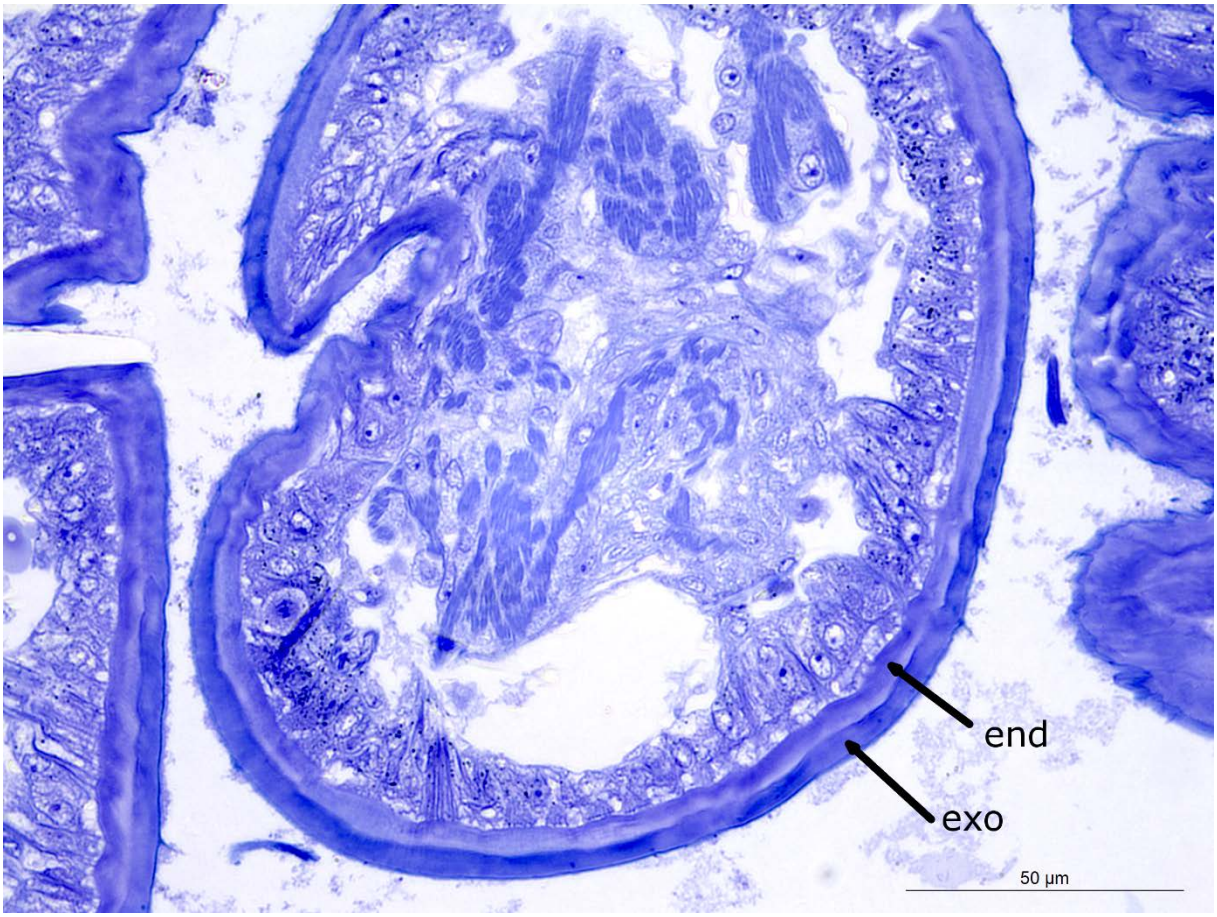

Figure 17: Histological section of the cirri, the layering of the endo- and exo-cuticle is indicated. End, endocuticle; exo, exocuticle. Scale bar: 50 µm.

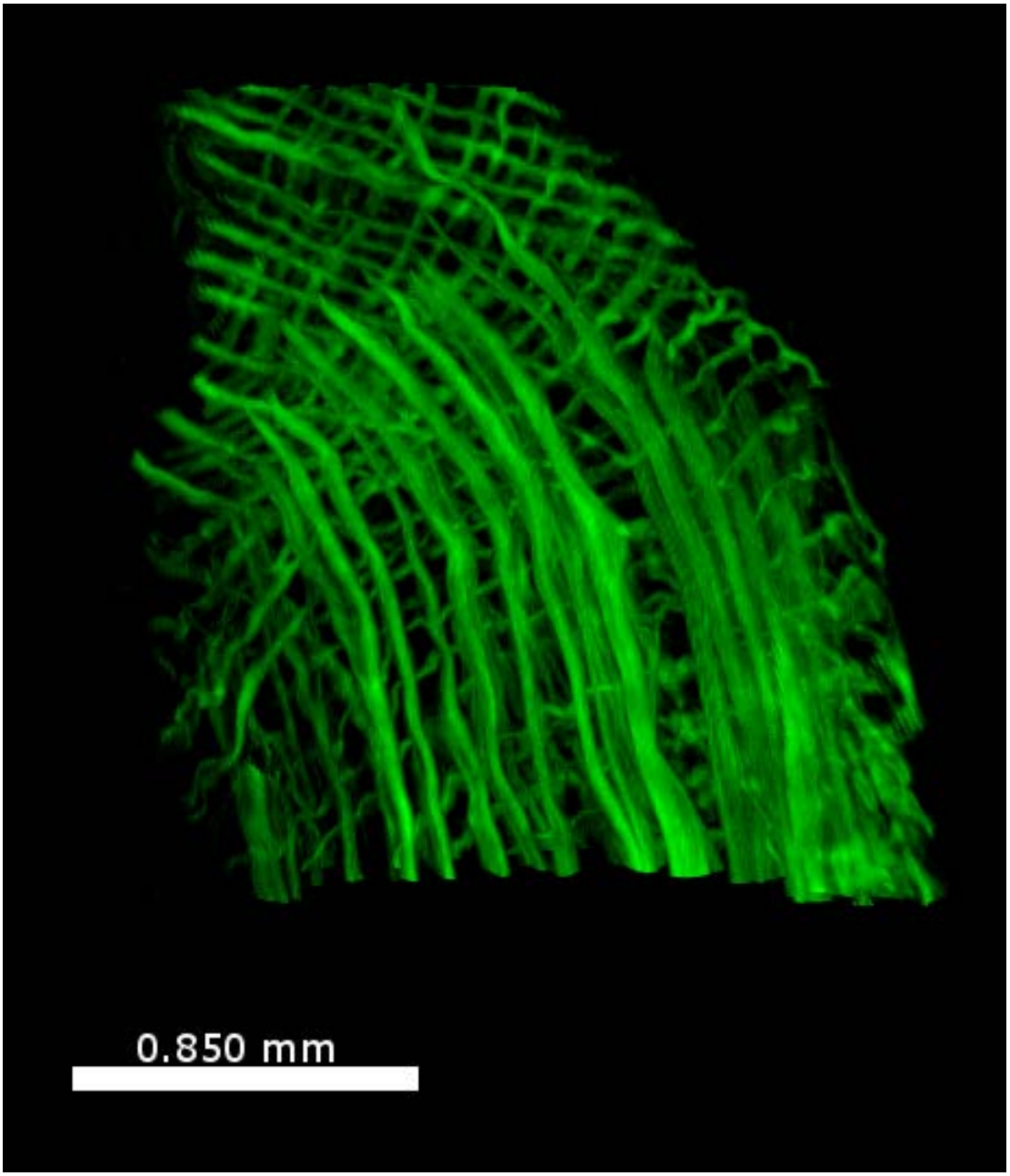

Figure 18: Imaris reconstruction of the muscle tissue surrounding the upper part of the peduncle of P1, 3 layers are visible. The inner layer, closest to the viewer, and the two oblique layers running perpendicular behind it. Scale bar: 0.850 mm.

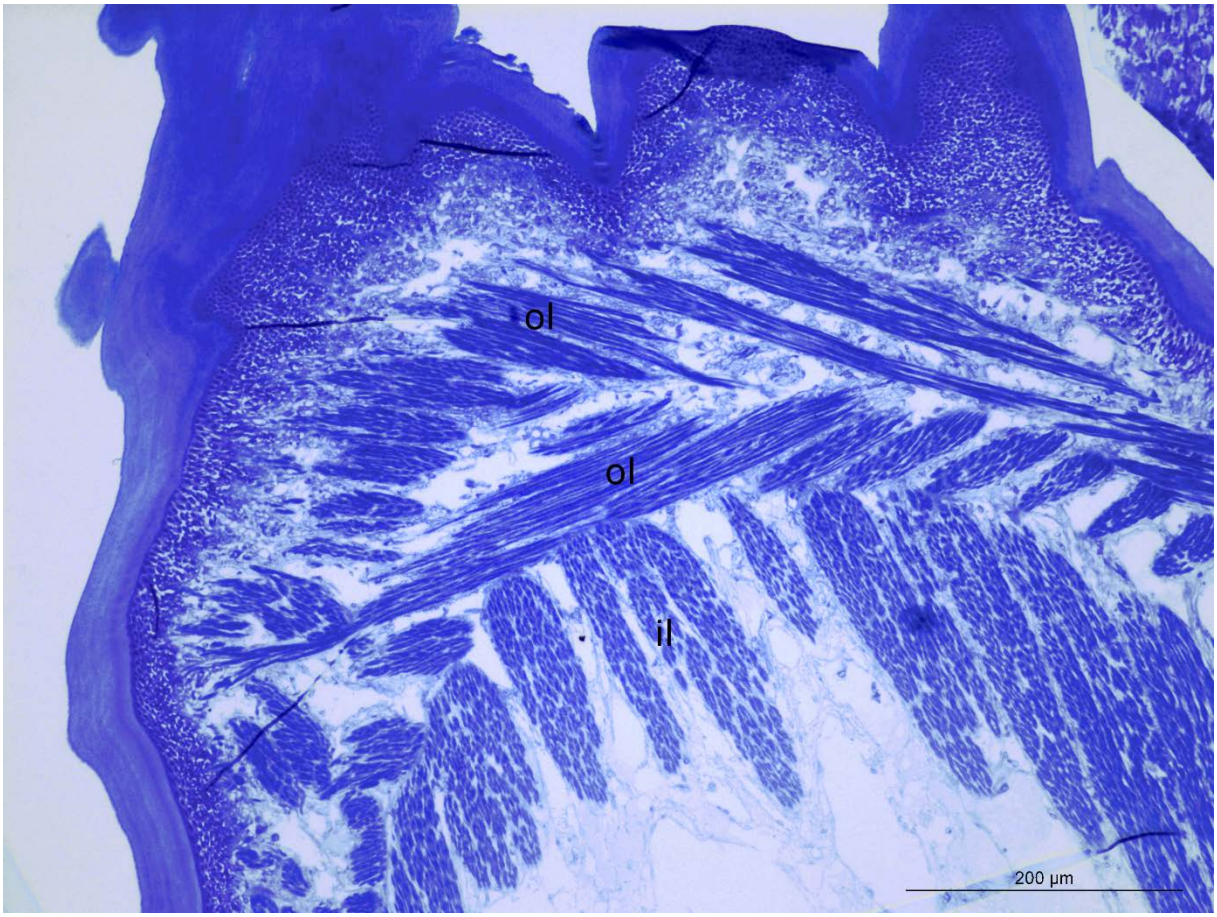

Figure 19: Histological section of the muscle fibers surrounding the top of the peduncle. Three individual muscle layers can be seen. The inner layer going from top to bottom and two layers running obliquely from top to bottom in opposite directions. Il, inner layer; ol oblique layers. Scale bar: 200 µm.

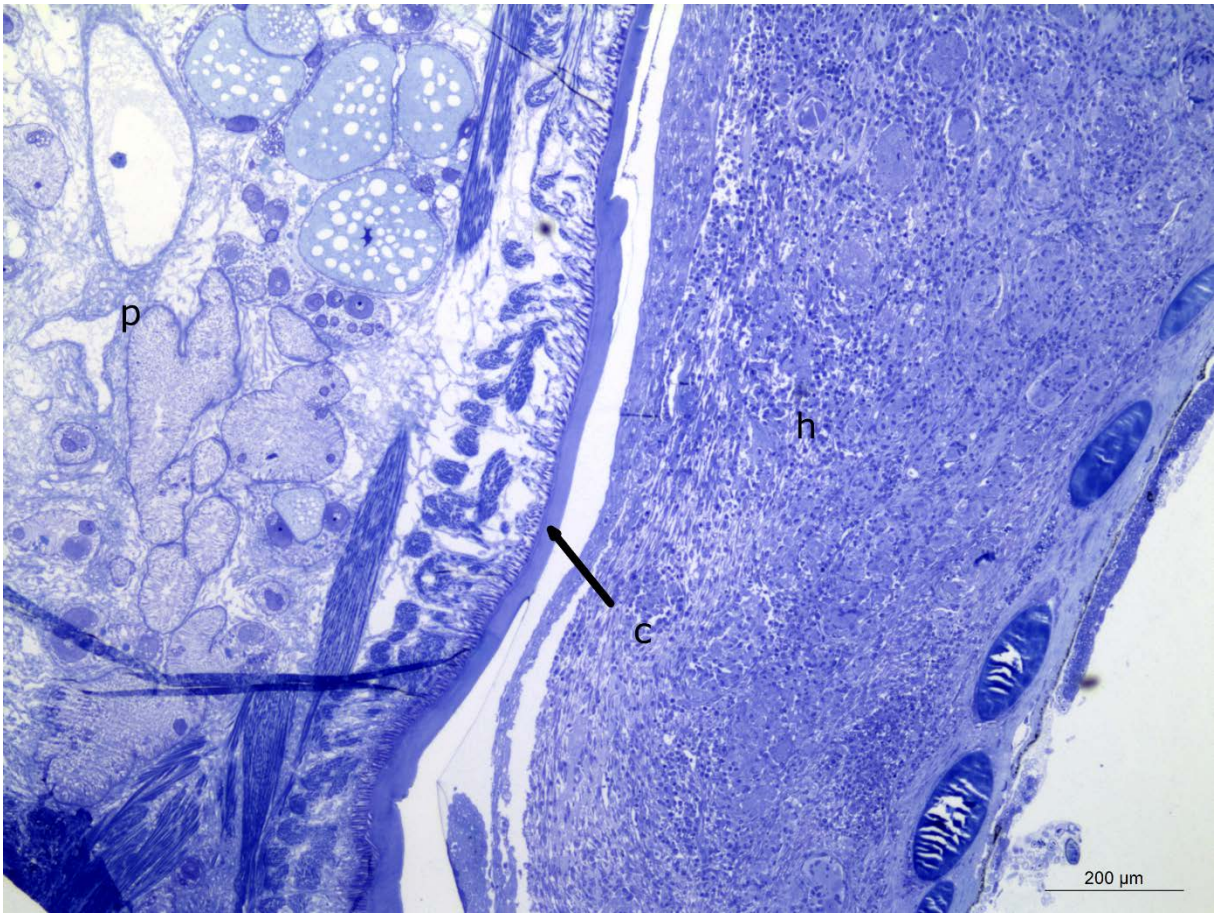

Figure 20: Histological section of the peduncle showing the cuticle from the waist and down the peduncle. The cuticle tapers off further down in the peduncle. (In the figure the mantle is facing downwards and the peduncle faces upwards). P, peduncle; h, host tissue; c, cuticle. Scale bar: 200 µm.

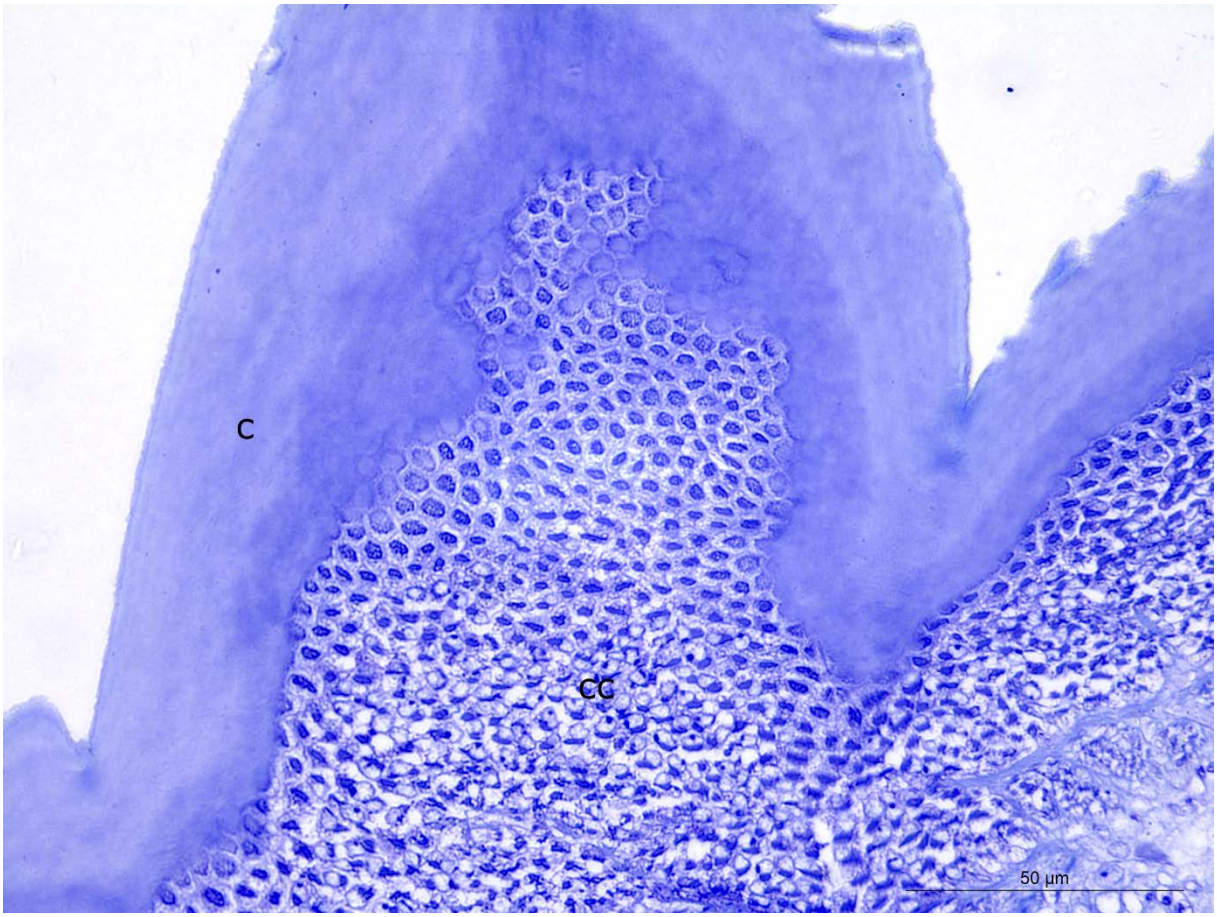

Figure 21: Histological section of mantle and the columnar cells below it. The section was taken in the same plane as the cuticle and shows a cross section of the cells. C, cuticle; cc, columnar cells. Scale bar: 50 µm.

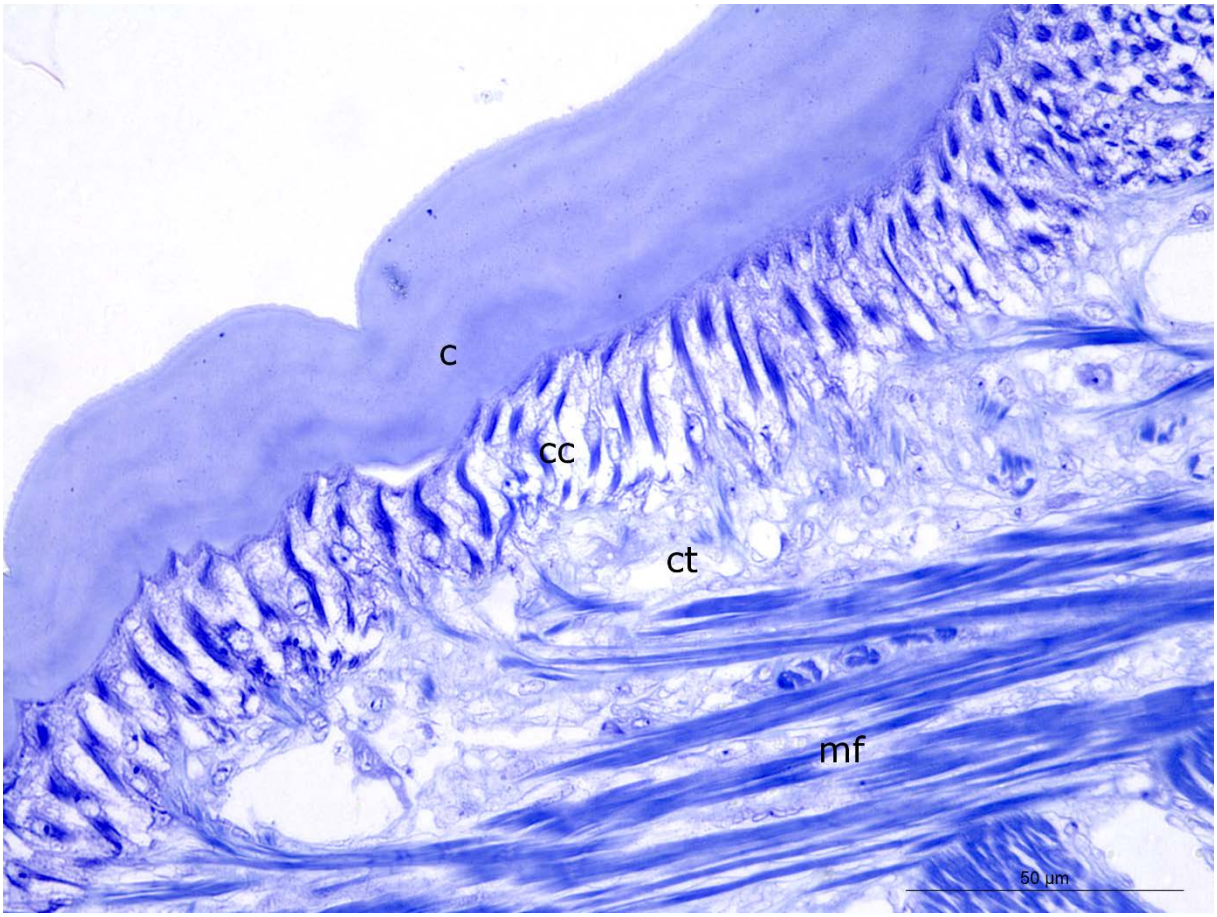

Figure 22: Histological section of the mantle and the columnar cells. The cross section was taken perpendicular to the mantle and shows the length of the columnar cells. C, cuticle; cc, columnar cells; ct, connective tissue; mf, muscle fibers. Scale bar: 50 µm.

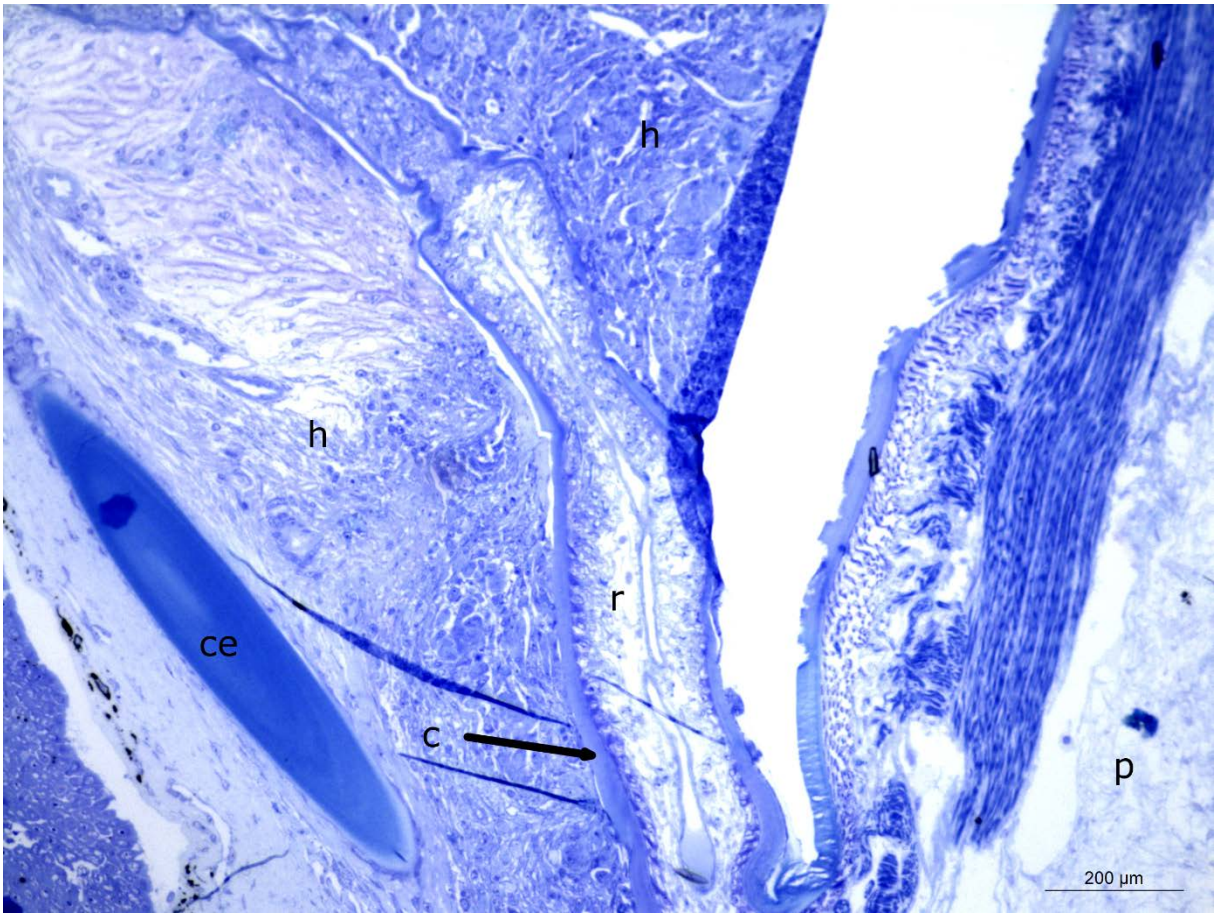

Figure 23: Histological lengthwise section of a root and the peduncle. The cuticle tapers off towards the tip of the root. H, host tissue; p, peduncle; ce, ceratotricia; r, root; c, cuticle. Scale bar: 200 µm.

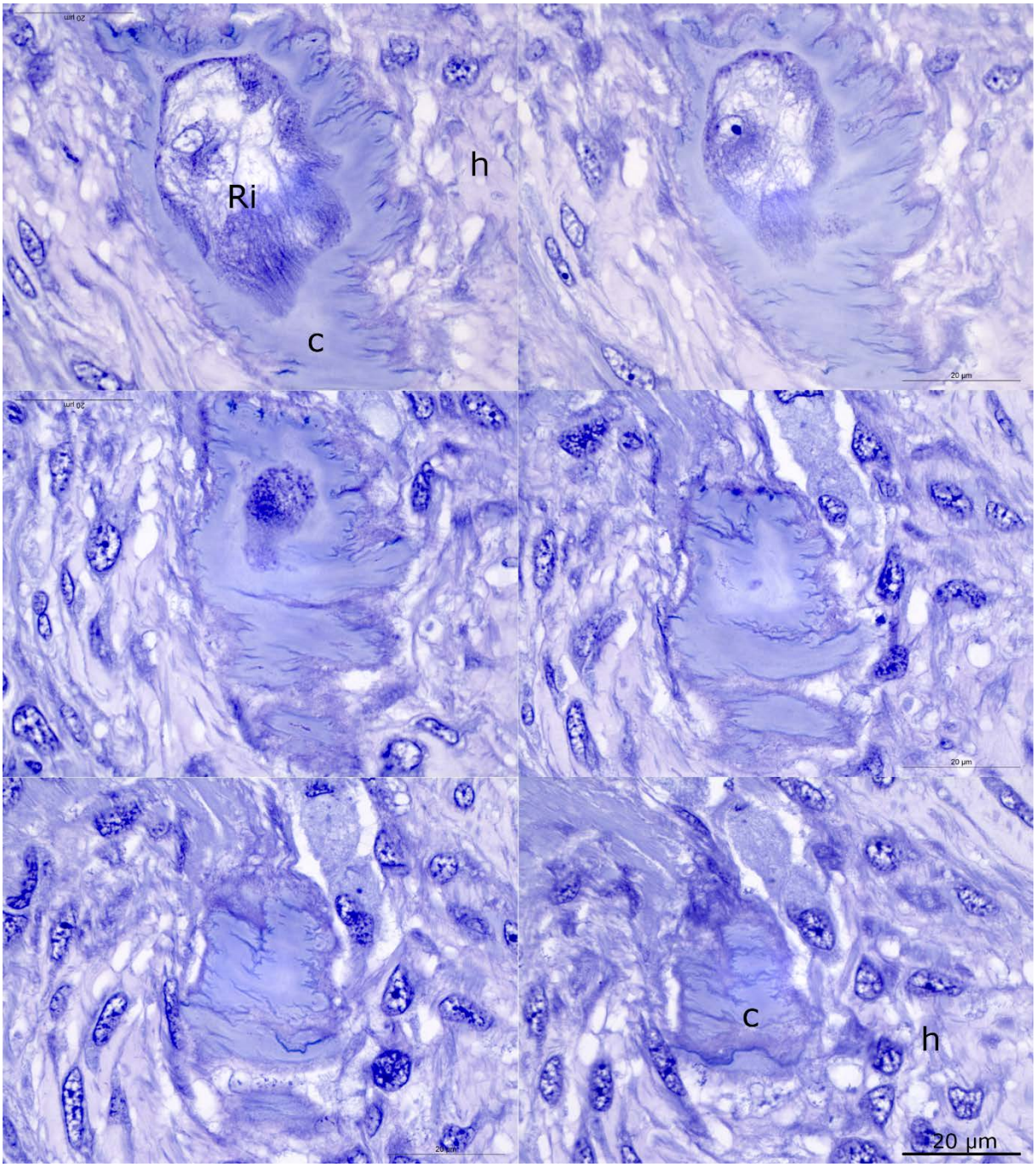

Figure 24: Histological serial sections of the tip of a root, showing the cuticle all the way to the end of the root. C, cuticle; Ri, root internae; h, host tissue. Scale bar: 20 µm.

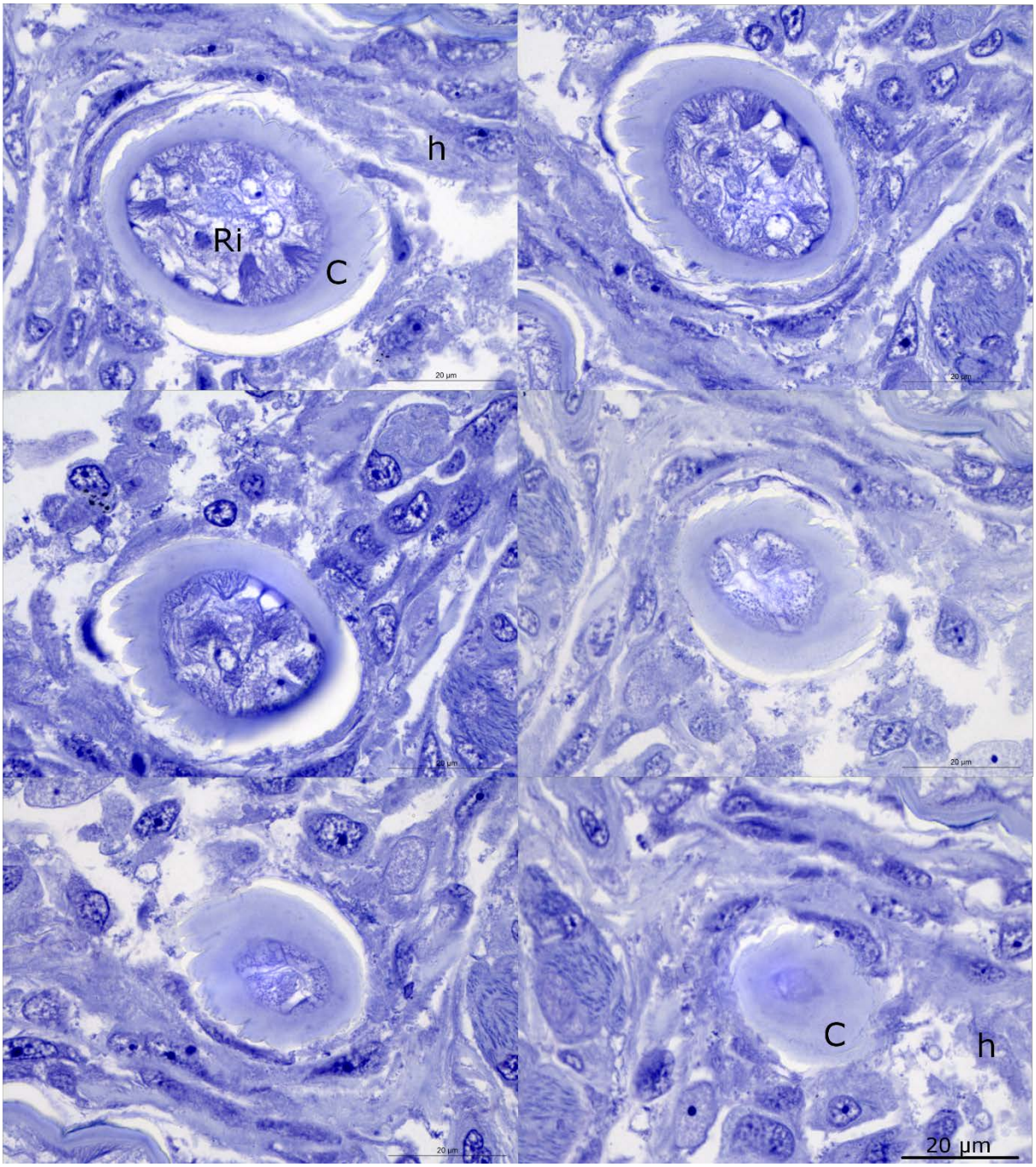

Figure 25: Histological serial sections of the tip of a root, showing the cuticle all the way to the end of the root. C, cuticle; Ri, root internae; h, host tissue. Scale bar: 20 µm.

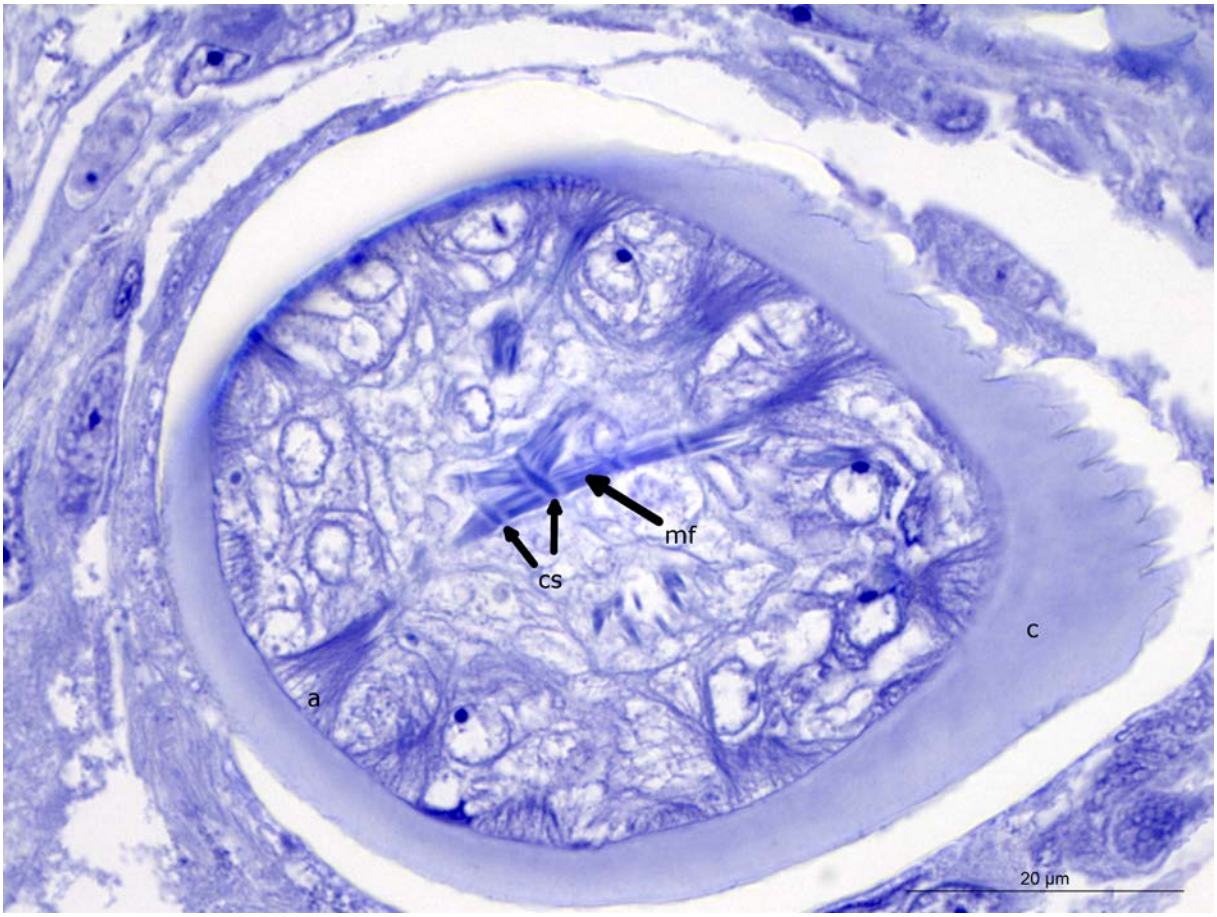

Figure 26: Histological cross section taken just before the tip of a root showing striped muscle fibers, the musculature can be seen crossing the roots from side to side and fanning out and anchoring in the cuticle. Mf, muscle fiber; cs, cross striping; c, cuticle; a, anchor point. Scale bar: 20 µm.

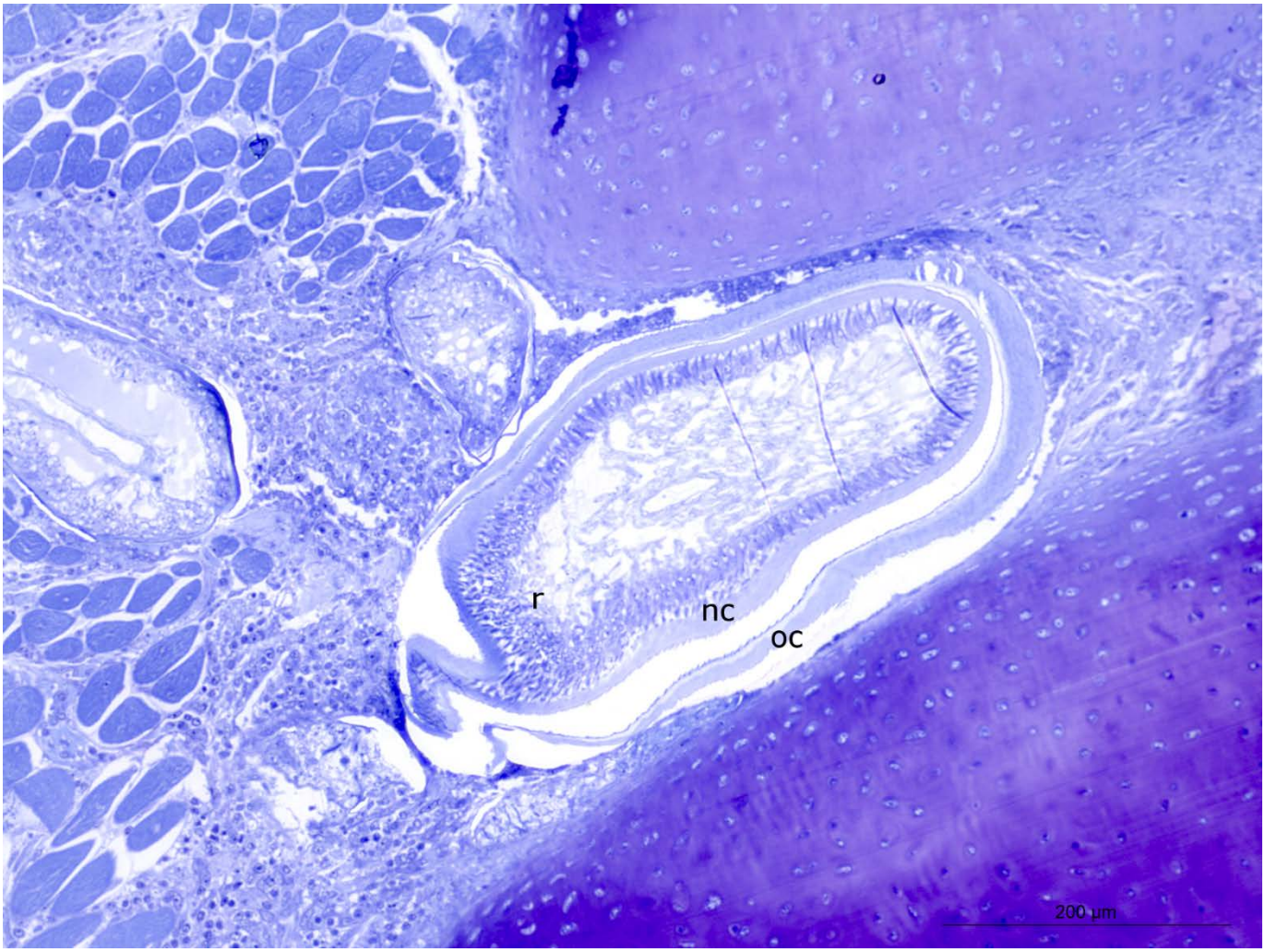

Figure 27: Histological section of a root in the process of molting. The new endocuticle can be seen covering the root. The old endocuticle can be seen detached from the new endocuticle and its inside is covered by the ecdysial membrane. Nc, new cuticle; oc, old cuticle; r, root. Scale bar: 200 µm.

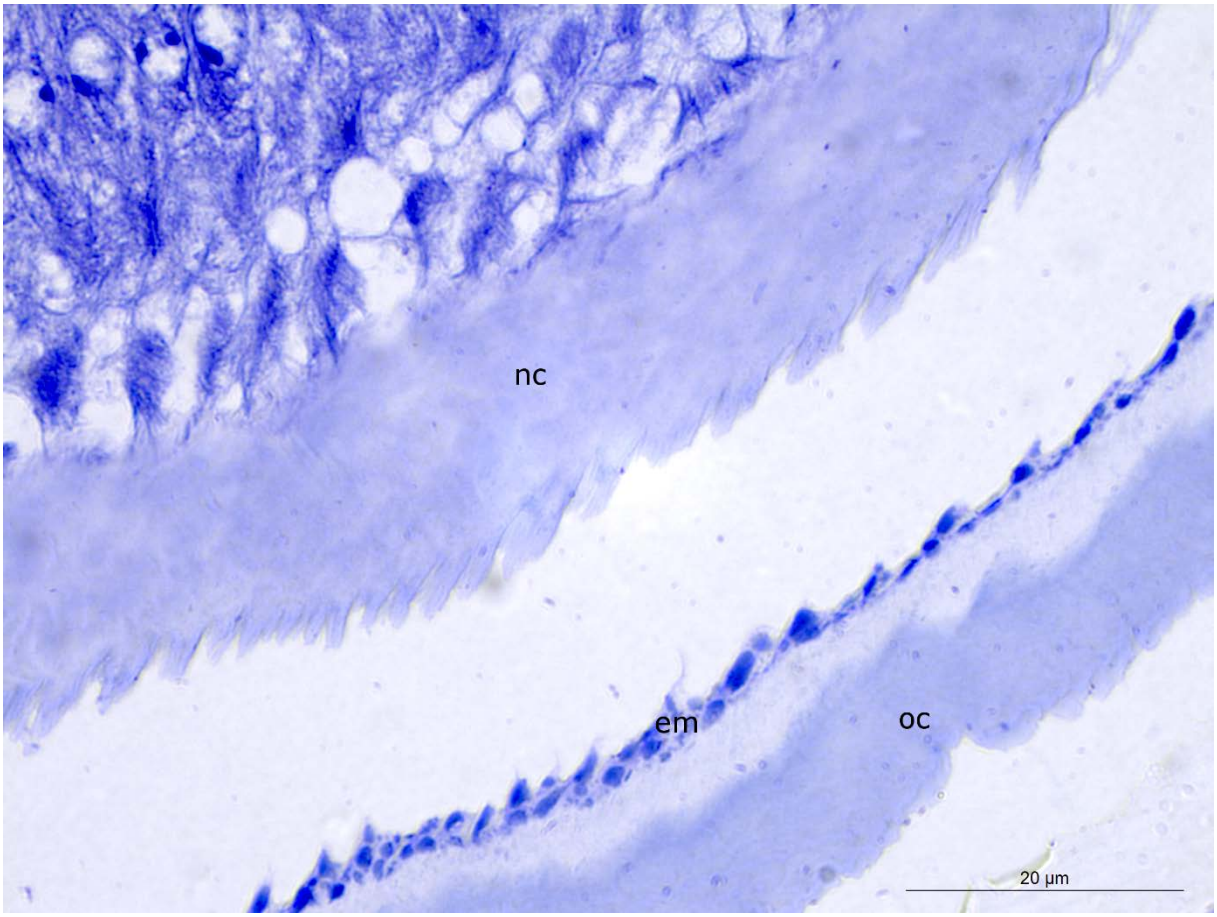

Figure 28: Histological section showing the ecdysial membrane between the new and old endocuticle. nc, new cuticle; oc, old cuticle; em, ecdysial membrane. Scale bar: 20 µm.

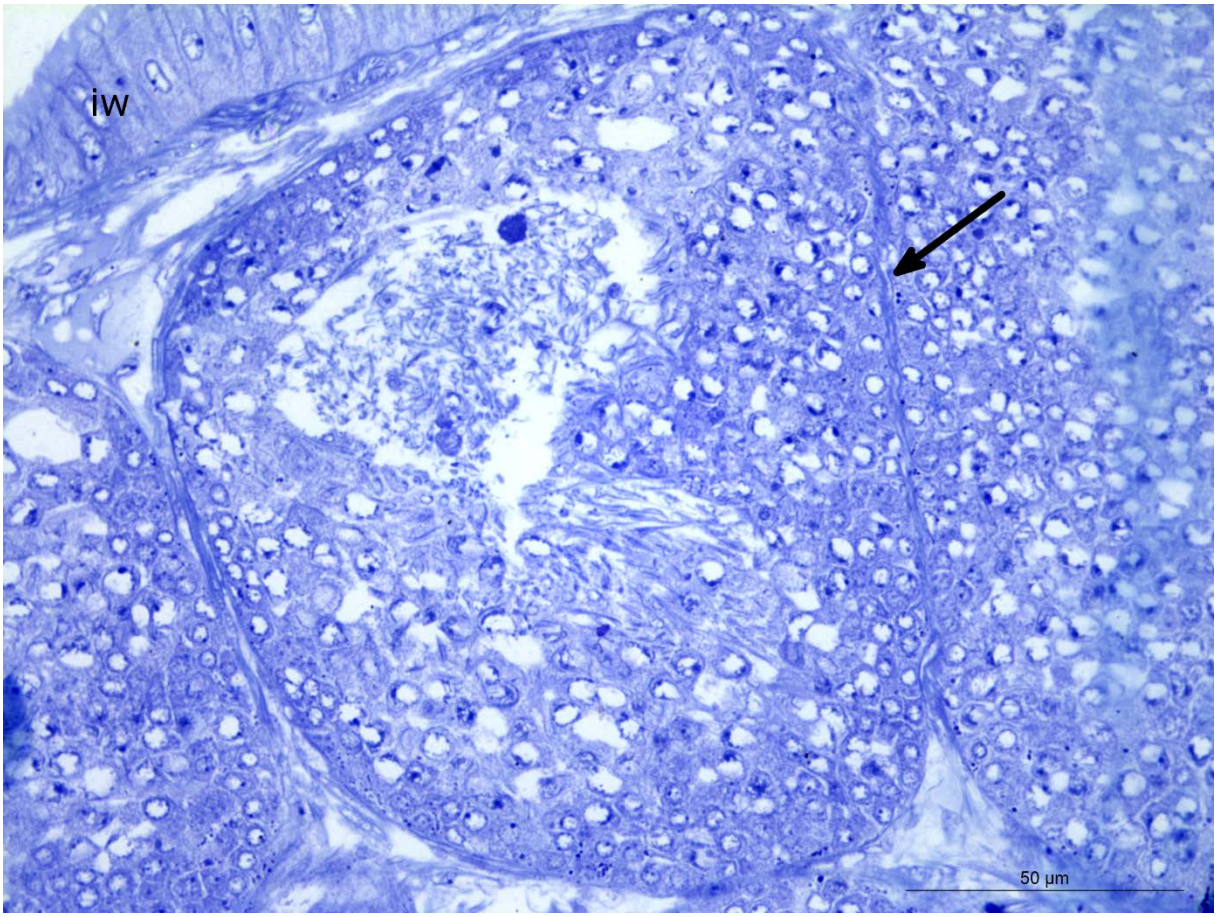

Figure 29: Histological section of testicular vesicle. The arrow is highlighting the connective tissue surrounding each separate vesicle. In the top left of the image the intestinal wall can be seen. iw, intestinal wall. Scale bar: 50 µm.

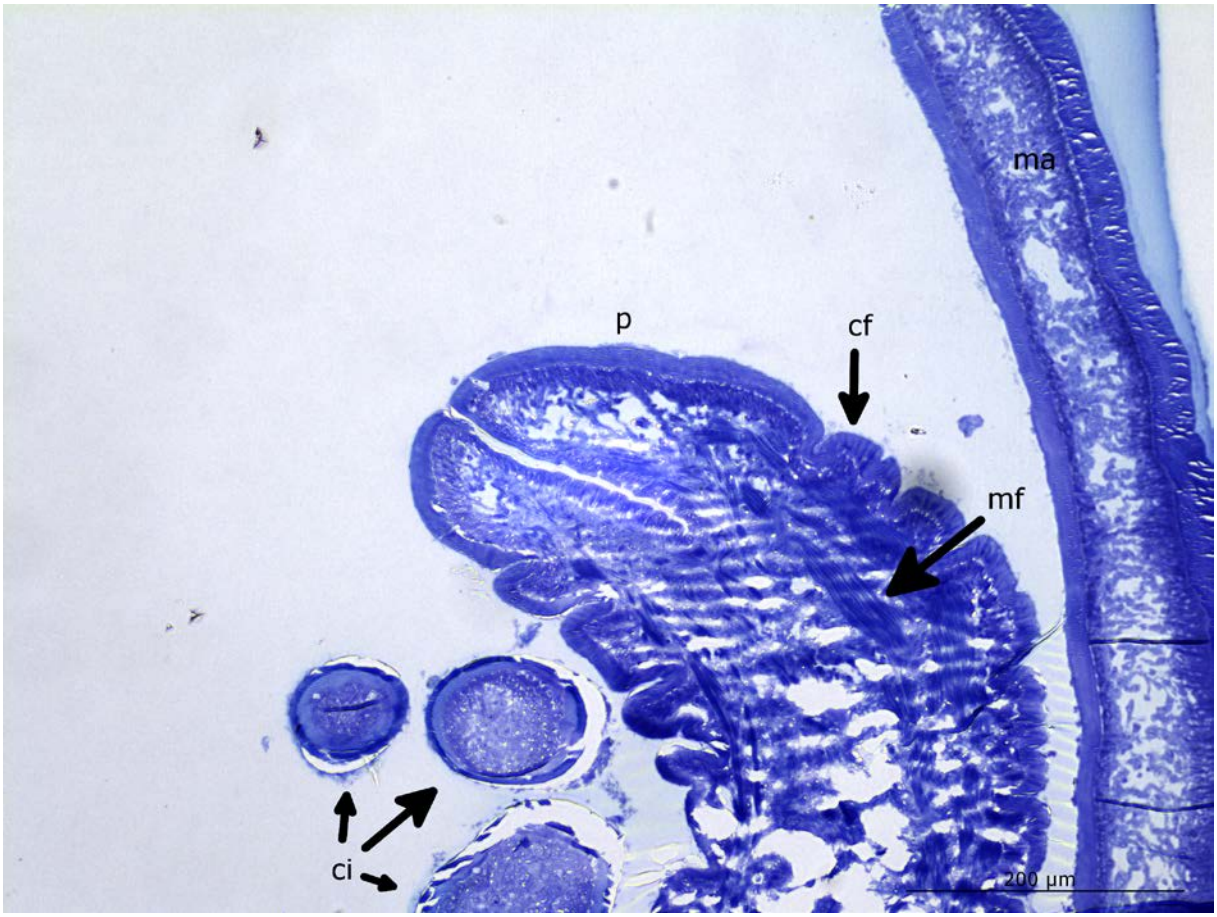

Figure 30: Histological section of the penis, showing a high degree of folding of the cuticle. The mantle can be seen to the right in the picture. Ci, cirri; mf, muscle fiber; cf, cuticle fold; p, penis. Scale bar: 200 µm.

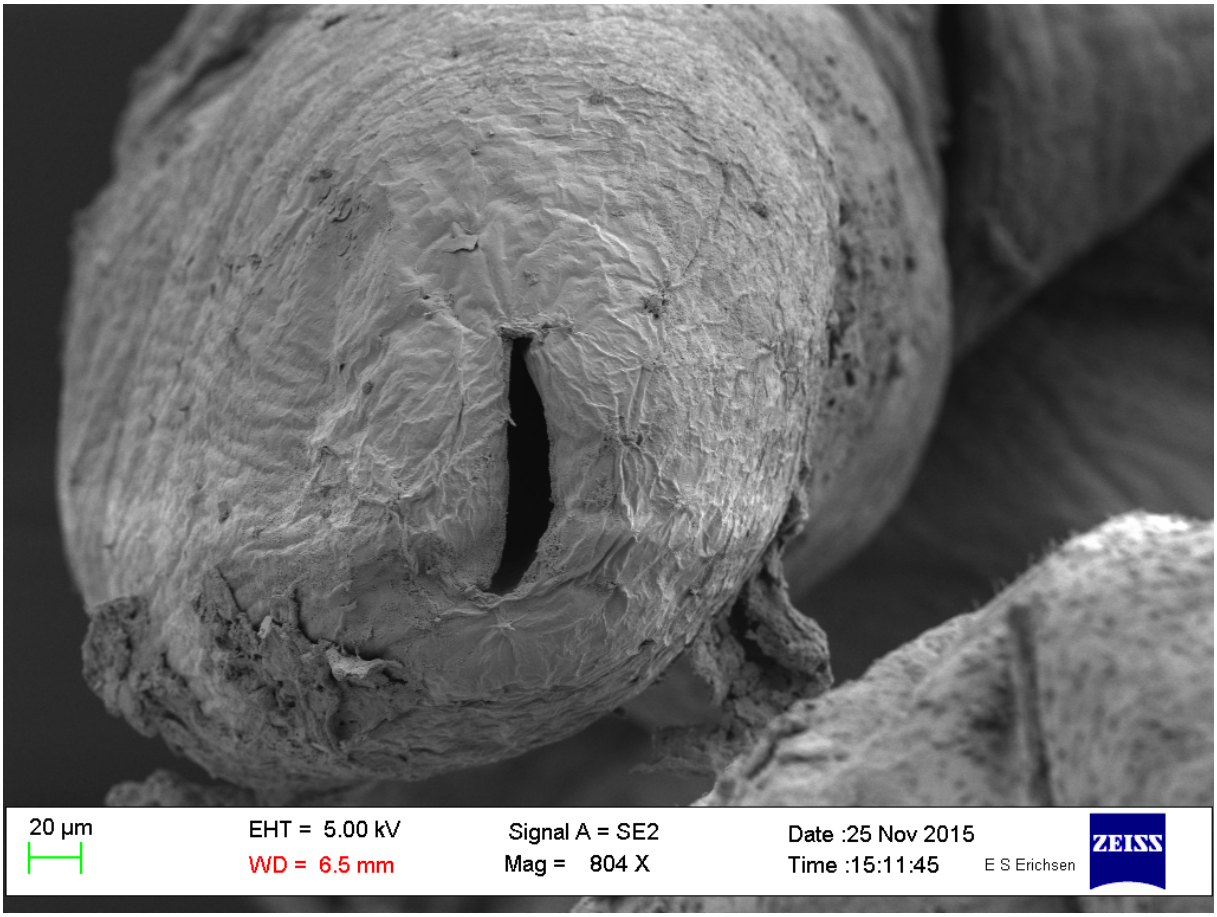

Figure 31: Scanning electron microscopy image of the secondary penis of p1 showing the urinary meatus. Scale bar: 20 µm.

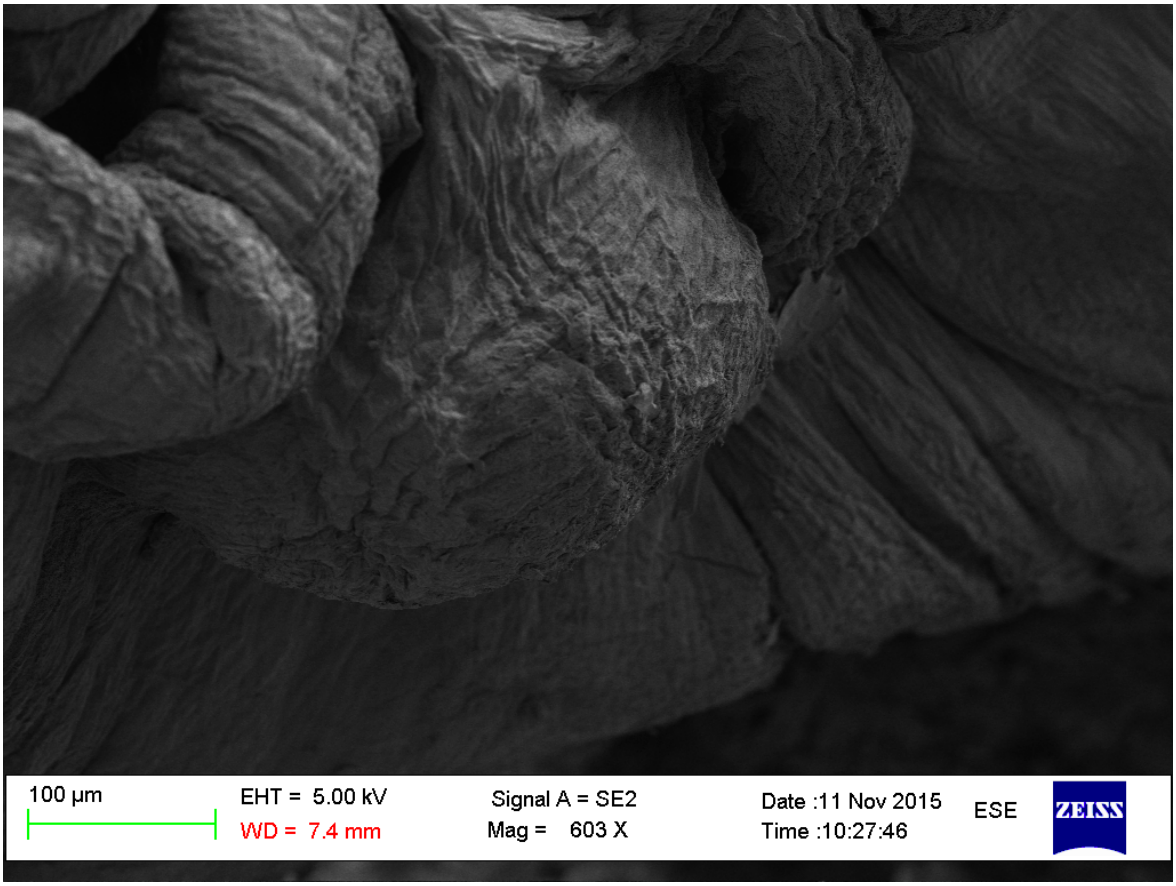

Figure 32: Scanning electron microscopy image of the oviducal bulb of p7.

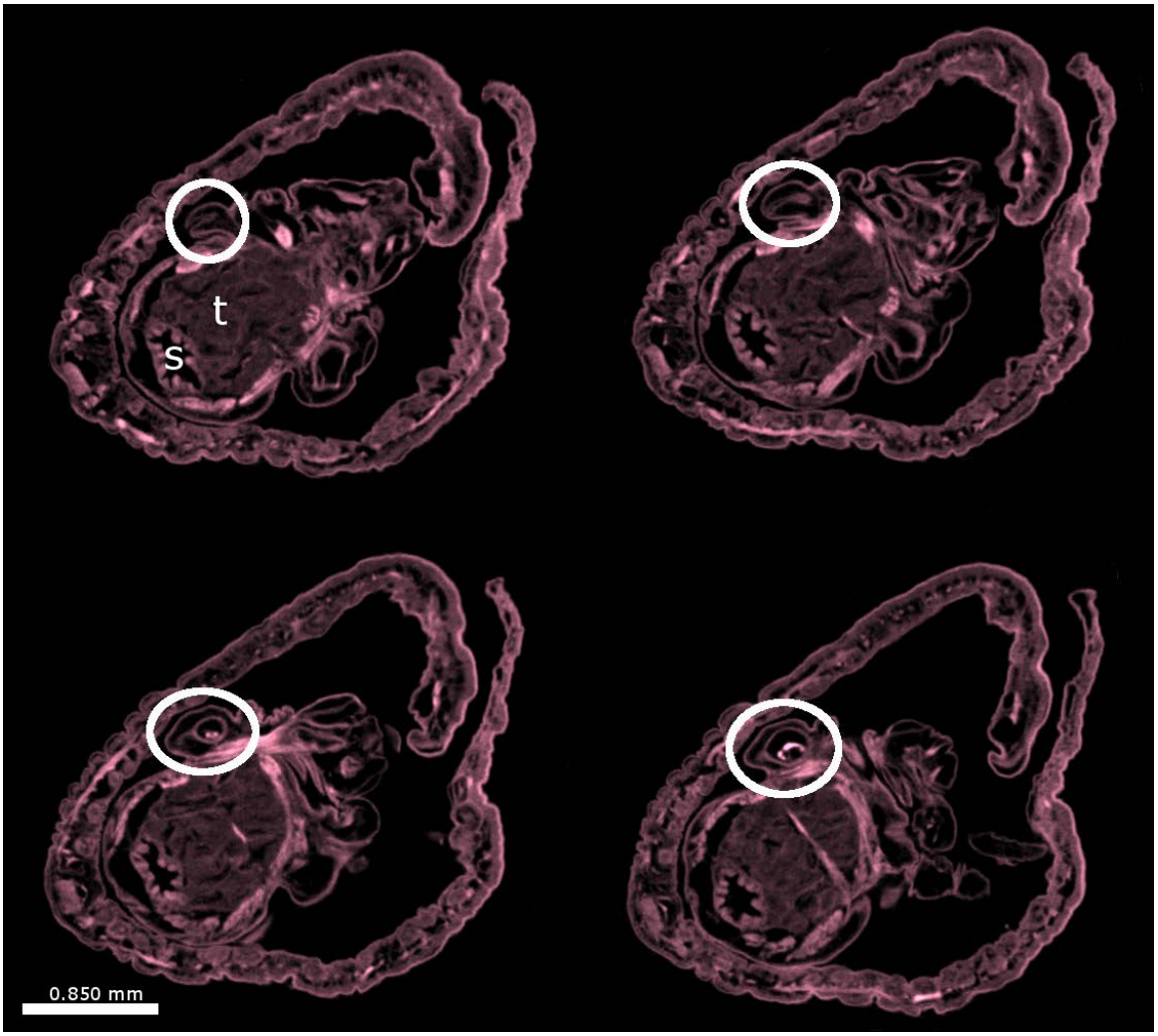

Figure 33: Cross sections of Imaris reconstruction of P1 showing the opening to the oviducal bulb, indicated by white circle. The testis and stomach is also visible in the sections and marked with S and t in the top left section. S, stomach; t, testies. Scale bar: 0.850 µm.

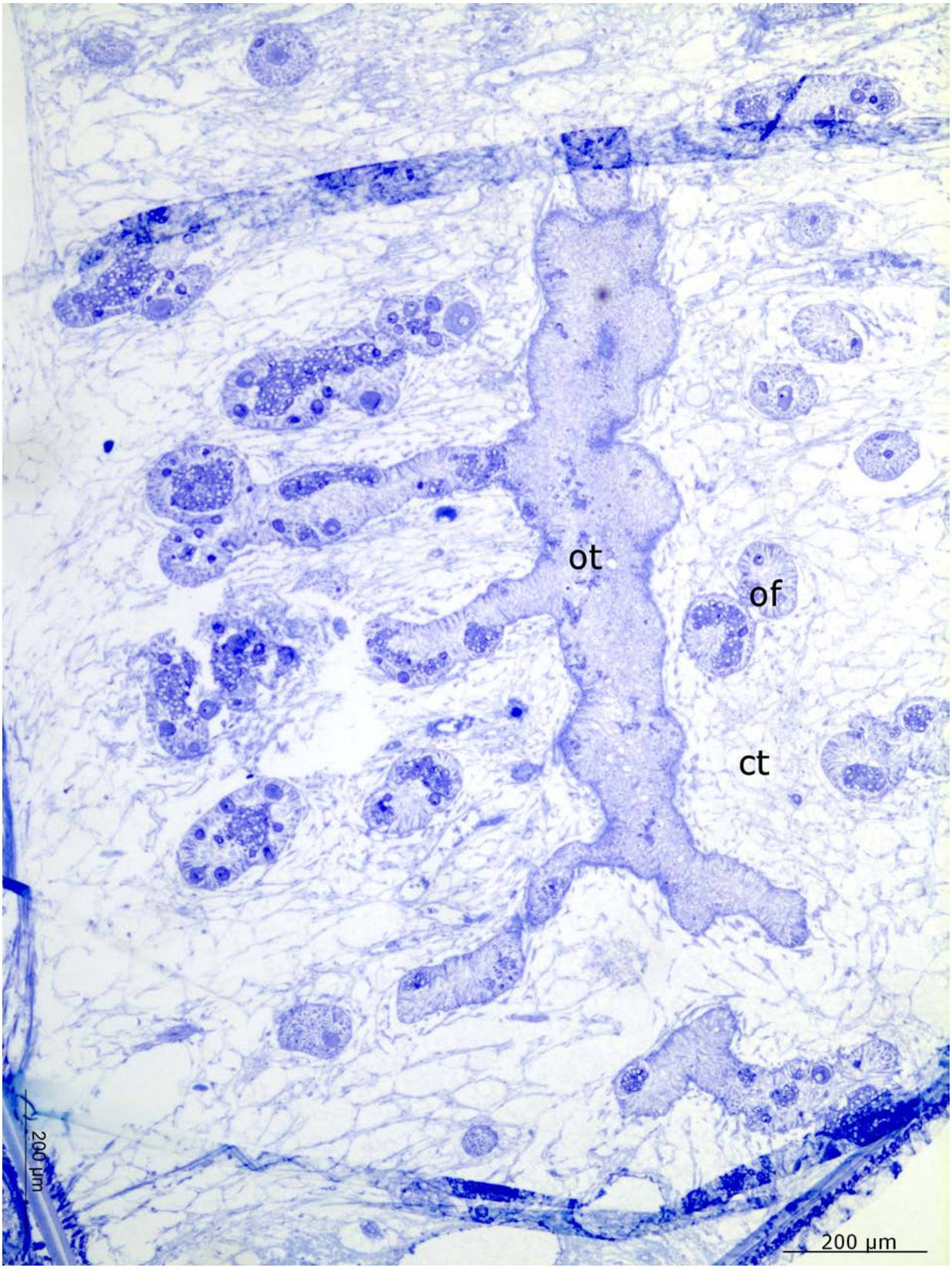

Figure 34: Histological section of p8 showing the branching of the ovarian tube and the ovarian follicles containing the oocytes. In the bottom left and right the cuticle covering the peduncle can be seen. Horizontal lines are artifacts from folding of the histological section. Ct, connective tissue; c, cuticle; ot, ovarian tube; of, ovarian follicles.

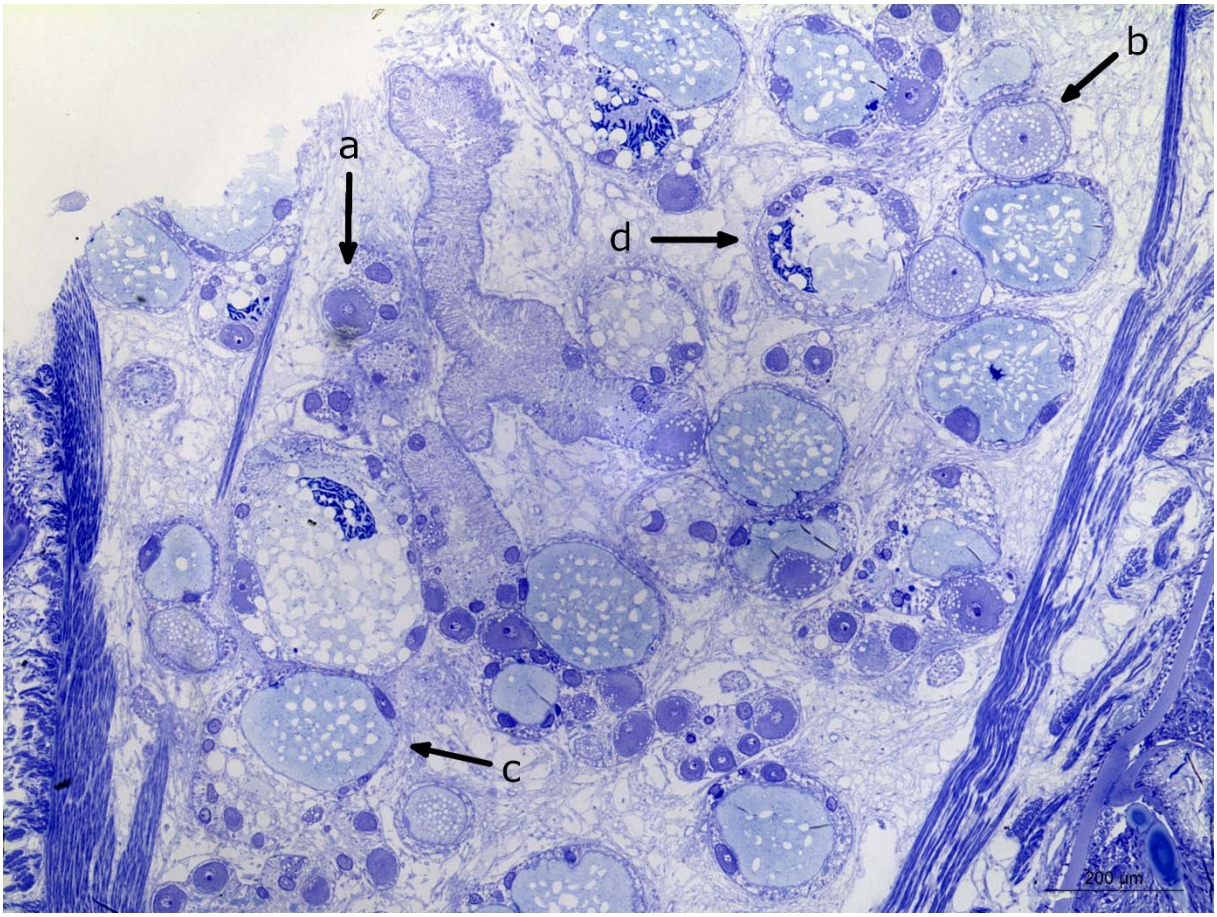

Figure 35: Histological section of the peduncle of p9 showing the ovarian tubes, follicles and developing oocytes. Four distinctly separate stages of maturity can be seen, ranging from immature oocytes (a), large oocytes with a finely granular yolk appendage (b), large oocytes with a granular yolk appendage (c) and oocytes undergoing atresia (d). See Fig. 36-38 for detailed images. Scale bar: 200 µm.

Figure 36: Histological section of a developing oozyte. The nucleus can be seen in the middle of the cell surrounded by the yolk appendage, consisting of lipids and granulated coagulum, and the granulosa cells. N, nucleus; li, lipids; gc, granulosa cells. Scale bar: 50 µm.

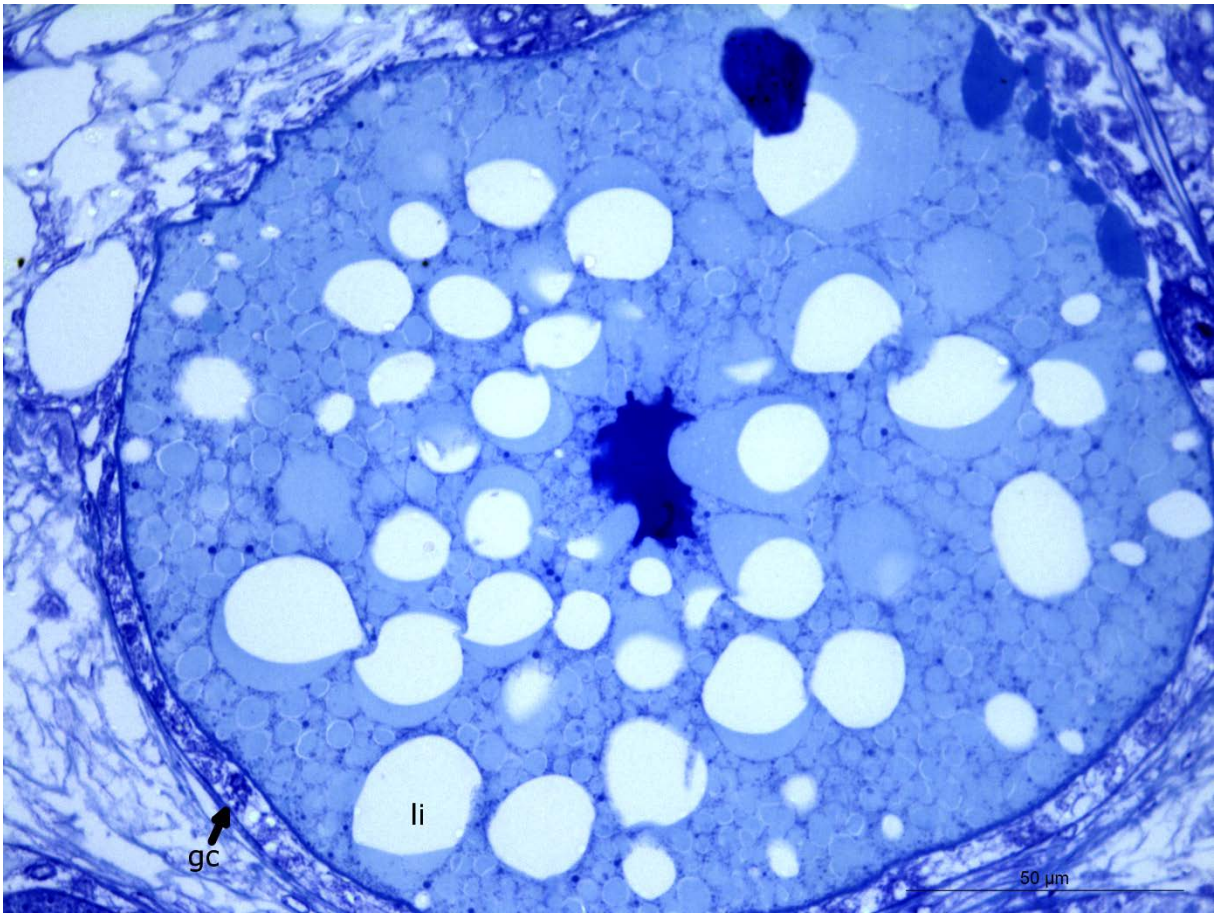

Figure 37: Histological section of a developing oozyte, the lipids form larger spheres than the oozyte in Fig. 36, and the remaining yolk content appear more granulated. Li, lipids; granulosa cells. Scale bar: 50 µm.

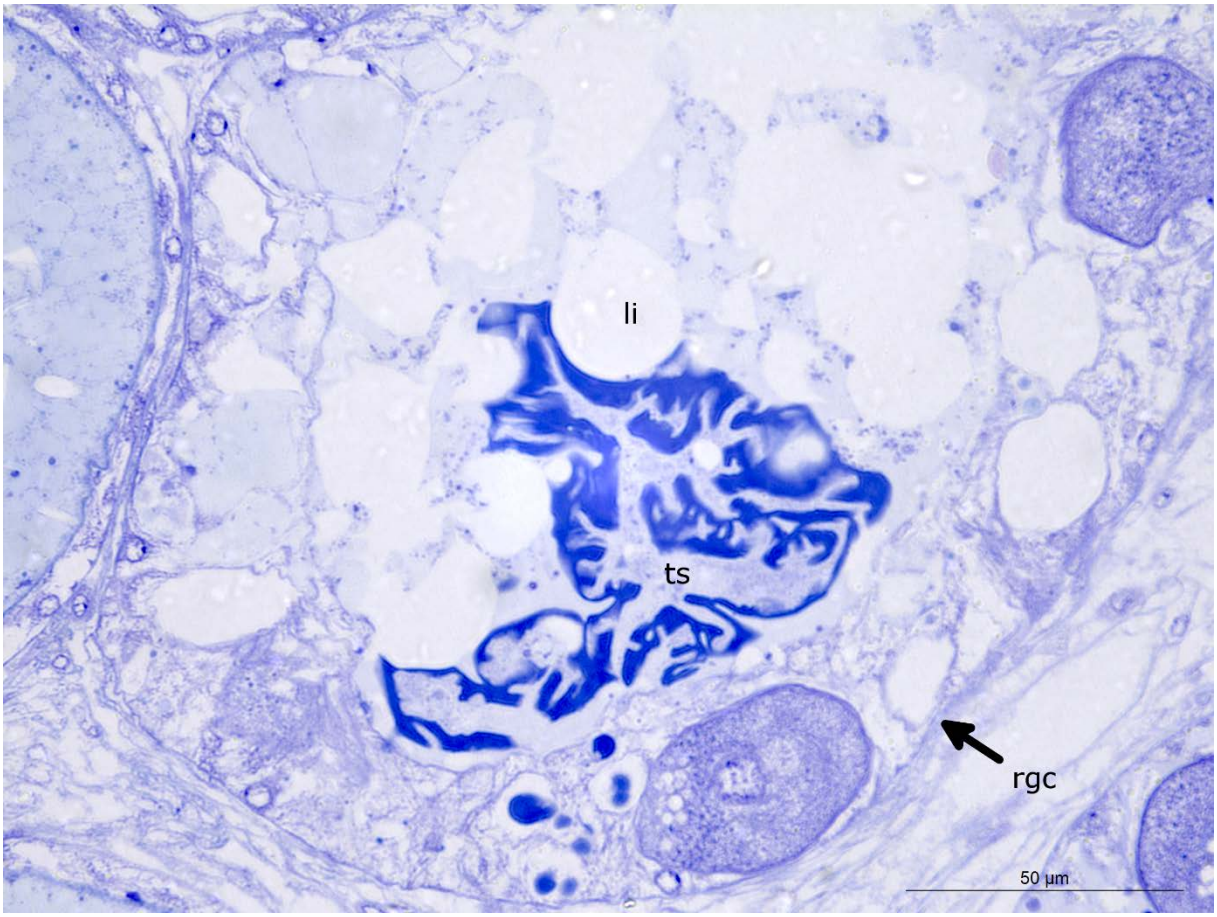

Figure 38: Histological section of oozyte undergoing atresia. They yolk appendage appears to be dissolved and the center of the cell is occupied by a tubular branching structure, the granulosa cells seen in the earlier stages no longer make up a clear border around the yolk. Li, lipids; rgc, remnant of granulosa cells; ts, tubular branching structure. Scale bar: 50 µm.

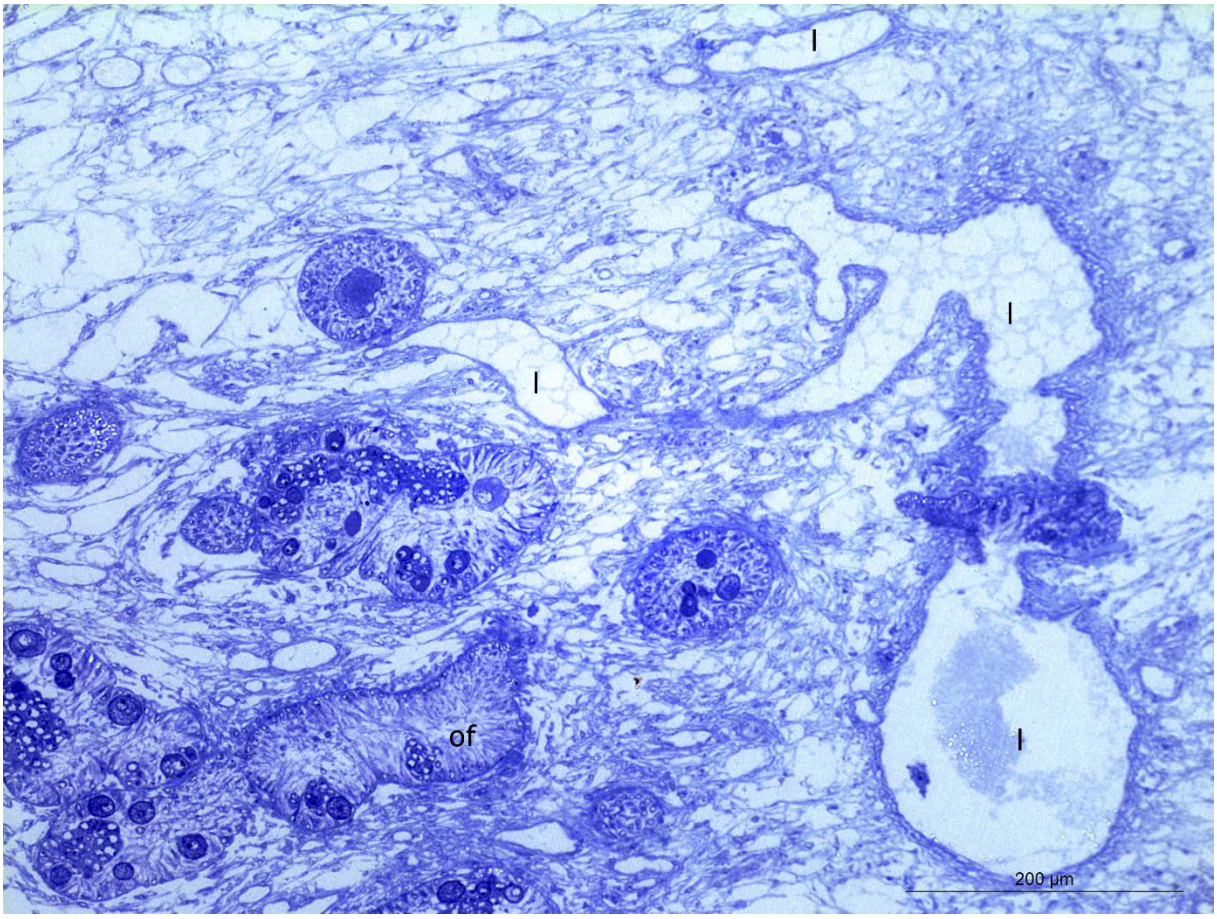

Figure 39: Histological section of the peduncle showing smaller lacunae running between the ovarian follicles. The walls of the lacunae can be seen as darker bands consisting of a dense layer of connective tissue. Of, ovarian follicle; l, lacunae. Scale bar: 200 µm.

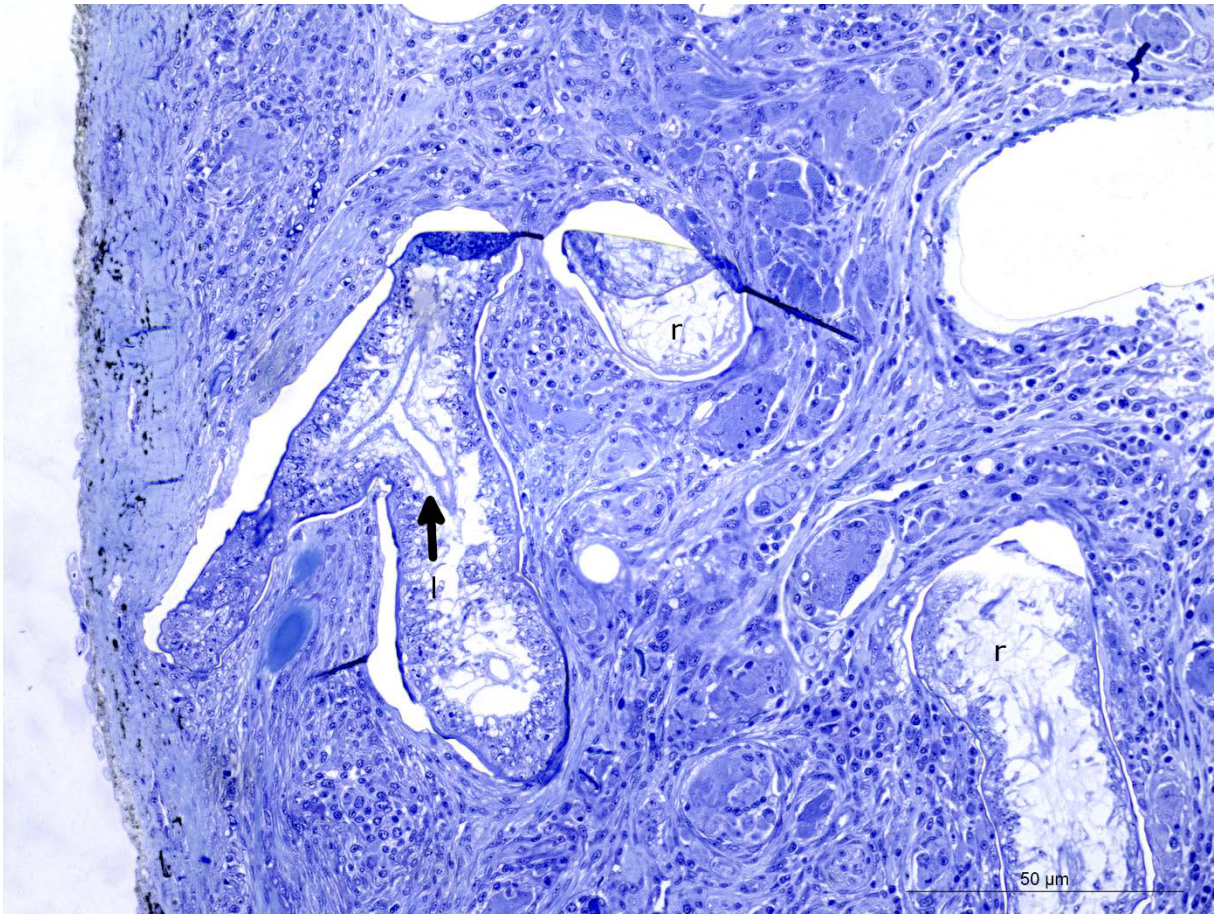

Figure 40: Histological section of a branching root, showing a lacunae diverging into both ends. L, lacunae; r, root. Scale bar: 50 µm.

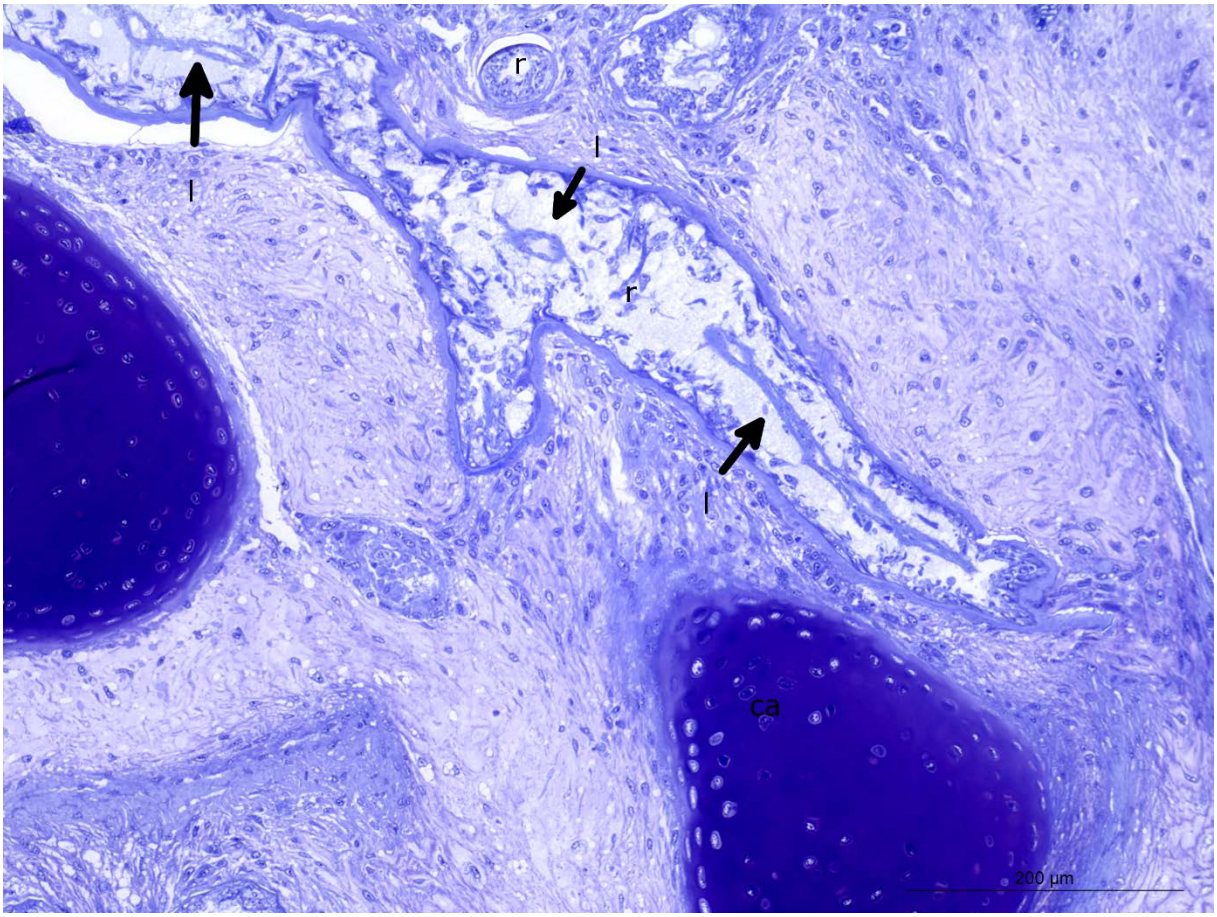

Figure 41: Histological section of a root showing the longitudinal extent the lacunae. ca, cartilage; r, root; l, lacunae. Scale bar: 200 µm.

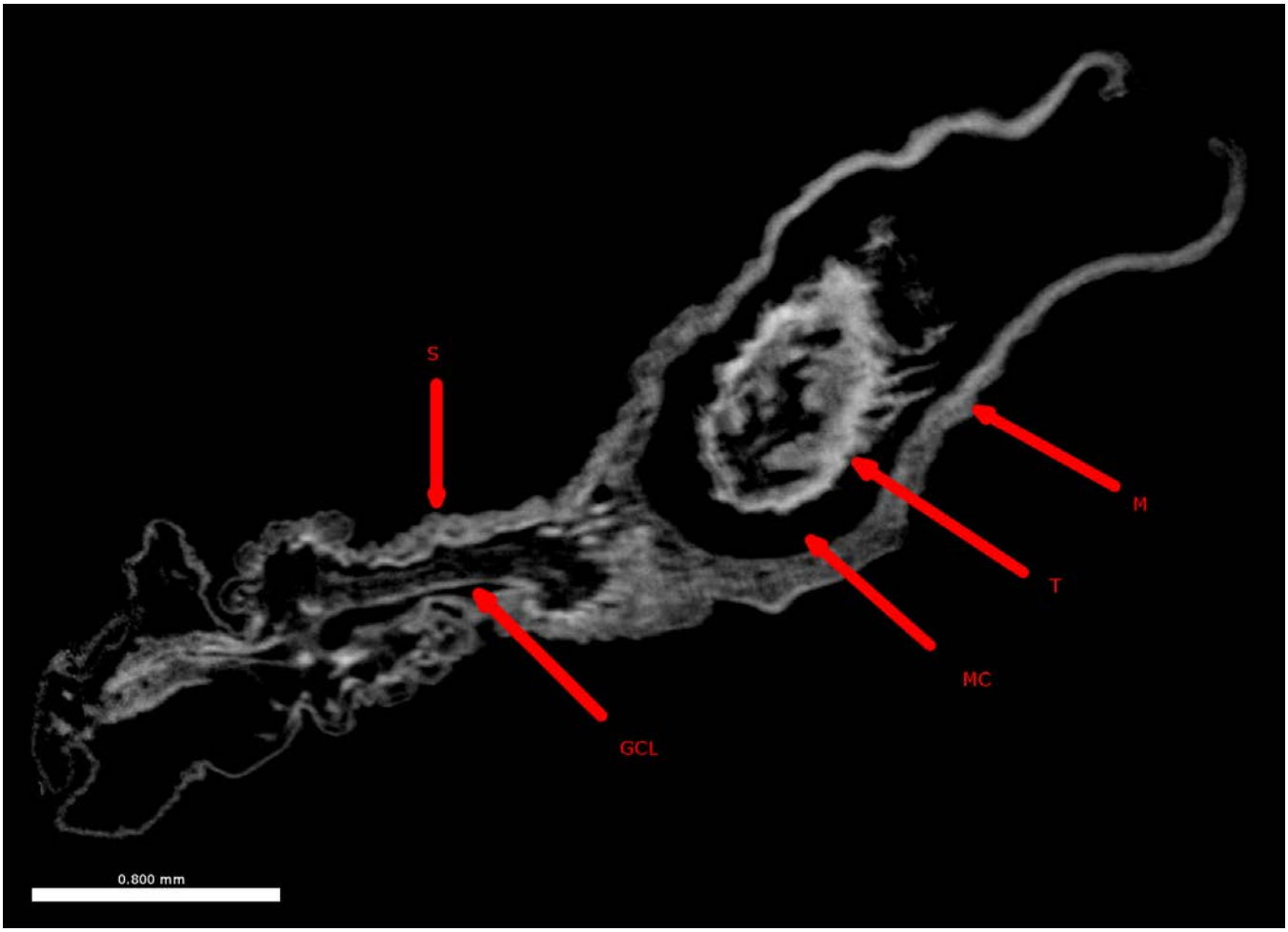

Figure 42: Cross section of MicroCT data for P1. Showing the mantle, mantle cavity, thorax, stalk and the great central lacunae. M, mantle; MC, mantle cavity; T, thorax; S, stalk; GCL, great central lacunae. Scale bar: 0.8 mm.

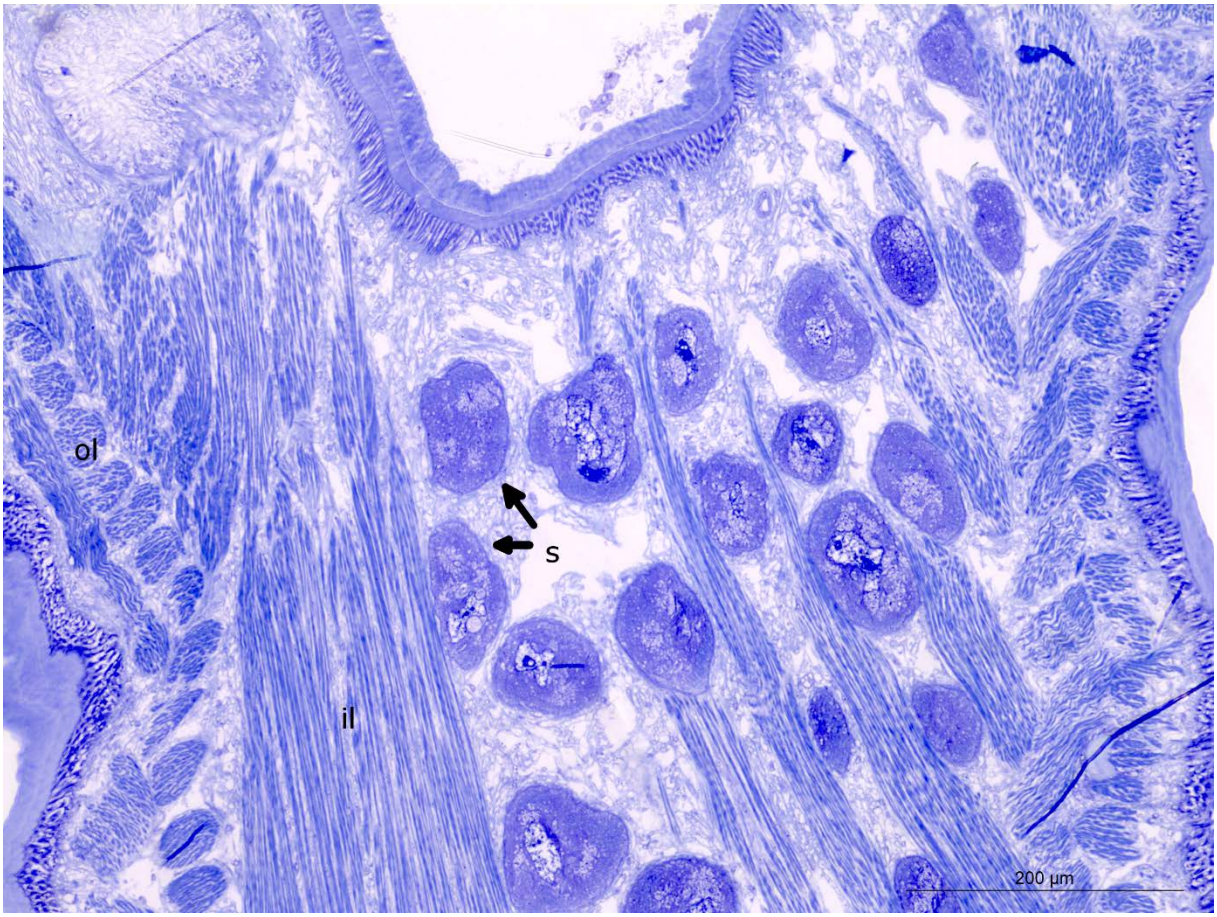

Figure 43: Histological section of the waist region of *Anelasma* where the majority of the cement glands can be found surrounded by the inner and oblique musculature of the peduncle. S, cement gland; ol, oblique layer; il, inner layer. Scale bar: 200 µm.

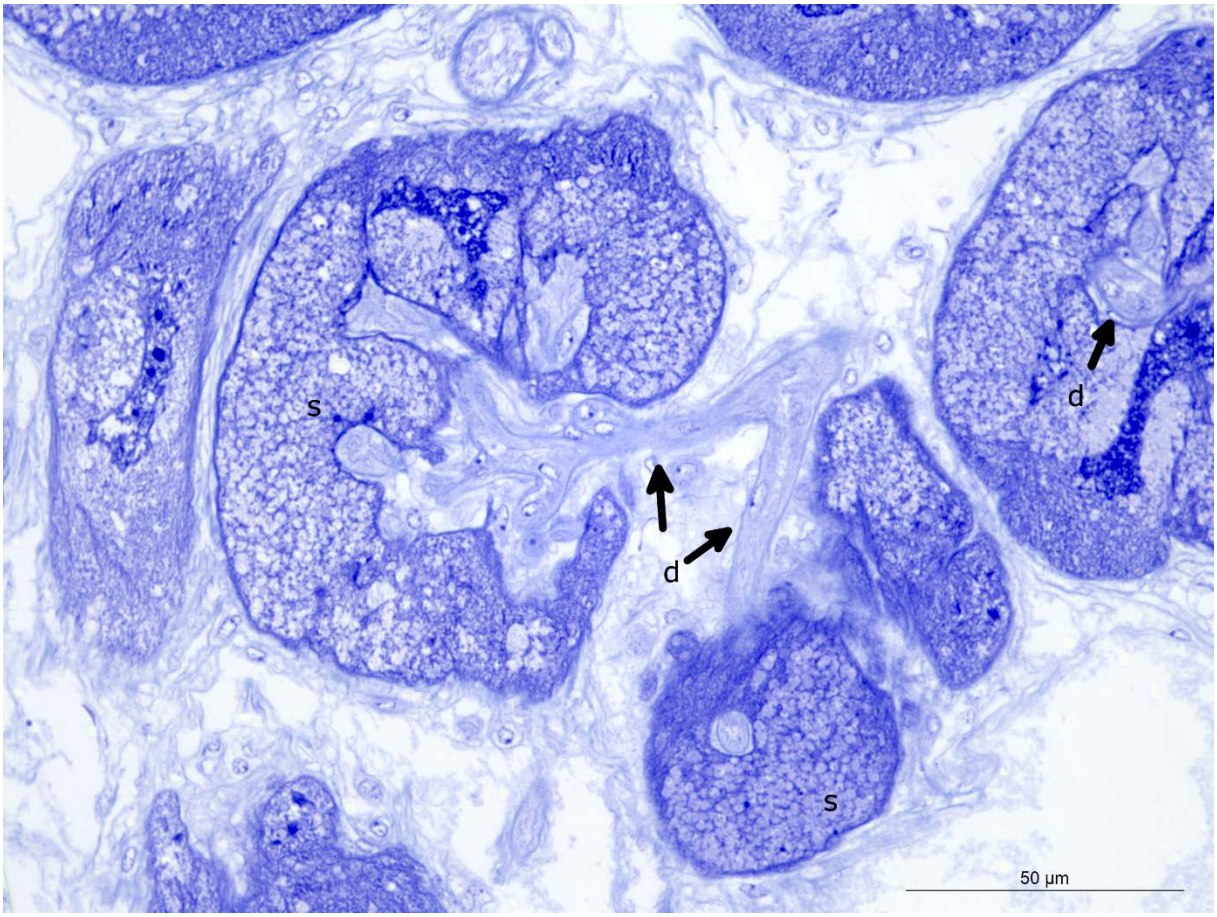

Figure 44: Histological section of the cement glands showing the ducts penetrating the center of the glands themselves and running out into the surrounding tissue where they connect with ducts from other cement glands. D, duct; s, cement gland. Scale bar: 50 µm.

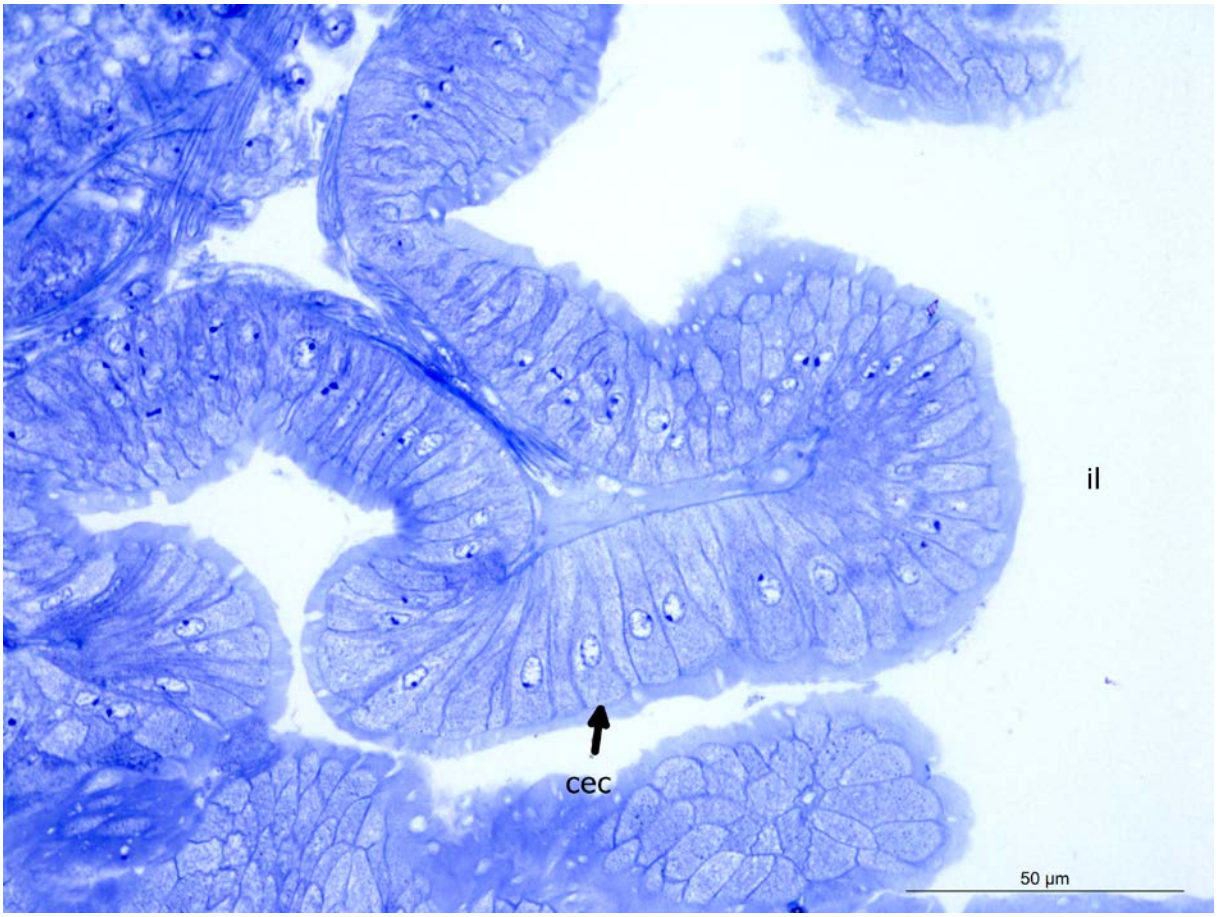

Figure 45: Histological section of folding in the digestive tract showing the cylindrical epithelial cells that line most parts of the intestine. Cec, cylindrical epithelial cell; il, intestinal lumen. Scale bar: 50 µm.

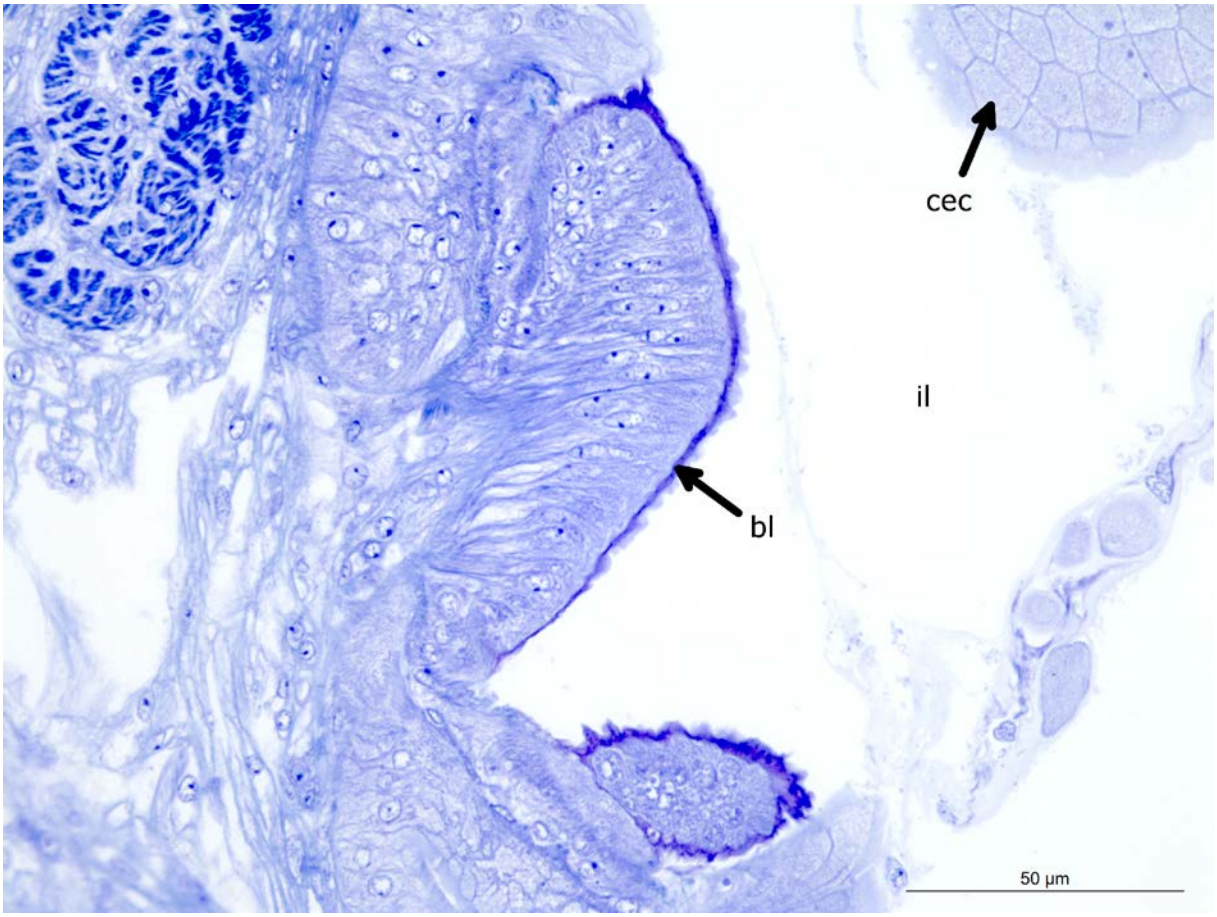

Figure 46: Histological section of the intestine showing cluster of smaller cells of unknown function. The boundary of the cluster has a much deeper stain than remainder of the intestinal surface. Cec, cylindrical epithelial cell; il, intestinal lumen; bl, boundary layer. Scale bar: 50 µm.

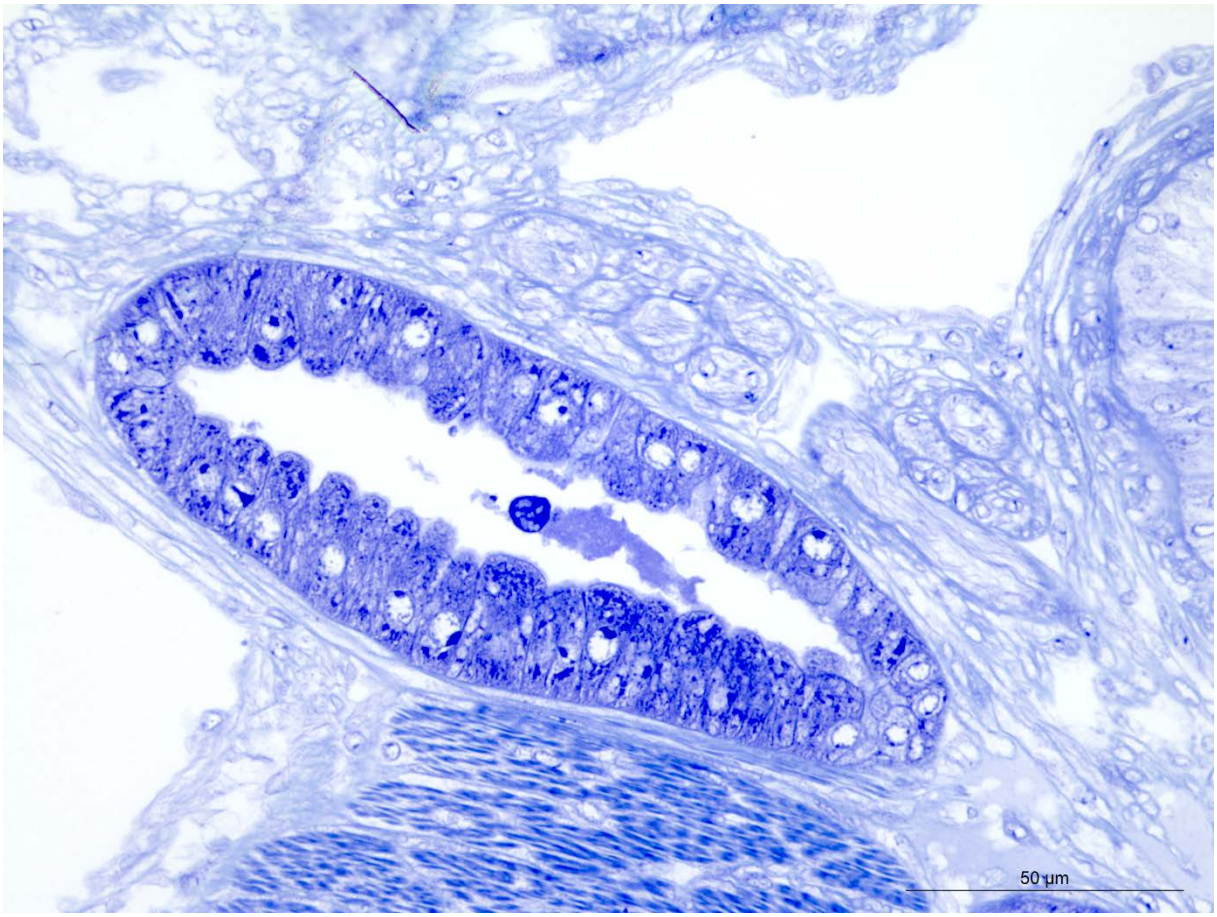

Figure 47: Histological section of digestive glands peduncular to the stomach consisting of cylindrical epithelial cells. Scale bar: 50 µm.

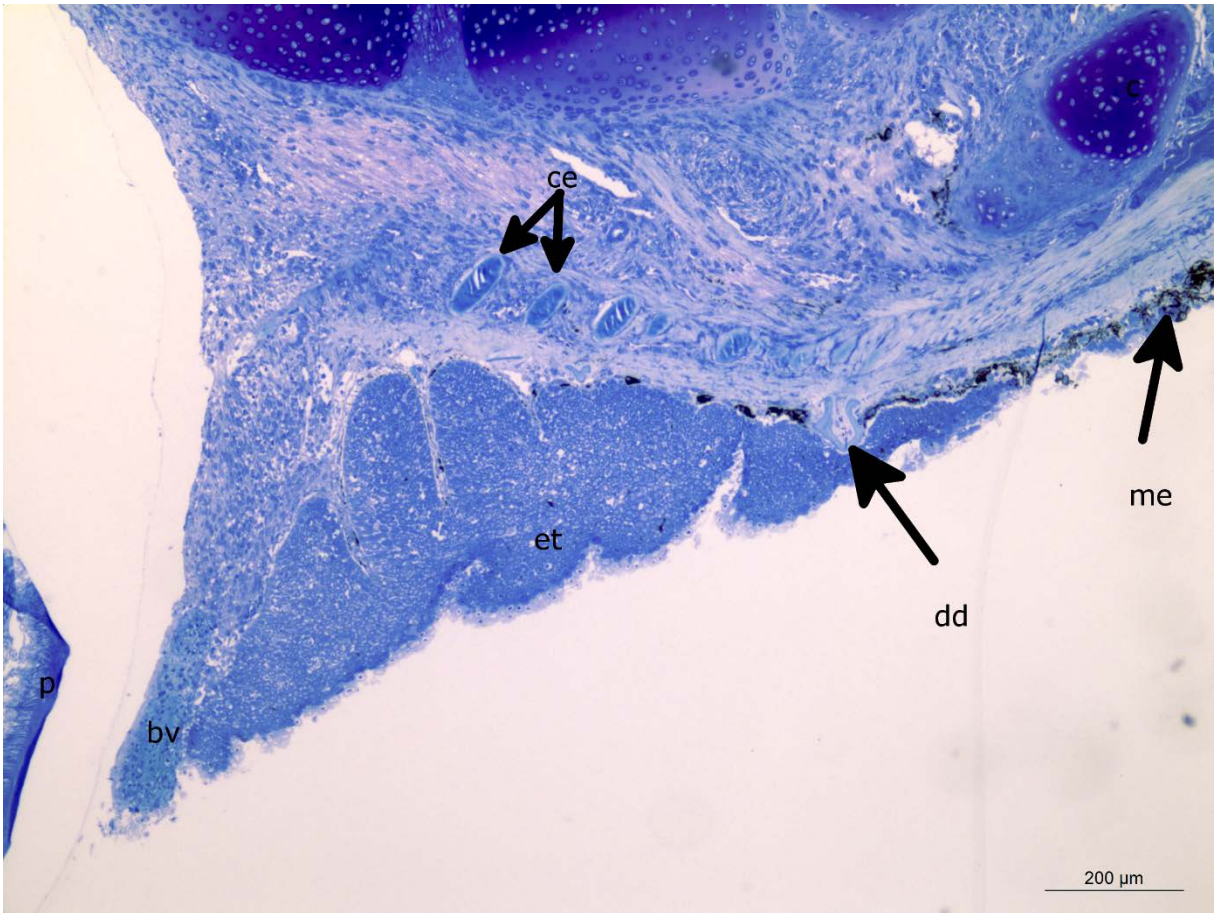

Figure 48: Histological section of the site of attachment. Close to the hole left by the peduncle there is a lack of Melanophores and a marked thickening of the epithelium. A large blood vessel can also be seen at the surface of the host tissue right next to the peduncle. P, peduncle; bv, blood vessel; et, epithelium; dd, dermal denticle; me, Melanophores; ce, ceratotricia. Scale bar: 200 µm.

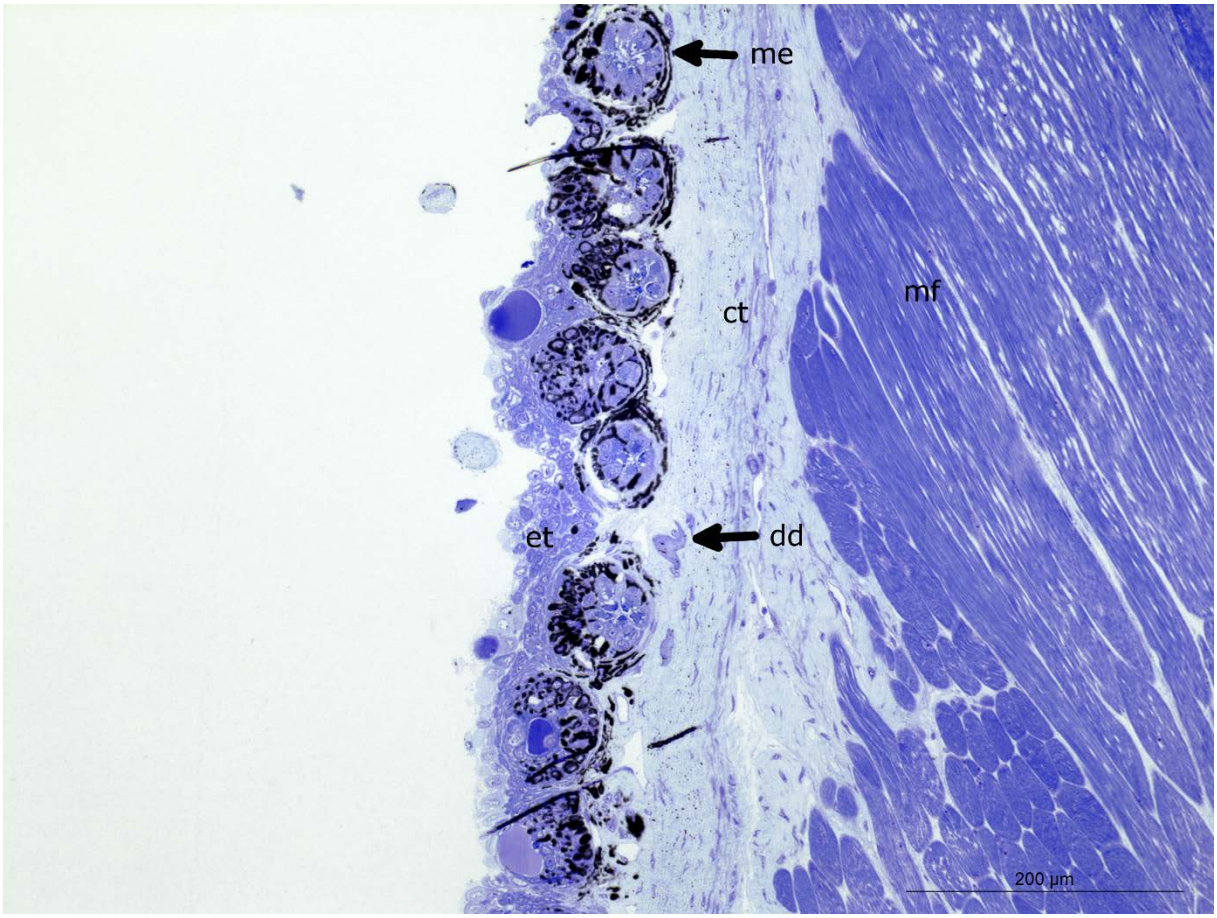

Figure 49: Histological section of a healthy section of host tissue. The epithelium forms an even layer and the Melanophores are evenly distributed. Between the Melanophores and muscle fibers a layer of connective tissue as well as the base of a dermal denticle can be seen. Me, melanophore; ct, connective tissue; mf, muscle fibers; et, epithelium; dd, dermal denticle. Scale bar: 200 µm.

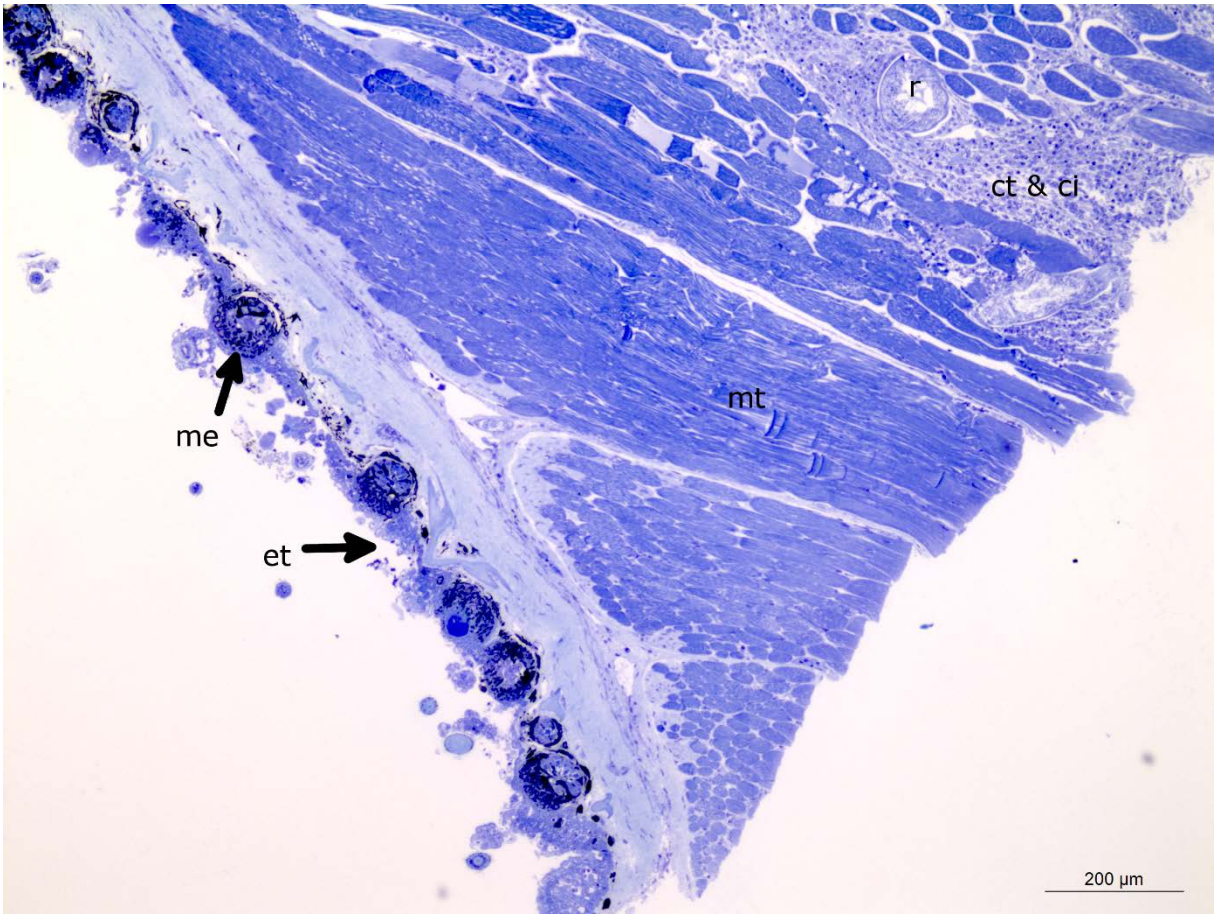

Figure 50: Cross section of tissue near the site of infection showing very localized damage to the tissue. At the bottom three intact myotomes can be seen, closer to the peduncle the layers are infiltrated by roots and muscle fibres are replaced by connective tissue and cellular infiltrates. Et, epithelium; me, Melanophores; mt, myotome; r, root; ct & ci, connective tissue and cellular infiltration. Scale bar: 200 µm.

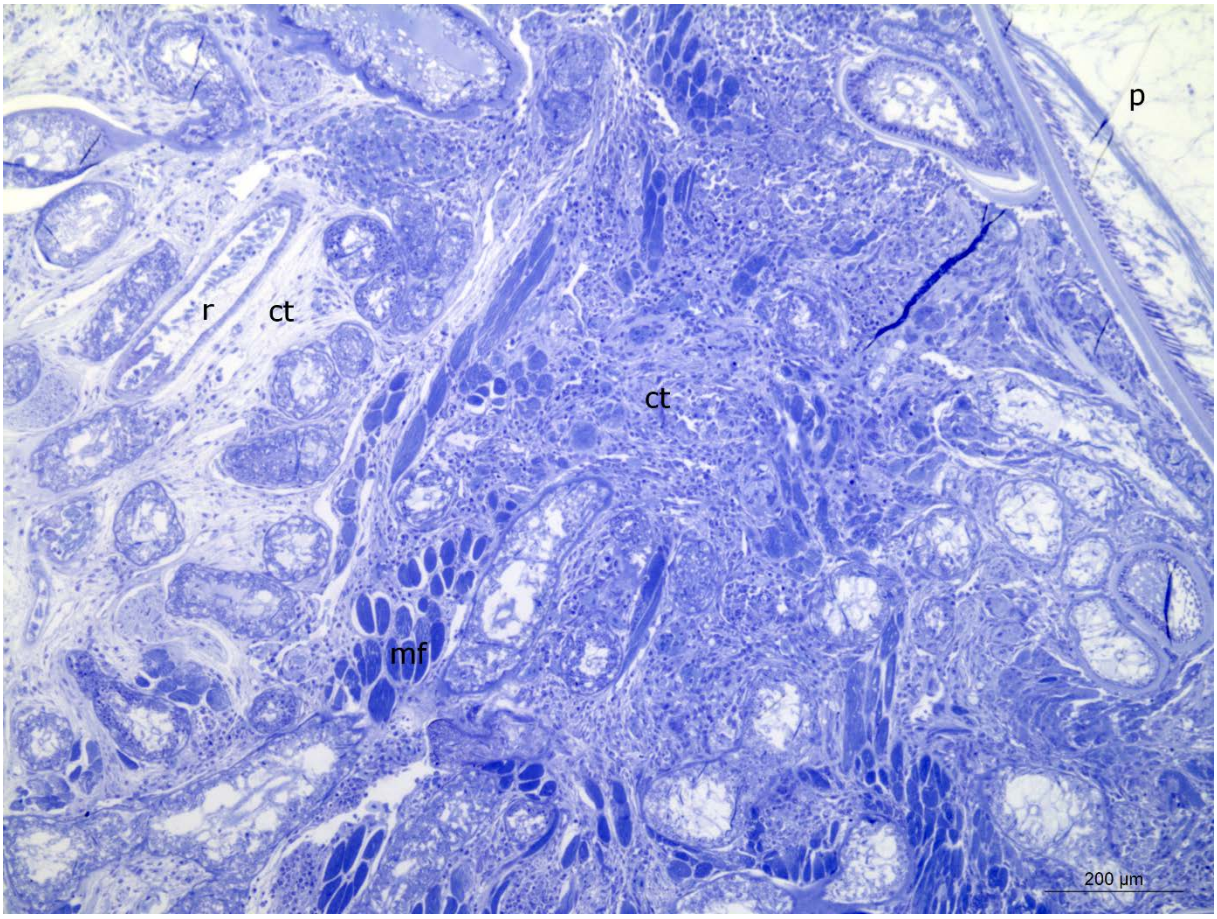

Figure 51: Histological section taken by the peduncle, the peduncle can be seen in the top right corner. The host tissue is riddled by roots and the repeating structure of the myotomes is completely gone. Some muscle fibers can still be seen but it is mostly replaced by connective tissue and roots. P, peduncle; ct, connective tissue; r, root (only one is marked in the image); mf, muscle fibers. Scale bar: 200 µm.

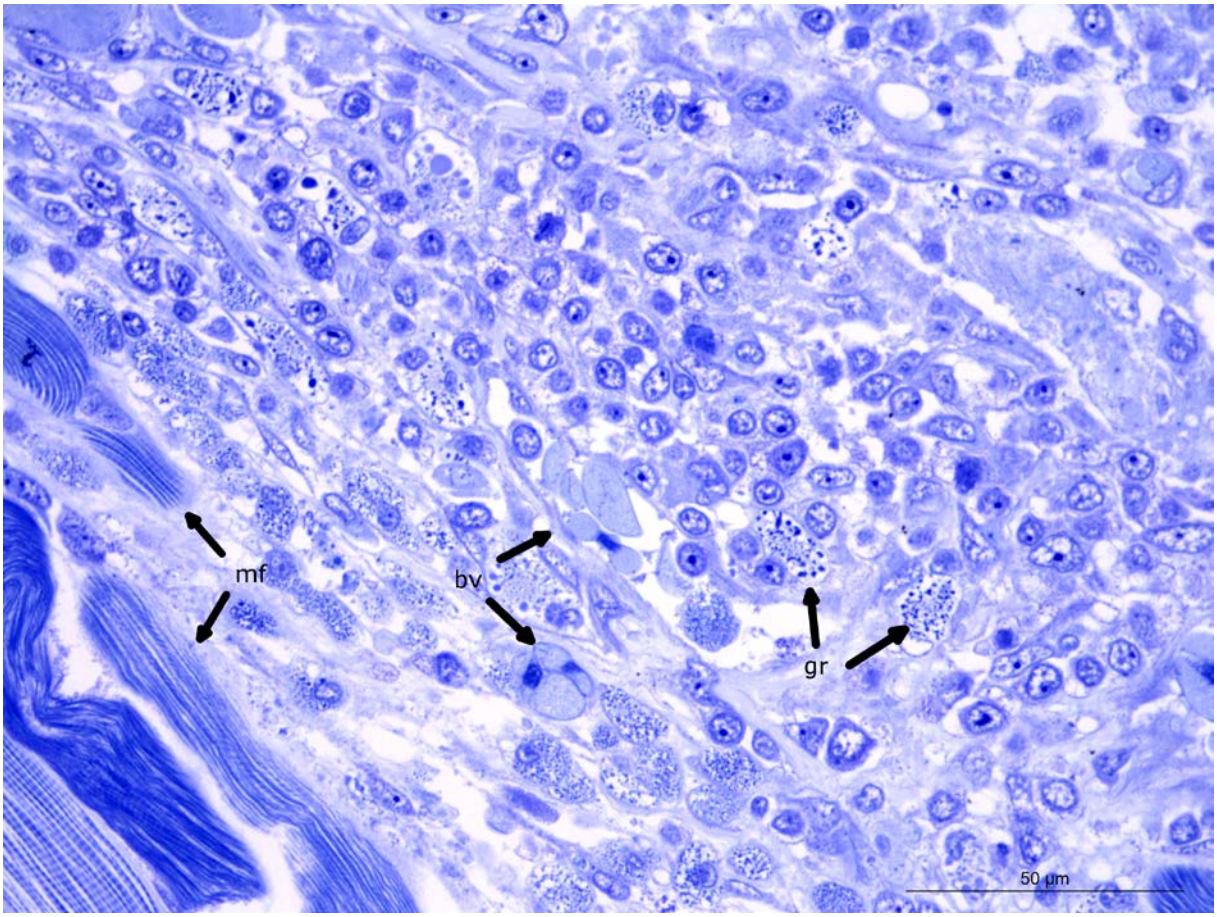

Figure 52: Histological section of host tissue infiltrated by granulocytes. Some muscle fibers are still visible. Mf, muscle fibers; bv, blood vessel; gr, granulocyte. Scale bar: 50 µm.

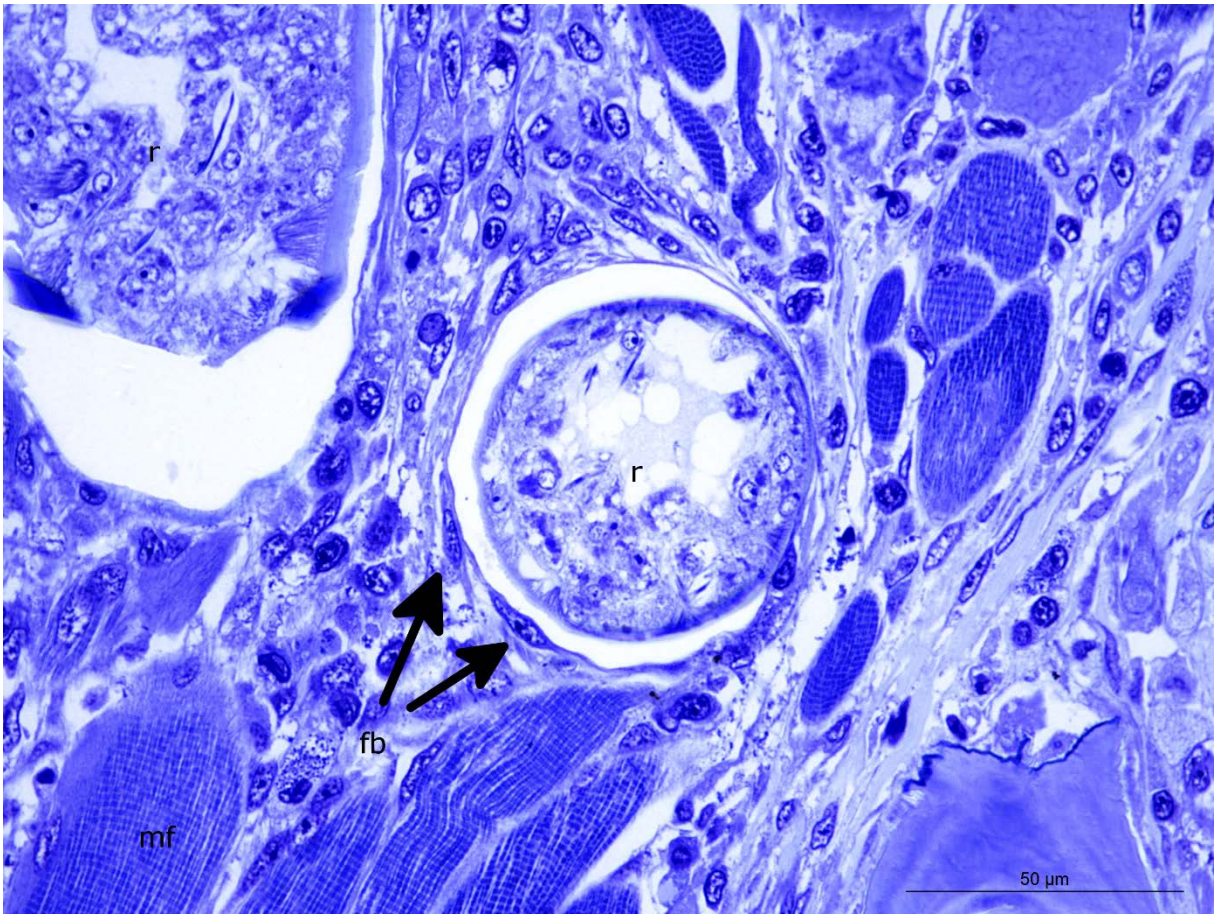

Figure 53: Histological section showing fibroblast cells encapsulating a root. R, root; fb, fibroblast; mf, muscle fiber. Scale bar: 50 µm.

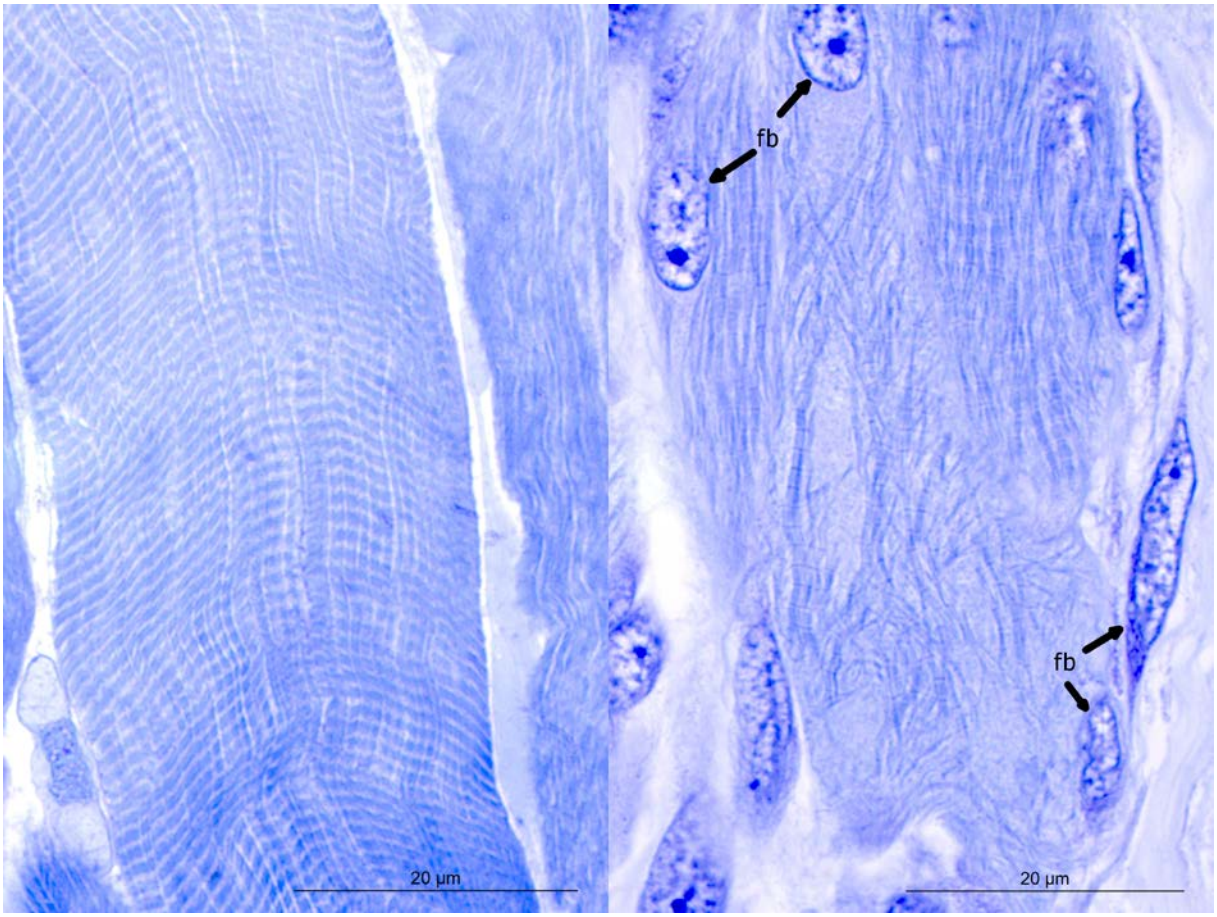

Figure 54: Histological section of muscle fibers. A shows a healthy muscle fiber with even striation. B shows a muscle fiber in close proximity of a root, in this one the striation of the musculature is degrading and fibroblasts can be seen in the musculature. Fb, fibroblast. Scale bar: 20 µm.

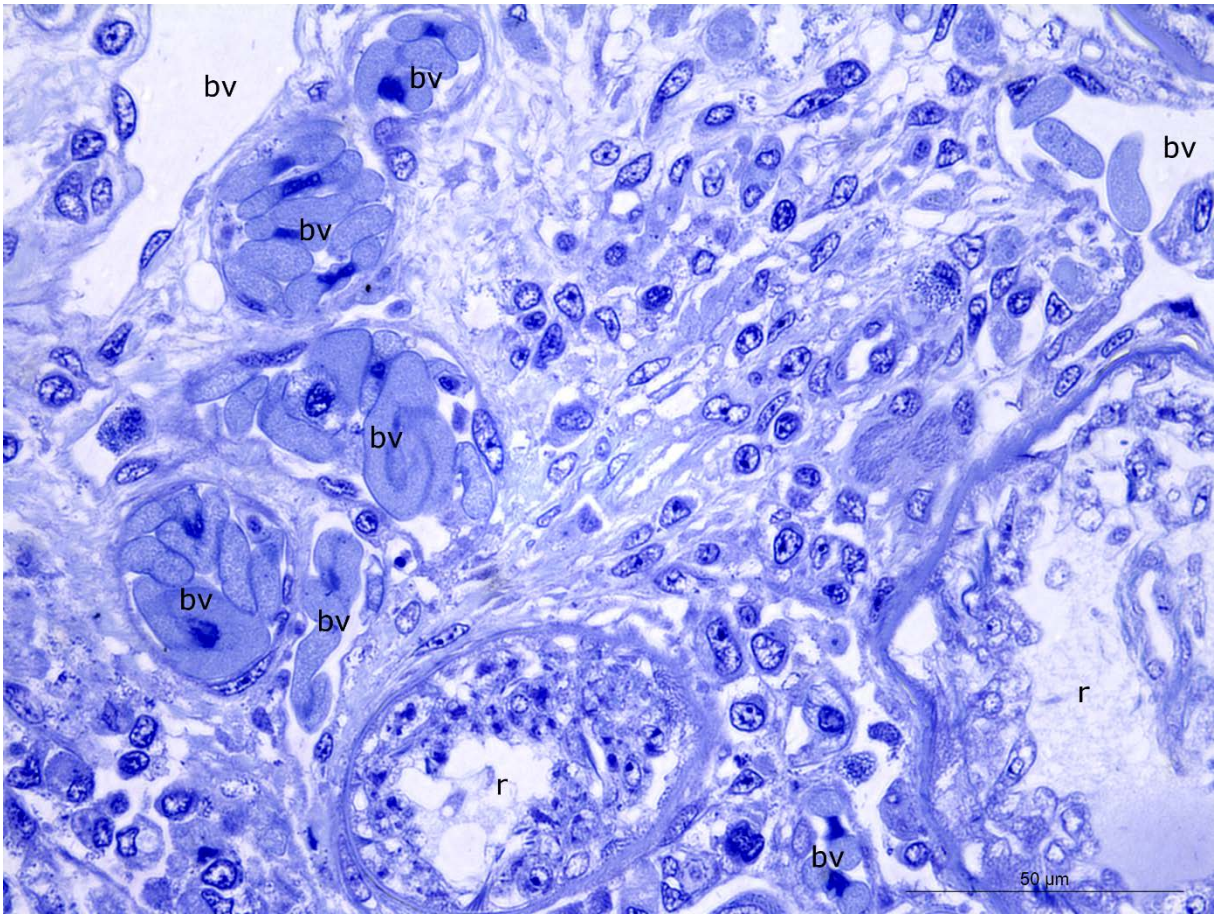

Figure 55: Histological section of host tissue, showing two roots and several capilaries. R, root; bv, capilary blood vessel. Scale bar: 50 µm.

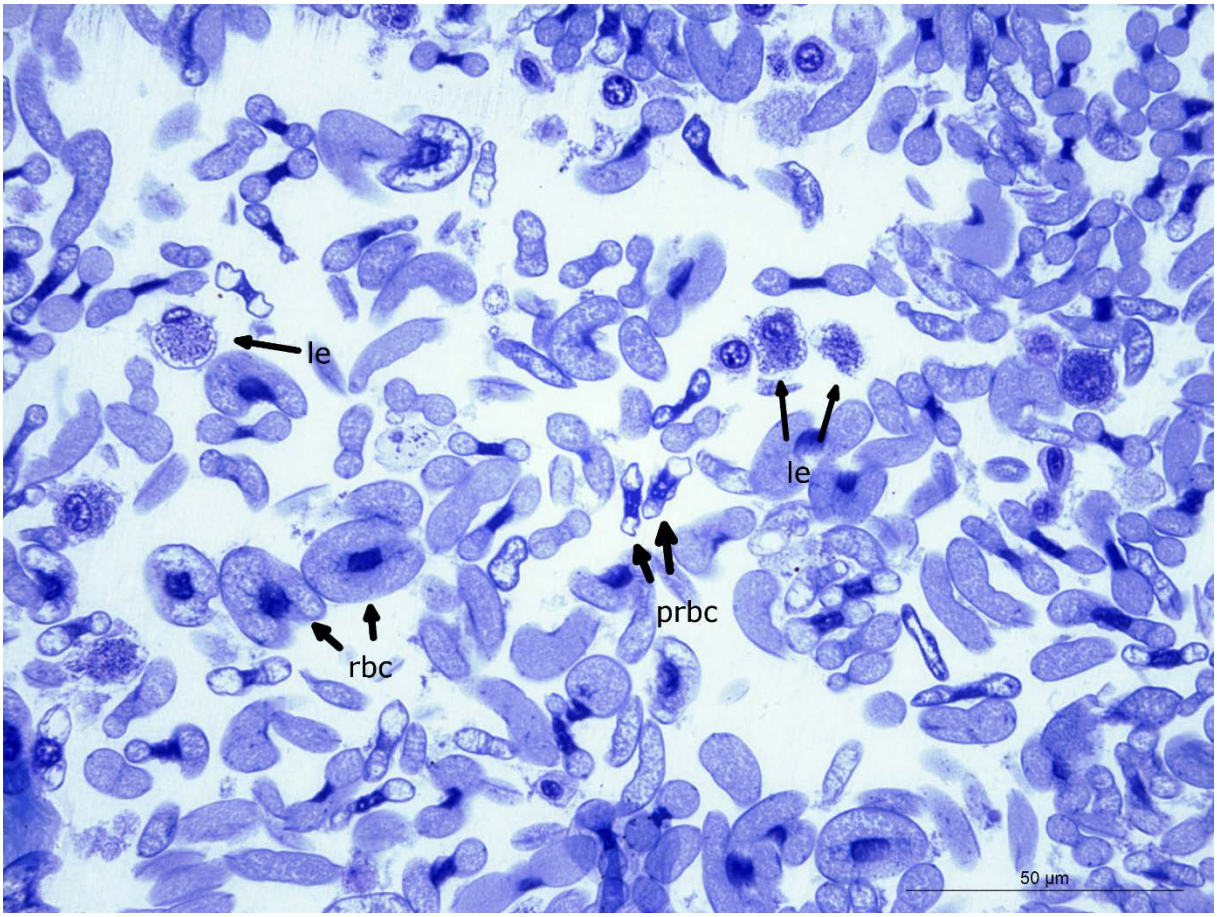

Figure 56: Histological section of a large blood vessel of e. spinax. Most of the red blood cells look healthy, but a number of small, pale red blood cells can also be seen. Some leucocytes can also be seen. Rbc, red blood cell; prbc, pale red blood cell; le, leucocyte. Scale bar: 50 µm.

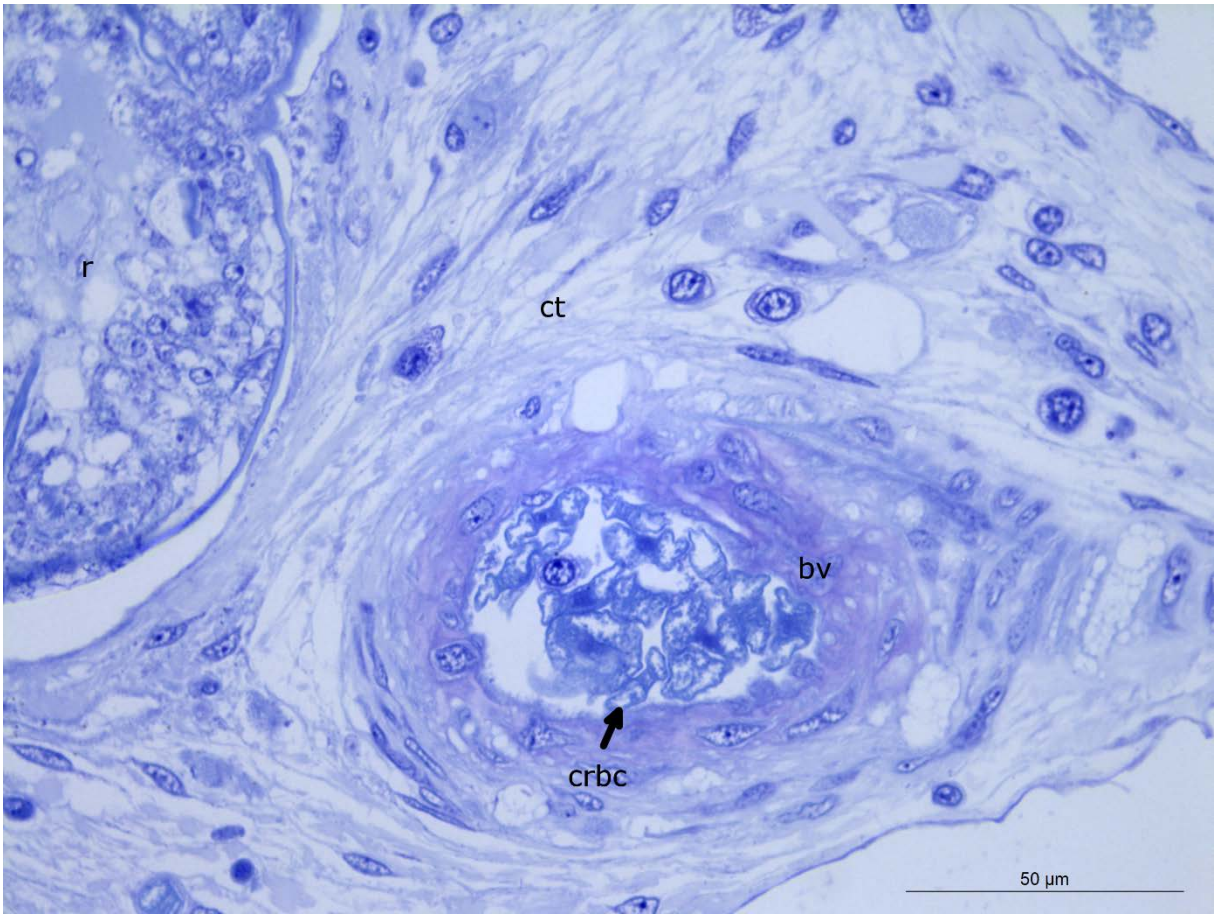

Figure 57: Histological section of host tissue showing a blood vessel. All the red blood cells in the vessel appear to be crenated. R, root; ct, connective tissue; bv, blood vessel; crbc, crenated red blood cell. Scale bar: 50 µm.

Discussion

General body form

Based on what is seen in the three 3D-models of *Anelasma* it seems as if there is a great deal of plasticity in the body shape going from recently settled to the mature individual. It appears as if both the stalk and the mantle is developed alongside the first few roots after *Anelasma* has settled on a host. This is of course highly speculative as no one has to my knowledge been able to keep any of its host species in captivity, and it has, therefore, not been possible to study the mechanism of attachment or the early development. There have however been successful experiments on a whale barnacle, *Coronula diadema*, where cyprids were incubated with a small piece of host tissue and settled and metamorphosed into juveniles (Nogata and Matsumura, 2006). If this would prove possible in *Anelasma*, it would allow for the study of its early development. In the juvenile the lower part of the opening to the mantle cavity can be seen high up on the stalk (Fig. 6, 3D-model of Small), while it can be seen just above the waist in P1 and P7 (Fig. 5 & 7, 3D-model of P1 & P7). This indicates that the stalk either has to be reduced, or that *Anelasma* burrows its stalk into the tissue of the host and it subsequently is modified into what we see as the peduncle in the mature individuals. The outer morphology of the juvenile barnacle closely resembles that of *Lepas antifera* (Lacombe, D., 1969), where the cement glands and ovaries are found just below the capitulum. Taking this into consideration it is probable that it is in fact the stalk seen in the juvenile that later make up the burrowed peduncle in mature specimen. The difference in the appearance of the peduncle between P1 and P7 is likely to be explained by P1 being mature, while P7 is still in a juvenile stage. This is supported by Hickling (1963) in that the peduncle first swells up after the maturation of the ovaries.

Unfortunately both P1 and P7 were cut down a little too much in preparation for micro-CT, but from what can be seen in histological sections it does not appear to be any major difference between the area that is visible in the 3D-models and the bottom of the peduncle.

External characteristics

The findings on the surfaces of the mantle cavity and cirri seem to be in strong contrast to what has been seen earlier. Johnstone and Frost (1927) reports the cuticle lining the mantle cavity to be “similar in every way to that which invests the outer surface of the mantle, thorax and peduncle”, indicating that it was entirely smooth. This holds true for the external cuticle

of the mantle (Fig. 8), but the mantle cavity is densely covered in retinacula (Fig. 9 & 10). The observed thickness of the cuticle is however just as reported in previous studies, with a markedly thicker cuticle on the outside compared to the cuticle of the mantle cavity (Fig. 11) The lack of retinacula in previous studies might be due to the retinacula only developing when the mantle is carrying eggs, or that previous investigators simply lacked the means to see them. The function of the retinacula is not known in *Anelasma, but* it has been speculated that they in *Rhizocephala* serve as chemoreceptors, hold the eggs in place or monitor the water current in the mantle (Rybakov and Høeg, 2002). Based on their shape alone they appear to be structural devices, and function in retaining the eggs in the mantle cavity *Anelasma.*

Looking at the cirri it is evident that they are highly reduced as stated by Ommundsen (2014, Fig. 12 & 13). They are however evenly covered in fan-shaped setules (Fig. 15) quite similar to those found in *Ibla cumingi* (Chan B. K. K. et. Al., 2008) as well as single spines (Fig. 16). Histological sections have also shown that there are bundles of longitudinal musculature in the cirri (Fig. 14) enabling the vigorous movement seen in live specimen. Regardless of this and their motility there is not much doubt that they are in fact completely ineffective for filter feeding.

The cuticle of the capitular region is much thicker than in the penduncular region, and in the cirri the endo- and exo- cuticle can be seen as two individual layers (Fig. 17), similar to that seen in prawns (Sharshar Kh. M. et. Al., 2008). This is a strong contrast to what is seen in the penduncular region, where the cuticle can be seen thinning from the waist down and the apparent reduction of the exocuticle (Fig. 20). The cuticle is supported by a dense layer of columnar cells (Fig. 21 & 22). The cuticle of the roots can be seen tapering off the closer it comes to the tips and show a reduction similar to that of the peduncle (Fig. 23). The roots also show signs of molting (Fig. 27 & 28) The loss of the exocuticle is likely to be an adaptation to the peduncle being buried in the host and therefore being incapable of shedding the old cuticle in the same manner as in the capitular region. As there were no traces of multiple layers of cuticle covering the roots and peduncle I expect that the endocuticle of the peduncle and roots is reabsorbed during the premolt, as seen in other crustaceans (Horst et. Al., 1993). The musculature of the peduncle appears to be well developed and forms three distinct layers (Fig. 18 & 19) and is most likely a means of expelling the mature ova from the peduncle, and into the mantle cavity. The roots of *Anelasma* have previously been reported to have “naked tips”, completely lacking cuticle (Brock, H., 1918), this does not appear to be the case, as every rootlet that could be traced to its end were completely covered by cuticle (Fig. 24 & 25).

The reproductive system

The male reproductive system is well developed and takes up most of the thorax (Fig. 5, 3D-model of P1), it is made up of numerous testicular vesicles (Fig. 29) and the general appearance appear much like what is described by Johnstone & Frost (1927) but due to poor fixation of the thorax it is difficult to draw any conclusions from the histological sections. The cuticle of the probosciform penis is highly folded (Fig. 30), and it can most likely be extended for some distance by turgor pressure. The longitudinal musculature of the penis is probably used in directing the penis during mating, and to contract the penis when not in use as seen in other cirripedes (Anderson, 1994). In micro-CT data it is possible to trace the paired vas deferentia running into the primary penis, and a single one that runs out into the secondary penis (Fig. 5, 3D-model of P1). The urinary meatus is also visible (Fig. 31) so it appears the secondary penis is somewhat functional. The presence of an ectopic penis may be a Hox phenotype, caused by a mutation in Abdominal-B which has been found to be expressed in the genital region of *S. carcini* (Brena et al., 2005) and is known to play a role in genital development in Drosophilia (Estrada B., et al., 2001).

The female reproductive system takes up most of the space in the peduncle and the ovarian ducts can be traced from deep within the peduncle where they branch out and end in ovarian follicles and up through the waist where they arch out to the oviducal bulbs at the base of the first pair of cirri (Fig. 5, 3D-model of P1 & Fig. 32). Johnstone and Frost (1927) were unable to make out the opening of the oviducal bulbs, but as seen in the 3D-reconstructions and micro-CT data they are clearly visible at the side of the oviducal bulb facing towards the bottom of the mantle cavity (Fig. 33), and there is no doubt they are connected to the ovarian tubes themselves. Histological sections of P8 reveals the highly branched ovarian tubes, as well as numerous immature ova (Fig. 34). In the histological sections of the peduncle of P9 Fig. 35), which was a mature individual, ova in varying stages of development are visible, ranging from small unyolked ova to large ova undergoing atresia. The maturing ova develop a large granular yolk appendage (Fig. 36 & 37), indicating that *Anelasma* has a rich supply of nutrients. In some of the larger ova the yolk appears to be dissolving and a deeply staining tubular structure can be seen in the center of the ova (Fig. 38), most likely aiding in its reabsorption. Based on this appears as if *Anelasma* is capable of continuously producing eggs, regardless of whether it is actively depositing the ova in the mantle cavity or not. The reason for this is unclear, but it could be due to a general scarcity of breeding opportunities and the high availability of nutrients.

Seeing that both the male and female reproductive system is well developed it is possible that *Anelasma* is capable of self-fertilization, but as they most often are found in pairs it is unlikely that they rely on this for reproduction.

The Lacunar system

The great central lacuna can be seen running axially through the body (Fig. 5, 3D-model of P1) and enveloping the female reproductive system (Fig. 39), it also radiates to the distal parts of the peduncle and into the roots (Fig. 40 & 41). The lacunar system seems to be well developed in the juvenile even before the peduncle develops (Fig. 42), indicating that it is important throughout all the life stages post settlement. The function of the lacunar system is likely to transport the absorbed nutrients from the roots to where it is used. This is supported by the large amount of lacunae surrounding the ovaries, which are likely to be the most nutrient demanding part of *Anelasma.* It has previously been hypothesized that the nutrients taken up by the roots were transported to the great central lacunae by peristalsis (Johnstone J, Frost WE, 1927), despite them not finding any clear signs of musculature in the roots. The striped musculature seen in the roots (Fig. 27) in the work for this thesis confirms their suspicions and support their hypothesis. It still remains unclear how the nutrients are transported across the cuticle and into the lacunar spaces as there were no clear signs of pores in the cuticle.

The lacunae all appear to be lined by a thin layer of epithelial cells (Fig. 39), if the cells are of endodermal origin it is possible that there is a physical connection between the lacunar system and the digestive system. If this is the case it is possible that the digestive system still functions as an excretory organ as suggested by Broch (1919) as he perceived it as rather highly developed considering the parasitic nature of *Anelasma.* On the other hand, the close connectivity between the lacunar system, the roots and the cement glands could point towards an epidermal origin. If this holds true it is likely that *Anelasma* would require an entirely different means of disposing of waste products. This could be achieved by excreting the waste products back into the host and relying on the host to excrete it.

The cement glands

As *Anelasma* no longer relies on being cemented to a substratum it would be expected that the cement glands would either be reduced, or that they have been adapted to another purpose. The cement glands are however well developed and are found in high numbers in the mantle and the upper parts of the peduncle (Fig. 5, 3D-model of P1 & Fig. 43). The substance produced in the cement glands is led out of the glands by small ducts (Fig. 44), merging to form the two efferent ducts that empty into the lacunae at the bottom of the peduncle. It has been proposed that the cement glands in *Anelasma* are modified to "provide some of the substance used in the elaboration of the food yolk" seen in the eggs (Johnstone J, Frost WE, 1927). This conclusion was drawn due to the high amount of nutrients in the eggs, the high degree of lacunae surrounding the ovaries and on Darwin's assumption that the cement glands were modified ovaries, this assumption was later dismissed by Darwin himself (Crisp, 1983). Given this it is unlikely that the cement glands would have acquired the necessary mutations to produce any of the nutrition for the eggs rather than *Anelasma* simply expanding on the structures already in place for producing nutrients. It is likely the cement glands have adapted to an entirely different function. One other example of barnacles using the cement glands for other means than adhesion is seen in the "Buoy Barnacle", *Dosima fascicularis*, where the cement is led through principal canals and excreted through pores on the bottom of the peduncle forming a float (Zheden et al., 2014). In *Amphibalanus reticulatus* the cement has even been found to corrode stainless steel (Sangeetha et al., 2010). Looking at the different utilization of the cement glands in other barnacles and the connections between cement glands, the lacunar system and the roots in *Anelasma* it is not unlikely that the secretions actual function is to aid in the digestion of or nutrient uptake from the tissue surrounding the roots as previously suggested by Broch (1919).

The digestive system

Apart from the general shape of the digestive tract (Fig. 5, 3D-model of P1) and the anterior placement of the digestive glands (Fig. 47) there isn't much to conclude from either histological sections or the 3D-reconstruction. The digestive system is largely covered by cylindrical epithelial cells (Fig. 45). The function of the small cluster of darker staining cells lining parts the intestine (Fig. 46) can only be speculated about, and no suggestions will be provided here. The stomach has been found to be completely empty and considered as no longer in use for feeding by previous investigators (Ommundsen A., 2014), to clarify if it still retains any function in excretion additional work would be needed.

Occurrence of *Anelasma* on the host

For the specimens of *Anelasma* with recorded attachment-sites they appear to be in the sites seen most often in previous studies. If there is any effect on *Anelasma* from where they are attached is not known, but it is likely that some attachment-sites can have a larger impact on *E. spinax's* ability to feed, i.e. the region around the mouth and eyes. It has also been hypothesized that *E. spinax* uses photophores to light up or mimic the shape of the dorsal spines as a warning display to potential predators (Claes et al., 2013), as *Anelasma* appears to most often attach next to the spines it is possible that it can interfere with this visual cue, and thereby reduce the survival rate of infected sharks.

Host reaction to the parasite

Comparing healthy skin tissue from *E. spinax* (Fig. 49) to the skin surrounding the waist of the peduncle of *Anelasma* (Fig. 48) the epithelium is noticeably thicker in proximity of the peduncle, and there is a reduction in the number of melanophores. The skin of *E. spinax* is pale and slightly raised (Fig. 3), but there does not appear to be any signs of secondary infections. Apart from a local change in epithelium stratification directly surrounding the parasite the penetration of the hosts skin does not appear to cause any major harm in itself.

The structure of the myotomes a short distance from the peduncle appears completely unaffected, but in proximity of the roots they are degraded and the tissue appears to be necrotic (Fig. 50). The degeneration of the myotomes is very local around the peduncle, and nearby the musculature is almost entirely replaced by connective tissue (Fig. 51). Comparing healthy musculature to the musculature affected by *Anelasma* one can clearly see the degradation of the striation and infiltration of fibroblasts (Fig. 54). The degradation of the host tissue is likely to be one of the steps by which *Anelasma* acquires its nutrients. Despite the degeneration being localized around the peduncle it is possible it has an effect on the hosts ability to swim and capture prey given the size of the peduncle compared to the host.

The increase in capillaries in the tissue affected by *Anelasma* (Fig. 55) could be induced by *Anelasma* to relocate more nutrients to itself as seen in parasitic helminths (Dennis, Schubert and Bauer, 2011), or it could simply be a host response as seen in tissue after inflammation. Apart from this an inflammatory response with infiltration of leucocytes can be seen (Fig. 52), as well as some degree of encapsulation of the roots by fibroblasts (Fig. 53).

In one of the large blood vessels there seems to be a mixture of healthy looking, and smaller pale erythrocytes (Fig. 56), while in a small vessel close to the roots of *Anelasma* all appear to be crenated (Fig. 57). If the apparent change seen in some of the erythrocytes is caused by *Anelasma* is uncertain, but it is most likely caused by the treatment of the specimens and the staining of the histological sections (pers. com. Kryvi, H.). To further elucidate this and if there is an increase in immune cells it would be helpful to obtain blood-smears from both infected and healthy individuals of *E. spinax.*

Main conclusions

- The general body form of *Anelasma* varies greatly by stage of maturity, and obtains its final form after maturity and swelling of the ovaries.
- The cuticle of the penduncular region of *Anelasma* is reduced, this is likely an adaption to the peduncle being buried in the flesh of its host while *Anelasma* still relies on molting to increase in size.
- Both the male and female reproductive system is well developed at the same time in *Anelasma,* but as they mostly appear in pairs it is unlikely that they rely on self-fertilization for reproduction.
- The lacunar system is very well developed and can be seen penetrating far into the tips of the roots of *Anelasma.* Its function is likely to transport and redistribution of the nutrients taken up by the roots of *Anelasma.* This is supported by the large amount of lacunae seen surrounding the ovaries.
- The cement glands close connectivity to the lacunar system and the roots indicates that the cement glands have adapted to play a role in nutrient uptake or digestion of the host tissue surrounding the roots.
- The presence of *Anelasma* appear to only have a very localized effect on its host.
- In conclusion *Anelasma* is in possession of several adaptations to a parasitic lifestyle.

Suggestions for further work

- Study the settlement and metamorphosis of the cyprid larvae of *Anelasma.*
- Investigate the ultrastructure of the roots of *Anelasma* to determine how nutrients are transported across the cuticle of the roots and if the roots themselves function as trophic organ as believed in *Rhizocephala* (Rybakov and Høeg, 2002).
- Investigate whether the lacunar walls are made up of epithelial cells and if there is any connection between the digestive tract and the lacunae.
- Investigate the function of the digestive tract and determine if it still has a role as an excretory organ.
- Investigate what genes are expressed in the cement glands and determine their function.
- Compare blood from infected and healthy individuals of *E. spinax* to investigate the host reaction.

References:

ANDERSON, D. (1994). *Barnacles*. London: Chapman & Hall.

BRENA, C., LIU, P., MINELLI, A. AND KAUFMAN, T. (2005). Abd-B expression in Porcellio scaber Latreille, 1804 (Isopoda: Crustacea): conserved pattern versus novel roles in development and evolution. *Evol Dev*, 7(1), pp.42-50.

BROCH, H. 1919. Anatomical studies on Anelasma and Scapellum. *Kongelige Norske Videnskabernes Selskabs Skrifter Trondhjem, 1, 1-28.*

CHAN, B., GARM, A. AND HEG, J. (2008). Setal morphology and cirral setation of thoracican barnacle cirri: adaptations and implications for thoracican evolution. *Journal of Zoology*, 275(3), pp.294-306.

CLAES, J., DEAN, M., NILSSON, D., HART, N. AND MALLEFET, J. (2013). A deepwater fish with 'lightsabers' – dorsal spine-associated luminescence in a counterilluminating lanternshark. *Sci. Rep.*, 3.

CRISP, D. (1983). Extending Darwin's investigations on the barnacle life-history. *Biological Journal of the Linnean Society*, 20(1), pp.73-83.

DARWIN, C. R. 1851. Living Cirripedia, A Monograph on the Sub-Class Cirripedia, with Figures of All the Species. The Lepadidæ; or, Pedunculated Cirripedes. London: *The Ray Society*, 1.

DENNIS, R., SCHUBERT, U. and BAUER, C. (2011). Angiogenesis and parasitic helminth-associated neovascularization. *Parasitology*, 138(04), pp.426-439.

ESTRADA, B ; SÁNCHEZ-HERRERO, E. (2001). The Hox gene Abdominal- B antagonizes appendage development in the genital disc of Drosophila. *Development*, 128 (2001), pp. 331–339

JOHNSTONE, J. & FROST, W. E. 1927. Anelasma squalicola Loven; its general morphology. *Proceedings and Transactions of the Liverpool Biological Society*, 41, 29-91.

HAYASHI, R., CHAN, B., SIMON-BLECHER, N., WATANABE, H., GUY-HAIM, T., YONEZAWA, T., LEVY, Y., SHUTO, T. AND ACHITUV, Y. (2013). Phylogenetic position and evolutionary history of the turtle and whale barnacles (Cirripedia: Balanomorpha: Coronuloidea). *Molecular Phylogenetics and Evolution*, 67(1), pp.9-14.

HICKLING C. F., 1963. On the small deep-sea shark Etmopterus spinax L. and its Cirripede parasite Anelasma squalicola (Loven). *J. Linn. Soc. Lond., Zoology*, 45 (303): 17-24.

KOSSMAN, R., (1874), Suctoria und Lepadidae. (Arbeiten aus dem Zoologisch-Zootomishen Institut) Würzburg.

LACOMBE, D. AND LIGUORI, V. (1969). Comparative Histological Studies of the Cement Apparatus of Lepas anatifera and Balanus tintinnabulum. *Biological Bulletin*, 137(1), p.170.

NOGATA, Y. AND MATSUMURA, K. (2006). Larval development and settlement of a whale barnacle. *Biology Letters*, 2(1), pp.92-93.

OMMUNDSEN, A. (2014). From suspension feeding to parasitism: The feeding mode of the shark barnacle Anelasma squalicoola (Lovén, 1844). Masters Thesis. University of Bergen.

REES, D. J., ET AL. (2014). "On the Origin of a Novel Parasitic-Feeding Mode within Suspension-Feeding Barnacles." *Current Biology* 24(12): 1429-1434.

RYBAKOV, A. AND HØEG, J. (2002). The Ultrastructure of Retinacula in the Rhizocephala (Crustacea: Cirripedia) and their Systematic Significance. *Zoologischer Anzeiger - A Journal of Comparative Zoology*, 241(2), pp.95-103.

SANGEETHA, R., KUMAR, R., DOBLE, M. AND VENKATESAN, R. (2010). Barnacle cement: An etchant for stainless steel 316L?. *Colloids and Surfaces B: Biointerfaces*, 79(2), pp.524-530.

SHARSHAR, K. AND AZAB, E. (2008). Studies on Diseased Freshwater Prawn Macrobrachium rosenbergii Infected with Vibrio vulnificus. *Pakistan J. of Biological Sciences*, 11(17), pp.2092-2100.

YANO, K. AND J. MUSICK (2000). "The Effect of the Mesoparasitic Barnacle Anelasma on the Development of Reproductive Organs of Deep-sea Squaloid Sharks, Centroscyllium and Etmopterus." *Environmental Biology of Fishes* 59(3): 329-339.

ZHEDEN, V., KOVALEV, A., GORB, S. AND KLEPAL, W. (2014). Characterization of cement float buoyancy in the stalked barnacle Dosima fascicularis (Crustacea, Cirripedia). *Interface Focus*, 5(1), pp.20140060-20140060.

Appendix

Reducing model size and exporting 3D-models to PDF

All rendered surfaces were exported from imaris using the “Export Selected Objects” option as “.vrml” files. The file extension was then changed to “.wrl” before importing to meshlab_64bit (Visual Computing Lab – ISTI – CNR) for size reduction. To reduce the file size the following steps were taken.

Filters -> Cleaning and Repairing -> Remove Unreferenced Vertex

Filters -> Cleaning and Repairing -> Remove Duplicated Vertex

Filters -> Remeshing, Simplification and Reconstruction -> Quadratic Edge Collapse Decimation

For the “Quadratic Edge Collapse Decimation” the “Target number of faces” were set to half the original value, “Quality threshold” to 0.5 and “Preserve Boundary of the mesh”, “Preserve Normal”, “Preserve topology”, “Optimal position of simplified vertices” and “Post-simplification cleaning” were checked.

Filters -> Smoothing, Fairing, Deformation -> Taubin Smooth

For “Taubin Smooth” lambda and mu were left as default, and smoothing steps were set to 10.

Quadratic Edge Collapse Decimation and smoothing were then repeated until the surfaces were of a more manageable size (11.5gb to ~100mb).

After reaching a desirable size all surfaces were exported as “.obj” files and imported to Deep exploration (v. 6.5.0.9181, Right Hemisphere). The surfaces were then named and ordered in the “Scene” view, and the surfaces were colored in the “Color Objects Settings” before exporting as “.u3d”. The “.u3d” files were then opened in Acrobat Pro, and saved as “.pdf”.

Recipes for histology

Toluidine blue (1%) (Philpott, 1966)

- 1.91 g borax (dinatriumtetraborat – decahydrat)
- 1.0 g toluidine blue
- 100 ml destilled water
- Borax is solved in water and toluidine blue is added. The solution is stored dark, and is filtradet before use. After coloring the sections are rinsed in running water, previous to drying and mounting with DPX.

PBS (0,2 M, pH 7.2)

- 8.0g NaCl
- 0.2 g KCl
- 14.4 g $Na_2HPO_4 \cdot 2H_2O$ (di – sodium phosphate – dihydrate)
- 2.3 g NaH_2PO_4 (Sodium phosphate – monohydrate)
- Solved in 1000 ml of distilled water
- pH adjusted to 7.2 using a pH-meter
- Stored at 4 ^{0}C

Casting in Technovit 7100 ((2-hydroethyl) – methacrylate)

-Preinfiltration: 1 part Technovit base and 1 part ethanol (96%), stirred for approx. 2 hours.

-Infiltration: 100 ml Technovit and 1 bag of hardener is mixed and added to the tissue, stirred for 12 hours.

-Casting: 15 ml Technovit with hardener is mixed with 1 ml of liquid hardener. The tissue is cast in molds together with a block-holder, and after polymerization the blocks are removed and stored in an air-tight environment.

Directions for viewing 3D-models

This document contains 3D-models (Figures 5, 6 & 7) and I highly recommend to open the models in a separate window while reading through the results and discussion. This will not only make it a lot easier to follow, but also provides a level of information on the morphology of *Anelasma* that would have been impossible to convey by text and images alone.

For full functionality "Adobe Acrobat Reader DC" is required.

It can be acquired from:

https://get.adobe.com/no/reader/ (for windows) or
https://www.adobe.com/support/downloads/detail.jsp?ftpID=5867 (for mac).

(In case the links do not work it can also be found by searching for "Adobe Acrobat Reader DC" at google.com.)

After installation right click this file and choose "open with" ("åpne i") and choose "Adobe Acrobat Reader DC". The figures can then be activated by left clicking the figure. Upon clicking the figure there will be a prompt, asking if you trust the document. By pressing "Trust this document once/always" ("Stol på dette dokumentet en gang/alltid") the figure is available for activation. By clicking the figure again, the 3D-model is activated. The model can be rotated by clicking and holding the left mouse button and dragging the mouse cursor. To zoom in or out, hold in the right mouse button and drag the mouse cursor up (to increase its size) or down (to reduce its size), the same can be achieved by using the mouse wheel. By pressing and holding in both mouse buttons the model can be moved around in its frame.

To access the different layers of the model the "Show/ hide model tree" ("Vis/skjul modelltre") button has to be pressed. It is visible in the menu displayed above the 3D-model after activation. An image of the button can be seen below.

This reveals a menu on the left hand side, where all the different layers can be seen. By unchecking the individual boxes under "model" the underlying surfaces can be seen (unchecking "Host tissue" reveals the "Parasite w/o interna" and so on). The surfaces are listed in descending order, and by unchecking from the top down every layer is displayed in turn. It is also possible to right click the names in the menu and choose to make individual layers transparent, showing the placement of the underlying surface within the transparent outer layer. This option is especially useful when applied to the "Host tissue" to see extent of the roots within the host tissue, and "Thorax" to see the placement and relative size of the internal organs of the thorax.

The models can be accessed by Dropbox and opened in a separate window by following the link below.

https://www.dropbox.com/sh/eoaefv5klue65ot/AACJN6q7ukkl4hcYjIAAC7oHa?dl=0